

# **Study of CO<sub>2</sub>-Absorption into Thermomorphic Lipophilic Amine Solvents**

Zur Erlangung des akademischen Grades eines

**Dr.-Ing.**

von der Fakultät Bio- und Chemieingenieurwesen  
der Technischen Universität Dortmund  
genehmigte Dissertation

vorgelegt von

M.Sc. Yudy Halim Tan

aus

Bandung

Tag der mündlichen Prüfung: 24 September 2010

1. Gutachter: Prof. Dr. David W. Agar
2. Gutachter: Prof. Dr. Arno Behr

**Dortmund 2010**

## Summary

CO<sub>2</sub> absorption is done physically and chemically in industrial practice. Chemical absorption using amine solvent is preferable for removal of CO<sub>2</sub> at low partial pressure below 140 mbar. However the regeneration of loaded solvent requires high amount of energy and causes corrosion problem. To circumvent these problems a novel solvent, called lipophilic amine solvent was investigated.

Lipophilic amine, which has limited aqueous solubility, forms biphasic – organic and aqueous phase solutions upon mixing with water. Depending on the composition of the solvent, it allows absorption starting from heterogeneous aqueous solution with high absorption rate and capacity surpassing those of conventional alkanolamines. The amine-rich organic phase disappears during absorption as the result of dissolution of ionic reaction products between CO<sub>2</sub> and amine into aqueous phase. Thus the loaded solvent is literally homogeneous liquid.

During regeneration at elevated temperature, the loaded solution undergoes thermally induced liquid-liquid phase separation. The regenerated amine forms a layer of organic phase at the top of the loaded solution which acts as a solvent to extract the subsequent regenerated amine and drives the equilibrium towards desorption side. With these characteristics, not only high loading approaching 1:1 (CO<sub>2</sub>:amine) at 1 atm partial pressure of CO<sub>2</sub> could be achieved but also regeneration at moderate temperature 80°C could be carried out.

In this work, systematic approach had been applied to investigate the lipophilic amine characteristics for CO<sub>2</sub> absorption, starting from identifying suitable lipophilic amine for CO<sub>2</sub> absorption, absorption mechanism, determination of mass transfer properties, reaction kinetics and enthalpy, thermodynamics modelling until optimisation of the solvent composition. Further investigation had yielded a new concept to regenerate the loaded lipophilic amine solvents by extraction using foreign inert solvent.

In brief, the lipophilic amine solvents provide a new degree of freedom for effective CO<sub>2</sub> absorption with low temperature and low cost regeneration.

## Abstract

CO<sub>2</sub> absorption is done physically and chemically in industrial practice. Chemical absorption is preferable for removal of CO<sub>2</sub> at low partial pressure below 140 mbar. For this purpose aqueous amine solutions are used widely as chemical solvent. In industrial application primary and secondary amines, designated activator, are mixed with tertiary amine to combine synergistic effects of fast reaction rate of the former with high capacity of the latter. As the carbamate ion resulting from amine reactions with CO<sub>2</sub> is stable, the application of amine leads to high energy demand for regeneration and additional corrosion problem. To circumvent these problems a novel solvent, called lipophilic amine was developed in this work.

The utilisation of new amine solvents for CO<sub>2</sub> absorption, which undergo thermally induced phase separation (thermomorphic phase separation) was investigated in this work. This type of amines, designated lipophilic amine, has limited aqueous solubility. Upon mixing with water, it forms biphasic conjugate solution of amine-rich organic phase and water-rich aqueous phase. Depending on the composition of the solvent, it allows absorption starting from heterogeneous aqueous solution with high absorption rate and capacity surpassing those of conventional alkanolamines. The amine-rich organic phase disappears during absorption as the result of dissolution of ionic reaction products between CO<sub>2</sub> and amine into aqueous phase. Thus the loaded solvent is literally homogeneous liquid.

During regeneration at elevated temperature, the loaded solution undergoes thermally induced liquid-liquid phase separation. The regenerated amine forms a layer of organic phase at the top of the loaded solution which acts as a solvent to extract the subsequent regenerated amine and drives the equilibrium towards desorption side. Therefore, the lipophilic amine solvents regeneration is enhanced by auto-extractive effect.

With these characteristics, not only high loading approaching 1:1 (CO<sub>2</sub>:amine) at 1 atm partial pressure of CO<sub>2</sub> could be achieved but also regeneration at moderate temperature 80°C could be carried out.

Systematic approach has been applied to investigate the lipophilic amine characteristics for CO<sub>2</sub> absorption.

- Suitable lipophilic amines, which fulfil the criteria for CO<sub>2</sub> absorption, were identified. As a result, N,N-Dipropylamine (DPA), a secondary amine, and N,N-Dimethylcyclohexylamine (DMCA), a tertiary amine were identified as suitable lipophilic amines for CO<sub>2</sub> absorption.

- The characteristics of lipophilic amines aqueous solubility were also investigated to get a deeper insight of the thermomorphic liquid-liquid separation properties.
- The required lipophilic amine solution properties, such as CO<sub>2</sub> diffusivity, CO<sub>2</sub> physical solubility, amine partitioning, viscosity and density were determined experimentally at elevated temperature.
- Practical thermodynamic modelling based on Kent-Eisenberg model was applied for CO<sub>2</sub> absorption into the lipophilic amine solution. As the results, the distribution of reactive species in the bulk liquid phase at various CO<sub>2</sub> loading was predicted. The results also explain the absorption mechanism into lipophilic amine solvents.
- For equipment design purpose, kinetics of CO<sub>2</sub> – lipophilic amine DPA and DMCA reaction were investigated.
- Absorption heat of CO<sub>2</sub> and lipophilic amine was also determined based on the Van 't Hoff equation. It concludes the similarity of lipophilic absorption heat to that of conventional alkanolamine.
- Experimental optimisation of lipophilic amine mixture performance under various operating condition and composition of mixture of lipophilic amines were determined.
- Preliminary degradation study of the lipophilic amine DPA and DMCA has successfully identified the thermal stability and susceptibility of the lipophilic amine solvents under high O<sub>2</sub> condition.
- Exploration of other lipophilic amine solvents suitable for amine system successfully indentified more lipophilic amines for the next generation projects.

To improve the regeneration of lipophilic amine, a new method by extractive regeneration was investigated. The idea is to destabilize the equilibrium of the loaded lipophilic amine solution by means of extraction using inert foreign solvent. This way the regeneration of lipophilic amine can be carried out even at low temperature (40°C) and the foreign solvent can be separated from the extracted amine by flashing or simple distillation at low temperature. Aspen simulations done on the separation indicates the feasibility of the lipophilic amine – foreign solvent separation.

In brief, the lipophilic amine solvents provide a new degree of freedom for effective CO<sub>2</sub> absorption with low temperature and cost regeneration. The exceptional characteristic of the solvent is the high net capacity and low regeneration temperature which leads to a very significant cost reduction. Regeneration using waste heat can be expected.

---

## Acknowledgements

I would like to thank Prof. D.W. Agar for the supervision of this doctoral study, for his guidance and support that motivated me to resolve problems occurred during completion of the degree. I'd like to thank Frank Geuzebroek and Xiaohui Zhang as supervisors from industrial side and Shell Global Solutions without whom the project could not be accomplished.

My gratitude is addressed to staffs of the institute of reaction engineering who have lent their hands and contributed to all of the aspect of the study, Michael Schlüter, Julian Gies, Bern Kissel and Noel Meyer for their willingness to provide me with technical help concerning experiments. Special thanks are addressed to staffs of the glass workshop, Heinz Karmazin and Klaus Hirschfeld without whom none of the experimental apparatuses could be set up very well.

I would like also to thank Angela Andrade-Sierra, Andreas Ufer, Ken Irawadi and Falk Lindner who are my partners in brainstorming process, for their willingness to give support and to share our ideas during the project. Without less respect also my appreciation for all of the colleagues at the institute of reaction engineering who give me a memorable wonderful time during the completion of the degree. My gratitude also for Ammar Mohd. Akhir, Ameya Savnal, Pavadee Pachariyanon, Robert Misch, Li Binbin, Hu Ming, Alvin, Zheng Guanghua, Wang Jian, Zhang Jiafei, Cai Yu and Abhijit Karle for their contribution. My deep gratitude is addressed to my family for their support and accompanying during the hardest time of the project. And without less respect I would like to thank all people, without whom this project would be less well completed.

## Table of Contents

<b>ABSTRACT</b> .....	<b>II</b>
<b>ACKNOWLEDGEMENTS</b> .....	<b>IV</b>
<b>TABLE OF CONTENTS</b> .....	<b>V</b>
<b>LIST OF FIGURES</b> .....	<b>VII</b>
<b>LIST OF TABLES</b> .....	<b>X</b>
<b>NOMENCLATURE</b> .....	<b>XI</b>
<b>1 INTRODUCTION</b> .....	<b>1</b>
1.1 CO <sub>2</sub> removal background.....	1
1.1.1 Global warming and energy sectors.....	1
1.1.2 Chemical industry requirements.....	2
1.2 CO <sub>2</sub> capture technologies.....	3
1.2.1 Post combustion capture .....	3
1.2.1.1 Physical absorption processes .....	4
1.2.1.2 Chemical absorption processes .....	5
1.2.2 Pre-combustion processes .....	6
1.2.3 Novel CO <sub>2</sub> removal processes.....	7
1.3 Project background.....	7
<b>2 THEORETICAL BACKGROUND</b> .....	<b>9</b>
<b>3 EXPERIMENTAL TECHNIQUE, CHEMICALS AND APPARATUSES</b> .....	<b>16</b>
3.1 Chemicals .....	16
3.2 Apparatuses.....	19
3.2.1 Double stirred cell reactor.....	19
3.2.2 Absorption unit .....	20
3.2.3 Capillary reactor.....	22
3.2.4 Gas-liquid reactor .....	23
3.2.5 Viscometer unit .....	23
3.2.6 Extraction reactor.....	24
3.2.7 Amine screening unit .....	25
3.2.8 Liquid phase analysis .....	26
<b>4 RESULTS AND DISCUSSION</b> .....	<b>29</b>
4.1 Concept .....	29
4.1.1 Absorption: homogeneous – regeneration: biphasic.....	29
4.1.2 Absorption: heterogeneous – regeneration: biphasic .....	31
4.1.3 CO <sub>2</sub> absorption mechanism in biphasic amine solution .....	35
4.1.4 Comparison of biphasic and homogeneous solvent for CO <sub>2</sub> absorption .....	36
4.2 Influence of lipophilic amine structure to its properties.....	38
4.2.1 Influence of amine structure to molecule base strength.....	38
4.2.1.1 Inductive effect.....	38
4.2.1.2 Solubilisation effect.....	40
4.2.1.3 Steric effect.....	41
4.2.1.4 Influence of amine structure to viscosity .....	42
4.2.2 Exploration for suitable lipophilic amines.....	43
4.3 Lipophilic amines applied in CO <sub>2</sub> absorption.....	45

---

4.3.1	N,N-dipropylamine (DPA)	47
4.3.2	N,N-dimethylcyclohexylamine (DMCA)	48
4.4	Physicochemical properties: DPA-H <sub>2</sub> O and DMCA-H <sub>2</sub> O	50
4.4.1	Density	50
4.4.2	Viscosity	51
4.4.3	Gas physical solubility	52
4.4.4	Diffusivity of CO <sub>2</sub> in amine solutions	54
4.5	Thermodynamic modelling	54
4.5.1	Mathematical modelling	55
4.5.2	CO <sub>2</sub> -aqueous phase DPA model	56
4.5.3	CO <sub>2</sub> -aqueous MEA model	59
4.5.4	CO <sub>2</sub> -aqueous DMCA model	60
4.5.5	CO <sub>2</sub> -aqueous MDEA model	62
4.5.6	CO <sub>2</sub> - 3 M DPA model	63
4.5.7	CO <sub>2</sub> - biphasic 3 M DMCA model	65
4.6	Kinetics of CO <sub>2</sub> -DPA and CO <sub>2</sub> -DMCA	68
4.6.1	Kinetics of CO <sub>2</sub> – organic phase DPA and DMCA	69
4.6.2	Kinetics of CO <sub>2</sub> – aqueous phase DPA and DMCA	72
4.6.3	Kinetics of CO <sub>2</sub> – biphasic DPA and DMCA	75
4.7	DPA precipitation phenomena	79
4.8	Enthalpic study of DPA and DMCA solutions	80
4.9	Mixtures of DPA and DMCA	82
4.9.1	Regeneration temperature	82
4.9.2	Influence of amine concentration	83
4.9.3	Influence of activator to tertiary amine ratio	85
4.9.4	Performance comparison with commercial mixed alkanolamine	88
4.9.5	Solvent degradation	91
4.9.5.1	Thermal degradation	91
4.9.5.2	Oxidative degradation	92
4.10	Extractive regeneration	97
4.10.1	Concept and solvent selection	97
4.10.2	Inert solvent performance	99
4.10.3	Inert solvent recovery	103
4.11	Exploration for new amine	105
4.11.1	Primary amines screening	105
4.11.2	Secondary amines screening	107
4.11.3	Tertiary amines screening	109
4.11.4	Lipophilic Amine Screening Summary	112
<b>CONCLUSIONS AND OUTLOOK</b>		<b>119</b>
<b>REFERENCES</b>		<b>121</b>

## List of Figures

Fig. 1: CO <sub>2</sub> removal processes [39]	3
Fig. 2: CO <sub>2</sub> loading characteristic of physical and chemical solvent	4
Fig. 3: Ideal solution	11
Fig. 4: Athermal solution	11
Fig. 5: Regular exothermic solution	11
Fig. 6: Regular endothermic solution	11
Fig. 7: Solvated solution	12
Fig. 8: Solvated, self associated and aqueous solution	12
Fig. 9: Solution with Upper critical temperature (A), lower critical temperature (B), upper and lower critical temperature (C)	12
Fig. 10: Double stirred-cell unit	20
Fig. 11: Absorption unit	21
Fig. 12: Absorption bubble column	21
Fig. 13: Capillary reactor	22
Fig. 14: Gas-liquid reactor	23
Fig. 15: Viscometer unit	24
Fig. 16: Extraction reactor	24
Fig. 17: Extraction unit	25
Fig. 18: Amine screening unit	25
Fig. 19: Hexylamine-water solubility equilibrium	30
Fig. 20: CO <sub>2</sub> absorption curve into hexylamine-water solvent	30
Fig. 21: Concept of biphasic amine solution application for CO <sub>2</sub> absorption	33
Fig. 22: Thermomorphic liquid phase separation phenomena ( $T_1 < T_2 < T_3$ )	34
Fig. 23: 2-methylcyclohexylamine precipitation (4.3M)	35
Fig. 24: CO <sub>2</sub> – biphasic amine absorption mechanism	35
Fig. 25: CO <sub>2</sub> absorption into homogeneous and biphasic dipropylamine solutions	37
Fig. 26: Regeneration of homogeneous and biphasic dipropylamine solutions	37
Fig. 27: Inductive effect range in an amine molecule	39
Fig. 28: Electronegativity of substituents groups	40
Fig. 29: DPA-H <sub>2</sub> O and DMCA-H <sub>2</sub> O solubility curves	45
Fig. 30: Solubility curve of ternary system DPA-DMCA-H <sub>2</sub> O (3.6 M amine)	46
Fig. 31: Thermomorphic liquid-liquid phase separation of CO <sub>2</sub> -loaded 3.6 M 1:2-DPA:DMCA	46
Fig. 32: CO <sub>2</sub> absorption into dipropylamine (DPA) (20mlN/min, 1atm CO <sub>2</sub> at 25°C)	47
Fig. 33: Dipropylamine (DPA) precipitation	47
Fig. 34: Dipropylamine (DPA) regeneration characteristics	48
Fig. 35: CO <sub>2</sub> absorption into dimethylcyclohexylamine (DMCA) (20mlN/min, 1atm CO <sub>2</sub> at 25°C)	49
Fig. 36: Dimethylcyclohexylamine (DMCA) regeneration characteristics	49
Fig. 37: Density of DPA-H <sub>2</sub> O and DMCA-H <sub>2</sub> O conjugate solutions	51
Fig. 38: Kinematic viscosity of DPA-H <sub>2</sub> O and DMCA-H <sub>2</sub> O conjugate solutions	52
Fig. 39: CO <sub>2</sub> physical solubility into DPA-H <sub>2</sub> O and DMCA-H <sub>2</sub> O conjugate solutions	53
Fig. 40: CO <sub>2</sub> -aqueous DPA concentration profile (254 mol m <sup>-3</sup> DPA at 40°C)	57
Fig. 41: CO <sub>2</sub> -aqueous DPA loading curve (254 mol m <sup>-3</sup> DPA at 40°C)	59
Fig. 42: CO <sub>2</sub> -aqueous MEA concentration profile (254 mol m <sup>-3</sup> MEA at 40°C)	59
Fig. 43: CO <sub>2</sub> -aqueous DMCA concentration profile (80 mol m <sup>-3</sup> DMCA at 40°C)	60
Fig. 44: CO <sub>2</sub> -aqueous DPA loading curve (254 mol m <sup>-3</sup> DPA at 40°C)	62
Fig. 45: CO <sub>2</sub> -aqueous MDEA concentration profile (80 mol m <sup>-3</sup> MDEA at 40°C)	62
Fig. 46: CO <sub>2</sub> -DPA concentration profile (3000 mol m <sup>-3</sup> DPA at 40°C)	63
Fig. 47: Loading of CO <sub>2</sub> in 3000 mol m <sup>-3</sup> aqueous DPA at 40°C	64
Fig. 48: Loading of CO <sub>2</sub> in 3000 mol m <sup>-3</sup> aqueous DMCA at 40°C	65
Fig. 49: Concentration profile in bulk phase aqueous phase DMCA ( $P_{CO_2} < 25kPa$ )	66

Fig. 50: Concentration profile in bulk phase organic phase DMCA ( $P_{CO_2} < 25\text{kPa}$ ) .....	67
Fig. 51: Concentration profile in bulk phase homogeneous DMCA solutions ( $P_{CO_2} > 25\text{kPa}$ ) .....	68
Fig. 52: Pressure profile of CO <sub>2</sub> – organic phase DPA.....	70
Fig. 53: Pressure profile of CO <sub>2</sub> – organic phase DMCA.....	70
Fig. 54: Danckwerts plot of CO <sub>2</sub> – pure DPA system 3500-7500 mol/m <sup>3</sup> at 40°C .....	71
Fig. 55: Danckwerts plot of CO <sub>2</sub> – DPA-H <sub>2</sub> O system 3200-6500 mol/m <sup>3</sup> at 40°C .....	71
Fig. 56: Danckwerts plot of CO <sub>2</sub> – DMCA-H <sub>2</sub> O system 6200-6800 mol/m <sup>3</sup> at 40°C.....	72
Fig. 57: Danckwerts plot of CO <sub>2</sub> – DPA system 0-300 mol/m <sup>3</sup> at 40°C.....	73
Fig. 58: Danckwerts plot of CO <sub>2</sub> – DMCA system 0-80 mol/m <sup>3</sup> at 40°C.....	73
Fig. 59: Danckwerts plot of CO <sub>2</sub> – MEA system 0-300 mol/m <sup>3</sup> at 40°C.....	74
Fig. 60: Danckwerts plot of CO <sub>2</sub> – DEA system 0-80 mol/m <sup>3</sup> at 40°C .....	74
Fig. 61: Flow map of CO <sub>2</sub> – organic phase – aqueous phase DPA in 2.3 mm glass capillary .....	76
Fig. 62: Flow patterns of CO <sub>2</sub> -organic phase DPA-aqueous phase DPA (1 scale = 10 mm) .....	76
Fig. 63: CO <sub>2</sub> loading profile in liquid phases in a capillary reactor (40 mLN/min CO <sub>2</sub> ).....	77
Fig. 64: CO <sub>2</sub> loading profile in liquid phases in a capillary reactor (elevated CO <sub>2</sub> flowrate) .....	78
Fig. 65: DPA-H <sub>2</sub> O-CO <sub>2</sub> precipitation diagram .....	79
Fig. 66: DPA-DMCA-H <sub>2</sub> O-CO <sub>2</sub> precipitation diagram.....	80
Fig. 67: CO <sub>2</sub> partial pressure at elevated temperature .....	81
Fig. 68: Regeneration characteristics of 2.5N DPA solutions at elevated temperature .....	83
Fig. 69: DPA-DMCA absorption characteristics with concentration increase.....	84
Fig. 70: DPA-DMCA regeneration characteristics of with concentration increase .....	84
Fig. 71: Net capacity of 3 M - 1:2 DPA:DMCA with concentration increase.....	85
Fig. 72: DPA-DMCA absorption characteristics with amine ratio variation .....	86
Fig. 73: DPA-DMCA regeneration characteristics with amine ratio variation.....	86
Fig. 74: 3 M 1:3 – DPA:DMCA regeneration process at 70°C.....	87
Fig. 75: Absorption comparison: DPA-DMCA mixture with alkanolamine mixtures .....	88
Fig. 76: Regeneration comparison: DPA-DMCA mixture with alkanolamine mixtures .....	88
Fig. 77: Net capacity comparison: DPA-DMCA mixture with alkanolamine mixtures.....	89
Fig. 78: Theoretical absorption-regeneration operating lines of 3 M 1:3 - DPA:DMCA .....	90
Fig. 79: Theoretical comparison of 3 M 1:3 – DPA:DMCA to standard solvents.....	90
Fig. 80: 3M 1:3 – DPA:DMC repetitive absorption-regeneration performance .....	91
Fig. 81: Chromatogram of 3M DPA-H <sub>2</sub> O-O <sub>2</sub> system (overall).....	93
Fig. 82: Oxidative degradation product in 3M DPA-H <sub>2</sub> O-O <sub>2</sub> system (molecular weight fragments) .....	94
Fig. 83: Chromatogram of 3M DMCA-H <sub>2</sub> O-O <sub>2</sub> system (overall) .....	95
Fig. 84: Oxidative degradation product in 3M DMCA-H <sub>2</sub> O-O <sub>2</sub> system (molecular weight fragments) .....	95
Fig. 85: Extractive regeneration concept.....	97
Fig. 86: Extractive regeneration performance with various solvents ( $\alpha_{\text{initial}} = 0.8$ ) .....	100
Fig. 87: DPA and DMCA partition coefficient with various solvents ( $\alpha_{\text{initial}} = 0.8$ ) .....	101
Fig. 88: DPA and DMCA partition coefficient (with pentane) at temperature increase ( $\alpha_{\text{initial}} = 0.931$ ) .....	101
Fig. 89: Extractive regeneration using pentane at temperature increase ( $\alpha_{\text{initial}} = 0.931$ ) .....	102
Fig. 90: Extractive regeneration using pentane at various inert solvent at 40°C ( $\alpha_{\text{initial}} = 0.952$ ) .....	102
Fig. 91: Relux ratio dependent on number of stages.....	103
Fig. 92: Primary amines absorption (eq. 30%wt. DPA, 25°C) .....	106
Fig. 93: Primary amines regeneration (eq. 30%wt. DPA, 80°C) .....	106
Fig. 94: Secondary amines absorption (eq. 30%wt. DPA, 25°C).....	107
Fig. 95: Secondary amines regeneration (eq. 30%wt. DPA, 80°C) .....	109

---

Fig. 96: Tertiary amines absorption (eq. 30%wt. DPA, 25°C) .....	110
Fig. 97: Tertiary amines regeneration (eq. 30%wt. DPA, 80°C).....	110
Fig. 98: CO <sub>2</sub> absorption into cyclic structure tertiary lipophilic amines .....	111
Fig. 99: N-methylcyclohexylamine absorption characteristics.....	112
Fig. 100: N-methylcyclohexylamine regeneration characteristics.....	113
Fig. 101: Di-sec-butylamine absorption characteristics.....	113
Fig. 102: Di-sec-butylamine regeneration characteristics.....	114
Fig. 103: Absorption comparison with 3M lipophilic amine solutions at 40°C.....	114
Fig. 104: Regeneration comparison with 3M lipophilic amine solutions.....	115
Fig. 105: CO <sub>2</sub> absorption into MCA-DSBA mixtures at various concentration (40°C, 1 bar CO <sub>2</sub> ) .....	116
Fig. 106: CO <sub>2</sub> absorption into 3 M MCA-DSBA at various amine ratio (40°C, 1 bar CO <sub>2</sub> ) .....	116
Fig. 107: Loading curve of 3M 1:3 MCA:DSBA at absorption and regeneration temperature.....	117
Fig. 108: Theoretical performance comparison of lipophilic amine solvent with standard alkanolamine .....	118

## List of Tables

Table 1: Industrial CO <sub>2</sub> removal purposes [53] .....	2
Table 2: Solution thermodynamical classification [84].....	10
Table 3: Standardisation of amine concentration determination.....	26
Table 4: Standardisation of BaCO <sub>3</sub> precipitation.....	27
Table 5: Standardisation of CO <sub>2</sub> loading in amine solutions.....	28
Table 6: Influence of secondary liquids presence in absorption processes [30] .....	32
Table 7: pK <sub>b</sub> values of amines in water at 25 °C (pK <sub>b</sub> , NH <sub>3</sub> = 4.79) [57] .....	39
Table 8: Base strength of amine with various alkyl structures .....	41
Table 9: Primary amines' boiling points [48] .....	43
Table 10: Secondary amines' boiling points [48] .....	43
Table 11: Secondary amines' boiling points [48] .....	44
Table 12: Density parameter constants refer to equation (24) .....	51
Table 13: Kinematic viscosity parameter constants refer to equation (25) .....	52
Table 14: Physical solubility parameter constants refer to equation (26) .....	53
Table 15: DPA equilibrium constant correlation refer to equation (42) .....	58
Table 16: Loading of CO <sub>2</sub> in 0.254 M Aqueous DPA at 40°C .....	58
Table 17: DMCA equilibrium constant correlation refer to equation (43) .....	61
Table 18: Loading of CO <sub>2</sub> in 80 mol m <sup>-3</sup> aqueous DMC at 40°C.....	61
Table 19: CO <sub>2</sub> - 3M DPA equilibrium constant correlation refer to equation (43).....	65
Table 20: CO <sub>2</sub> – biphasic 3MDMCA equilibrium constant correlation refer to equation (43) .....	68
Table 21: Kinetics parameters of organic phase lipophilic amines .....	72
Table 22: Kinetics parameters of aqueous lipophilic and alkanolamines .....	75
Table 23: CO <sub>2</sub> absorption rate at various flowrates of organic and aqueous phase DPA...	78
Table 24: Absorption enthalpy of CO <sub>2</sub> - lipophilic and alkanolamines .....	81
Table 25: Solubility parameters of various solvents [35] .....	99
Table 26: Heat duty for pentane recovery .....	104

## Nomenclature

a	Specific surface area	[m <sup>2</sup> m <sup>-3</sup> ]
	Parameter constants	[-]
A	Area	[m <sup>2</sup> ]
AMP	2-amino-2-methyl-1-propanol	
c	Constant	[-]
D	Diffusivity	[m <sup>2</sup> s <sup>-1</sup> ]
DEA	Diethanolamine	
DMCA	Dimethylcyclohexylamine	
DPA	Dipropylamine	
DSBA	Di-sec-butylamine	
E	Polarity parameter	[-]
f	Fugacity	[Pa]
g	Molar free Gibb's energy	[kg m <sup>2</sup> s <sup>-2</sup> mol <sup>-1</sup> ]
G	Gas component	
h	Molar enthalpy	[kg m <sup>2</sup> s <sup>-2</sup> mol <sup>-1</sup> ]
H, h	Henry constant	[mol m <sup>-3</sup> Pa <sup>-1</sup> ]
Ha	Hatta modulus	[-]
k	Kinetics constant	arbitrary
	Mass transfer coefficient	[m s <sup>-1</sup> ]
K	Equilibrium constant	arbitrary
	Viscometer correction constant	[-]
LL	Liquid-liquid phase transition time (2 to 1 phase or 1 to 2 phases)	
m	Reaction order	[-]
MCA	Methylcyclohexylamine	
MEA	Mono-Ethanolamine	
MDEA	Methyldiethanolamine	
N	Normal condition	
n	Quantity constant	[-]
P	Pressure	[Pa]
R	Hydrocarbon chain	

---

	Reaction rate	[mol m <sup>-3</sup> s <sup>-1</sup> ]
	Specific absorption rate	[mol m <sup>-2</sup> s <sup>-1</sup> ]
	Gas constant	[kg m <sup>2</sup> s <sup>-2</sup> mol <sup>-1</sup> K <sup>-1</sup> ]
Re	Reynolds number	[-]
s	Molar entropy	[kg m <sup>2</sup> s <sup>-2</sup> mol <sup>-1</sup> K <sup>-1</sup> ]
	Spreading coefficient	[kg s <sup>-2</sup> ]
Sc	Schmidt number	[-]
Sh	Sherwood number	[-]
T	Temperature	[K]
TPT	Thermomorphous phase transition temperature from 2 to 1 phase	[°C]
t	Time	[s]
U	Internal energy	[kg m <sup>2</sup> mol <sup>-1</sup> s <sup>-2</sup> ]
v	Molar volume	[m <sup>3</sup> mol <sup>-1</sup> ]
V	Volume	[m <sup>3</sup> ]
w	Weight fraction	[-]
X	Mole fraction	[-]

### Greek symbols

$\alpha$	CO <sub>2</sub> loading in liquid phase	[-]
$\delta$	Solubility parameter	[kg <sup>0.5</sup> m <sup>-0.5</sup> s <sup>-1</sup> ]
$\Delta$	Difference	
$\varphi$	Fugacity coefficient	[-]
$\Phi$	Liquid volume fraction	[-]
$\gamma$	Activity coefficient	[-]
$\nu$	Kinematic viscosity	[m <sup>2</sup> s <sup>-1</sup> ]
$\sigma$	Surface tension	[kg s <sup>-2</sup> ]
$\Omega$	Number of molecular configurations	[-]

**Superscript**

*	Equilibrium condition
0	Reference point
Mix	Mixture
n	Normalised condition

**Subscript**

0	Reference point
a	Aliphatic amine
A	Aqueous phase
B	Base
D	Dispersive interaction
G	Gas component
H	Hydrogen bonding interaction
i	Component
k	Constant
L	Liquid component
Mix	Mixture
O	Organic phase
P	Polarity interaction
V	Vaporisation

## 1 Introduction

Carbon dioxide, one of the green house gases, presents in atmosphere and many industrial processes streams, causing undesired effects to the systems. The nature of carbon dioxide molecule, which is relatively stable at normal temperature and pressure, causes less usage of chemical conversion to convert it into economically valuable compounds. Moreover the CO<sub>2</sub> removal from low concentration and mobile sources is more complex and costly. As a comparison, Air is composed of 380 ppm CO<sub>2</sub>, which is 100 fold lower than industrial flue gas stream [39]. Thus it is economically more feasible and reasonable to focus the researches on CO<sub>2</sub> removal from larger sources.

### 1.1 CO<sub>2</sub> removal background

The presence of CO<sub>2</sub> in process streams and its excessive amount in the atmosphere results in many undesired effects to the systems. Two of the most important calls for CO<sub>2</sub> removal are from environmental and chemical sectors.

#### 1.1.1 Global warming and energy sectors

Carbon dioxide shares the major part of green house gases such as methane (CH<sub>4</sub>), nitrous oxide (N<sub>2</sub>O), Chlorofluorocarbon and Ozone (O<sub>3</sub>) which are involved in human caused enhancement of the greenhouse effect [37]. These gases change the earth's energy balance by absorbing longwave radiation emitted from the earth's surface, preventing it from subzero temperature, which is -18 °C without their presence. The concentration of carbon dioxide in atmosphere has been increasing from industrial revolution era (1700) at about 280 to 380 ppm in 2005. Its gradual increase in atmosphere is believed to cause global climate change which calls for lower CO<sub>2</sub> emission requirement.

The energy sectors are the major contributor of the CO<sub>2</sub> emission where fossil fuels are burned to generate electricity and steam. Roughly 85% of commercial energy use domestically and globally relies on fossil fuel [58]. For power generation, coal is used more widely than any other fossil fuels. Even with the growing influence of natural gas to substitute coal, coal's share in electricity generation is still projected to reach about 44% in 2020, which is higher than today [31]. Thus the CO<sub>2</sub> removal from the flue gas will still be a major issue in couple of decades.

### 1.1.2 Chemical industry requirements

The separation of CO<sub>2</sub> from mixtures with other gases is a process of substantial industrial importance. The reasons and the degree of carbon dioxide removal are varied and depend on the final use of the treated gases [53]. Typical industrial CO<sub>2</sub> removal purposes are given in Table 1.

Table 1: Industrial CO<sub>2</sub> removal purposes [53]

<b>Reasons for CO<sub>2</sub> removal</b>	<b>Specifications</b>
<b>Poison to catalysts</b>	
NH <sub>3</sub> synthesis	5-10 ppm (vol.)
Hydrocracker	50-100 ppm (vol.)
Hydrodesulfurization	
<b>Recovery of CO<sub>2</sub> for subsequent process</b>	
Urea manufacture	98-99%
Liquid CO <sub>2</sub> and dry ice	83-99%
Secondary oil recovery	
<b>Fuel gas heating value (Btu improvement)</b>	
High CO <sub>2</sub> natural gas	1-3%
SNG from liquid hydrocarbons or coal	0.1-2%
<b>Adjustment of gas composition</b>	
Methanol synthesis	1%
Oxo synthesis	0.1-0.6%
Iron ore reduction (FIOR process)	1%
Fischer-Tropsch	1-2%
<b>Avoid solid CO<sub>2</sub> plugging in cryogenic plants</b>	
Nitrogen wash of NH <sub>3</sub> synthesis gas	1 ppm
Air separation plants	
Liquefied natural gas	50-150 ppm (vol.)
Expander hydrocarbon recovery plants	
<b>CO<sub>2</sub> removal for sour gas sweetening</b>	1-3%

Industrial processes are developed to utilize CO<sub>2</sub> for chemical reactions; however their consumption is far below emitted CO<sub>2</sub>.

## 1.2 CO<sub>2</sub> capture technologies

CO<sub>2</sub> capture technologies can be divided into four major processes. Their process flow diagrams are depicted in Fig. 1.

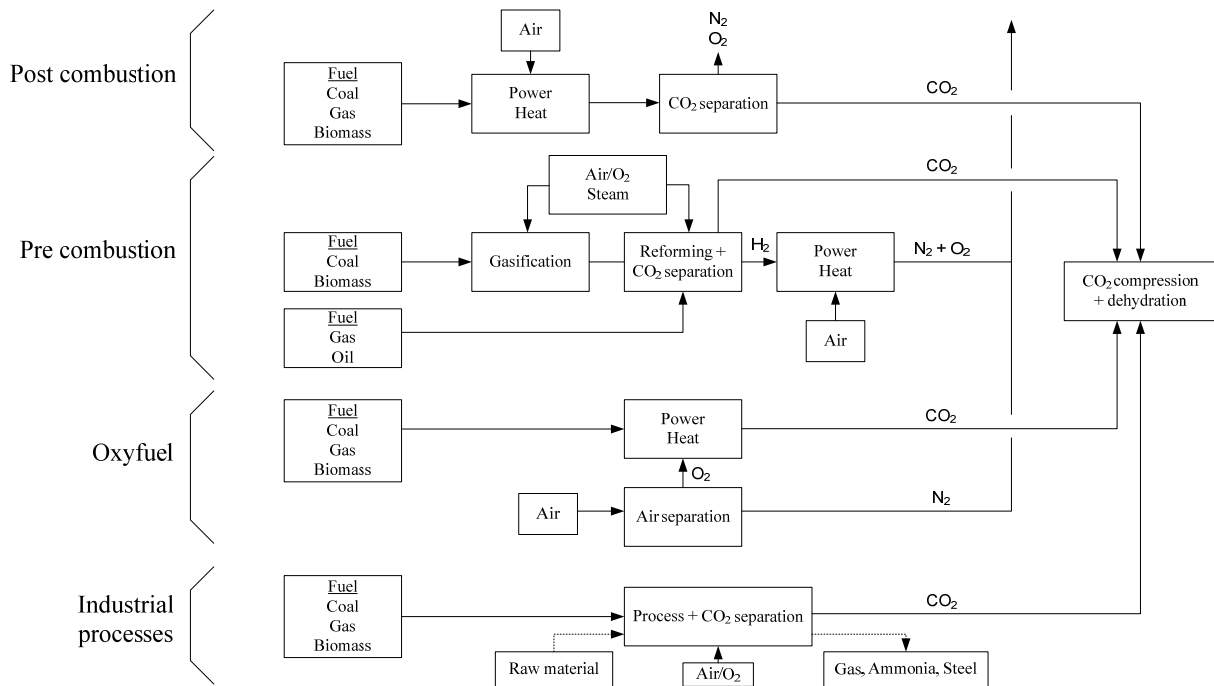


Fig. 1: CO<sub>2</sub> removal processes [39]

The process selection depends mainly on the flue gas characteristics such as CO<sub>2</sub> partial pressure, presence of other acid gases (SO<sub>x</sub>, NO<sub>x</sub>), content of hydrocarbon vapour, etc [58].

### 1.2.1 Post combustion capture

Post combustion capture refers to CO<sub>2</sub> capture from flue gas streams resulted from fuel combustion using aerial oxygen. Dependent on the fuel used, the flue gas contains mainly N<sub>2</sub>, steam, CO<sub>2</sub>, NO<sub>2</sub>, NO, SO<sub>2</sub>, SO<sub>3</sub>. The absorption using chemical or physical solvent is in fact most well developed technology for post combustion CO<sub>2</sub> removal.

The absorption processes are carried out by dissolving CO<sub>2</sub> into organic solvents or simultaneous absorption and reaction into aqueous base solutions designated chemical absorption. The process selection depends mainly on the inlet CO<sub>2</sub> partial pressure, degree of removal and also the energy requirement. The energy requirements are dependent mainly on

circulation rate, the temperature difference between the absorber and the regenerator and the degree of heat exchange and solvent chemistry.

### 1.2.1.1 Physical absorption processes

Processes designed based on pure physical absorption are more likely to be applicable when a high percentage of carbon dioxide is to be removed from high pressure gas. If the absolute carbon dioxide partial pressure is above 13.8 bar, the solvent process will generally tend to be more economical with respect to circulation rate than chemical solvent processes. This can be deduced from the equilibrium characteristic of physical solvent compare to chemical solvent as shown in Fig. 2.

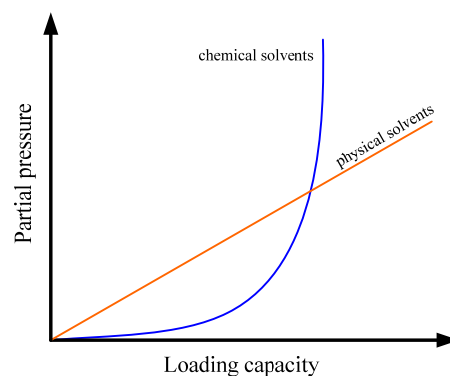


Fig. 2: CO<sub>2</sub> loading characteristic of physical and chemical solvent

At high available partial pressures of carbon dioxide the physical solvent system is capable of attaining a higher loading of the scrubbing solution and therefore will require lower solution circulation rates for the same degree of carbon dioxide removal. The price of solvents and their toxicity are also of important consideration.

The principal energy requirement is for circulating solution and refrigeration, since the solubility of carbon dioxide is greatly increased by operating less than ambient temperature. The typical operating condition is at high pressure (6.89-68.95 bar) and low temperature (313-373 K) [3]. Alcohol and polyalcohol are widely used as physical solvent. Some examples of physical absorption process are Allied Selexol process which utilizes polyethylene glycol as solvent, Fluor Solvent process which utilizes propylene carbonate, Lurgi Purisol process which utilizes n-methyl-2-pyrrolidone and Rectisol process which utilizes cold methanol as the solvent [53].

### 1.2.1.2 Chemical absorption processes

The chemical absorption method is effective to remove CO<sub>2</sub> at low partial pressure below 150mbar. For the chemical absorption process, the energy requirement is the decisive parameter to determine feasibility of the process. The principal energy requirement is heat to carry out the stripping, usually supplied in the form of low pressure steam. The heat energy requirement can be broken down into three components [43],[53]:

- Energy to heat the solution from temperature of absorber outlet entering the regenerator to reach reboiler temperature.
- Energy to reverse the chemical reaction between carbon dioxide and the active components in chemical solvent.
- Energy to provide a sufficient ration of steam to carbon dioxide leaving the top of regeneration column so that adequate driving force for stripping is provided.

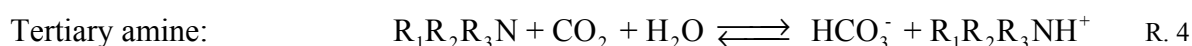
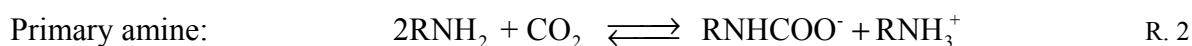
Most of the solvents applied in chemical absorption are inorganic alkalines or organic bases and their reactions with CO<sub>2</sub> are based on acid-base neutralisation reaction.

Among the used alkaline solution such as sodium carbonate, phosphate, borate, arsenite and phenolate, the potassium carbonate was the most extensively used with additional catalysts. Some aqueous alkaline processes were Catacarb process, Benfield process and Giammarco-Vetrocoke process which utilize aqueous potassium carbonate based on the reaction R. 1 [39].



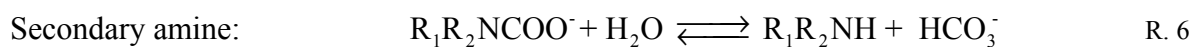
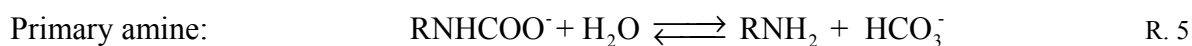
The absorption taking place at either ambient temperature or close to that required for regeneration of solution. Due to their low removal efficiency and high steam requirement (potassium is a stronger base than amines), aqueous alkaline processes have been largely superseded by newer developments.

Organic base being widely applied as solvent for chemical absorption is amine. Dependent on the amount of hydrogen substituent at the nitrogen atom, the amines are classified into primary, secondary and tertiary aqueous amine. Primary and secondary amines react with CO<sub>2</sub> based on alkanolamine solution based on the reactions R. 2, R. 3, R. 4.



The hydroxyl group of alkanolamine contributes to the solubility of entire molecule in water and high boiling point while the amino group contributes to the base strength required for the reaction with sour gas.

Some of the alkanolamine-based process utilize monoethanolamine (MEA), diethanolamine (DEA), triethanolamine, diglycolamine (DGA), diisopropanolamine (DIPA), methyldiethanolamine (MDEA) dissolved in water. MDEA known since 1950 is gradually displacing DIPA in these applications, however its use in industrial processes has only become important in recent years. Proprietary formulations comprising mixtures of the amines, usually based on MDEA, are widely used along with other additives [43]. Small amount of primary or secondary amines is added into aqueous MDEA as an activator to improve the reaction rate since tertiary amine has lower reaction rate than the primary and tertiary alkanolamines. Besides the corrosion problem due to usage of primary and secondary alkanolamine for carbon dioxide absorption, they lead to formation carbamate salts which are relatively stable. The stability of carbamate and low rate of their hydrolysis reactions R. 5, R. 6, as regeneration reaction of amine leads to high energy consumption [43].



Sterically-hindered amine is also introduced for CO<sub>2</sub> absorption due the selectivity consideration and also bulk alkyl groups lie close to amino group could instabilise carbamate leading to more effective carbon dioxide desorption . Study of carbon dioxide absorption using amine in nonaqueous solvents [81] as well as solid-immobilized amine [68], [86] was also investigated.

### 1.2.2 Pre-combustion processes

In pre-combustion process the fuel is first converted into synthetic gas by gasification or partial oxidation. The synthetic gas is furthermore reformed to yield hydrogen and carbon dioxide. Due to the high CO<sub>2</sub> concentration, it is removed normally using physical solvent prior to hydrogen combustion.

### 1.2.3 Novel CO<sub>2</sub> removal processes

A novel process utilising ammonia for absorption, designated chilled ammonia, was also introduced to overcome the high energy demand for CO<sub>2</sub> capture [60]. The process is operated at very low absorption temperature (2-16°C) to overcome ammonia loss. High concentration of ammonium carbonate / ammonium bicarbonate is obtained due to high CO<sub>2</sub> loading while the regeneration was carried out at least at 20 bar pressure to save the work contributed to compression prior to absorption.

Recent novel process introduced by Arlt et. al. utilises branched and hyperbranched polymer solutions, namely polyethers, polyesters and polyamines as physical and solvents for CO<sub>2</sub> absorbent. The solvents are proven to be CO<sub>2</sub> selective, have high loading and also flexible to tailor. The absorption enthalpy ranges from that of physical to chemical absorbent is a sign for lower regeneration energy requirement [63].

## 1.3 Project background

Aqueous amine solutions are widely used in CO<sub>2</sub> removal processes. Mixtures of primary or secondary with tertiary amines combine fast absorption rate of the former with the high absorption capacity of the latter [43]. The formation of stable carbamates by the reaction of primary and secondary amine with CO<sub>2</sub> has main disadvantage high energy demand for regeneration that the overall plant is considered as heat sink and they are also more corrosive. Approximately 30% loss of efficiency in coal-based power plant is contributed to the energy required for the post combustion CO<sub>2</sub> removal plant [62].

Thus, in the overall absorption process, not only the kinetics of reaction is important criterion, but also the amount of energy required to regenerate the loaded solution. In fact, current research emphasises the second criterion more than the first as solutions to a global energy and climate crisis make it more critical.

Several concepts have been investigated to circumvent the high energy demand, for example the application of sterically hindered amines or of solid activators [69], [86]. As a matter of fact, AMP (2-amino-2-methyl-1 propanol), the first sterically hindered amine discovered 24 years ago [67], which has a rate constant lower than its corresponding primary amine form, ethanolamine, due to steric effect is still very promising and is still being investigated today [16], [33], [20]. Low carbamate stability due to steric effect results in lower energy consumption for regeneration.

A novel solvent presented in this dissertation was investigated to circumvent the energy requirement. The new class of solvent investigated has thermomorphic (thermally induced) liquid-liquid phase transition during regeneration. The initial aqueous amine solutions might be single or biphasic dependent on their composition. The biphasic solution achieved homogeneous phase during absorption and becomes heterogeneous phase due to heating during regeneration. By promoting liquid-liquid phase separation during regeneration to recover regenerated amines in organic phase from the aqueous solution, the regeneration equilibrium can be displaced favourably. For this purpose, lipophilic amines of limited solubility in water were employed.

Taking advantage of the nature of equilibrium reaction, according to Le Chatelier's principle, the carbamate hydrolysis reaction can be enhanced by removing the regenerated amine from the aqueous reaction system by promoting phase separation. The reaction involving thermomorphic transition to multiphase system had been carried out in manufacturing of organic compounds involving homogeneous catalyst. Behr et.al. investigate deeply various operating schema of homogeneous catalyst recovery using thermomorphic system and employ it in manufacture of organic compounds [7],[9],[10],[11],[8]. By exploiting the solution entropy effect, the regeneration of the biphasic amine solution is expected to be carried out below temperature applied in industrial process. Thus it offers more degree of freedom for cost reduction.

## 2 Theoretical background

Thermodynamics study had been developed to predict the behaviour and possibility of liquid mixing. Among parameters used to characterize the behaviour of liquid mixing, enthalpy, entropy and free mixing energy are the most sophisticated besides volume of mixing. Indeed, these parameters are used to define types of solutions, as given in Table 2 and Fig. 3- Fig. 8 [84]

- $\Delta g^{\text{mix}}$  (free energy of mixing)  
→ Summary of energy barrier for obtaining mixing

$$\left(\frac{\partial g}{\partial p}\right)_T = v = \frac{RT}{P} \quad (1)$$

$$\Delta g_i^{\text{mix}}(P, T) = g_i - g_i^0 = RT \ln \frac{f_i}{f_i^0} \quad (2)$$

As for ideal condition: Fugacity of component-i in mixture at standard  $P_0$  and  $T$  equal to partial pressure of component-i ( $f_i = P_i$ ) and fugacity of pure component-i equal to total pressure ( $f_i^0 = P$ ). For non-ideal condition, the fugacity terms consist of fugacity coefficients  $\phi$  that can be transformed into activity coefficient term  $\gamma$  accordingly.

$$\Delta g_i^{\text{mix}}(P, T) = RT \ln \left( \frac{X_i \phi_i P}{\phi_i^0 P_0} \right) = RT \ln(X_i \gamma_i) \quad (3)$$

For total free energy of mixing is sum of all component molar free energy of mixing:

$$\Delta g^{\text{mix}}(P, T) = \sum_i^n X_i \Delta g_i^{\text{mix}}(P, T) = \sum_i^n RT X_i \ln X_i + \sum_i^n RT X_i \ln \gamma_i \quad (4)$$

$$\Delta g^{\text{mix}}(P, T) = \Delta g^{\text{ideal}}(P, T) + g^{\text{excess}} \quad (5)$$

The excess property terms summarize all non-ideality of the solution interaction.

Mixing favors negative free energy.

- $\Delta s^{\text{mix}}$  (entropy of mixing)  
→ Degree of randomness of solute-solvent molecular distribution in a continuum  
→ Mixing favors positive entropy of mixing

$$\Delta s^{\text{mix}} = R \ln \frac{\Omega_{\text{mixture}}}{\Omega_{\text{separate phases}}} \quad (6)$$

$\Omega_{\text{mixture}}$  : Number of forms in which a given number of molecules can be arranged in the mixture

$\Omega_{\text{separate phases}}$  : Number of forms in which the molecules of the mixture can be arranged that would constitute two phases

$$s = - \left( \frac{\partial g}{\partial T} \right)_p \quad (7)$$

$$\Delta s^{\text{mix}}(P, T) = - \sum_i^n R X_i \ln X_i - \sum_i^n R X_i \ln \gamma_i \quad (8)$$

▪  $\Delta h^{\text{mix}}$  (enthalpy of mixing)

→ Energy gap between interaction of same molecules (cohesive forces) with interaction between different molecules (adhesive forces) that can be measured experimentally.

→ Mixing favors negative enthalpy of mixing

$$\Delta h^{\text{mix}} = h_{\text{mixture}} - (h_{\text{solute}}^{\text{pure}} + h_{\text{solvent}}^{\text{pure}}) \quad (9)$$

$$\Delta h^{\text{mix}} = \Delta g^{\text{mix}} + T \Delta s^{\text{mix}} \quad (10)$$

▪  $\Delta v^{\text{mix}}$  (volume of mixing)

→ Shrinkage or volume expansion of the solution

$$\Delta v_{\text{mix}} = v_{\text{mixture}} - (v_{\text{solute}}^{\text{pure}} + v_{\text{solvent}}^{\text{pure}}) \quad (11)$$

Table 2: Solution thermodynamical classification [84]

Solution types	$\Delta V^{\text{MIX}}$	$\Delta H^{\text{MIX}}$	$\Delta S^{\text{MIX}}$	$\Delta G^{\text{MIX}}$
Ideal	0	0	$= -R \sum X_i \ln X_i$	$= RT \sum X_i \ln X_i$
Athermal	-	0	$< -R \sum X_i \ln X_i$	$> RT \sum X_i \ln X_i$
Regular -	-	-	$= -R \sum X_i \ln X_i$	$< RT \sum X_i \ln X_i$
Regular +	+	+	$= -R \sum X_i \ln X_i$	$> RT \sum X_i \ln X_i$
Solvated	-	-	$< -R \sum X_i \ln X_i$	$< RT \sum X_i \ln X_i$
Self-associated	+	+	$> -R \sum X_i \ln X_i$	$> RT \sum X_i \ln X_i$
Solvated, self associated, aqueous	0	+	$\approx -R \sum X_i \ln X_i$	$> -RT \sum X_i \ln X_i$

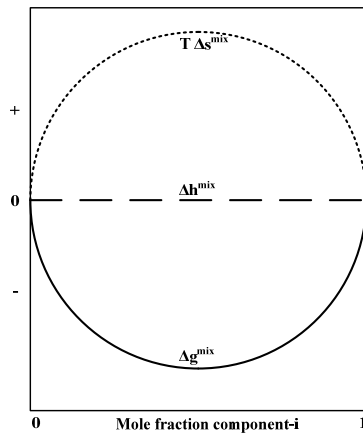


Fig. 3: Ideal solution

Ideal solution comprises solute and solvent molecules whose interaction among different molecules is similar to that of pure component. Ideal solution can be expected from mixture of similar size, non-polar, non-hydrogen bonding components.

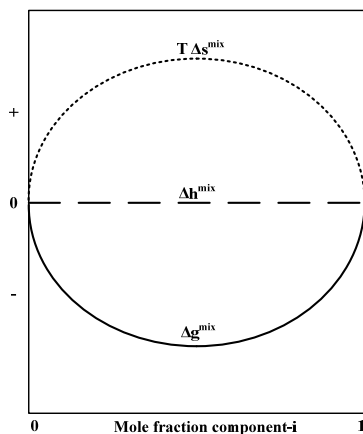


Fig. 4: Athermal solution

Athermal solution comprises solute and solvent molecules of different size that are more densely packed into non-random arrangement in a continuum than an ideal solution.

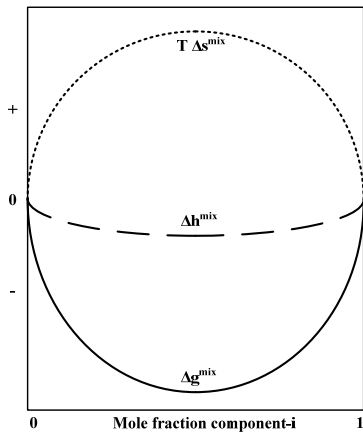


Fig. 5: Regular exothermic solution

Regular solution is designated for solution having small energy changes upon mixing that has no significant effect on  $\Delta h^{\text{mix}}$  and  $\Delta s^{\text{mix}}$ .

Regular exothermic solution comprises molecule with stronger adhesive than cohesive forces.

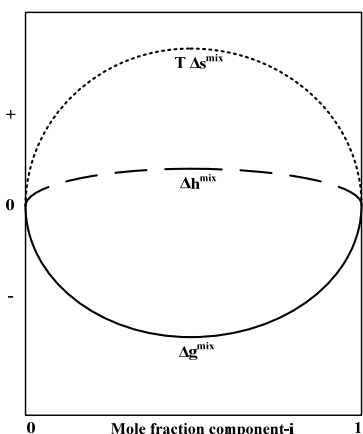


Fig. 6: Regular endothermic solution

Regular endothermic solution comprises molecules with similar size and non-identical but similar polarities, leading to stronger cohesive than adhesive forces.

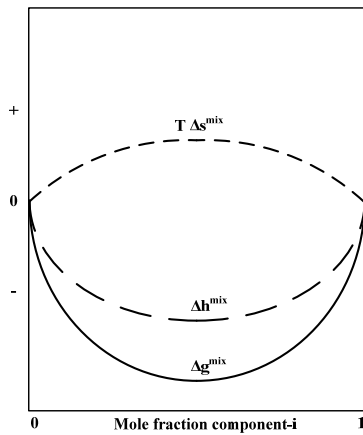


Fig. 7: Solvated solution

Solvated solution comprises molecules with stronger adhesive than cohesive interaction due to specific interaction between solute-solvent that doesn't exist in pure compounds, i.e. hydrogen bonding donor and acceptor mixture.

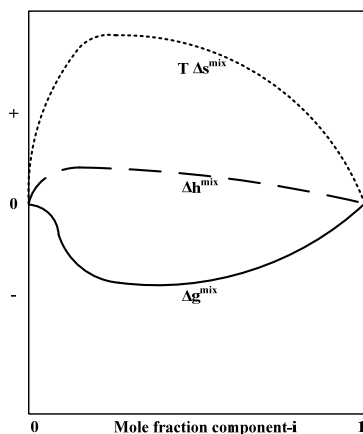


Fig. 8: Solvated, self associated and aqueous solution

One component of this solution can accept and donate hydrogen bond, the other can only donate or only accept or both.

Aqueous solution can be both self association ( $\Delta h^{\text{mix}} > 0$ ) or solvated ( $\Delta h^{\text{mix}} < 0$ ) and the outcome depends heavily on the types of solutes' functional groups.

As the result of all thermodynamic parameter contribution, several types of deviations from ideal solubility are found. Some solutions exhibit a miscibility gap where they are not completely miscible. Three basic types of deviations had been observed as follow.

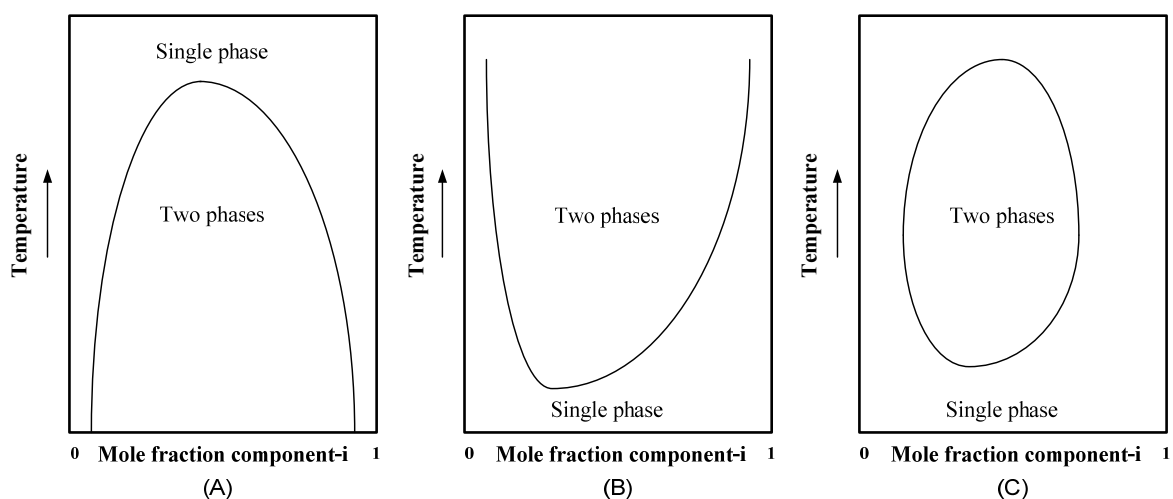


Fig. 9: Solution with Upper critical temperature (A), lower critical temperature (B), upper and lower critical temperature (C)

Solution with upper critical temperature exhibits phase splitting at lower temperature as at low temperature molecules move less intense than at high temperature and the nature of molecules to group within similar molecules prevails, leading to phase splitting. Solution with lower critical temperature achieved phase splitting at higher temperature. This indicates that the dissolution of solute in the solvent is induced by other interaction that that appears in their pure component. Increasing temperature will weaken this interaction thus phase splitting will occur after the interaction energy be overcome.

One may think that solution with upper and lower critical temperature will be less frequently found than the former two. In fact solutions with lower critical temperature will have upper critical temperature if the complete solubility can be achieved before achieving their boiling point. The thermodynamic approach can be used to explain partial miscibility behaviour.

Even though the thermodynamic properties of solutions discussed above can be used to predict mixing, it is time consuming to generate experimentally produced thermodynamic properties for multi component system with almost infinity possibilities of liquid combination. This drives engineers to use readily available parameters that are measured from pure components that can be used to predict their solubility with other components. Some of the parameters are Hildebrand's solubility parameter [5],[35], Hansen's solubility parameter [35], miscibility numbers (M-numbers) [32] and polarity parameter [59].

The solubility parameter of Hildebrand ( $\delta$ ) is defined as square root of cohesion energy as indicated in equation (12).

$$\delta = \left( \frac{\Delta U_v}{v_{\text{solvent}}} \right)^{1/2} = \left( \frac{\Delta H_v - RT}{v_{\text{solvent}}} \right)^{1/2} \quad (12)$$

$\Delta U_v$ ,  $\Delta H_v$  and  $v_{\text{solvent}}$  are molar energy, molar enthalpy of vaporization for a gas of zero pressure and molar volume of the solvent respectively. The enthalpy of vaporization is taking into account due to the fact that at boiling condition, all liquid inter and intra molecular forces are broken ( $\delta = 0$  for gas). As an analogy during mixing process the like molecules of each component in a mixture are separated from one another to an infinite distance comparable to what happens in vaporization process.

Literally  $\delta$  stands for the work necessary to separate the solvent molecules (i.e. disruption and reorganization of solvent-solvent interactions) to create a suitable sized cavity, large enough to accommodate the solute [59].

Accordingly, as a rule of thumb, good solvent for a certain non-electrolyte has  $\delta$  value close to that of solutes and they differ no more than 3.5 fold [5]. However by neglecting intermolecular interactions during determination of solubility parameter leads to exclusion for some applications. Some compounds having similar  $\delta$  are not miscible while compounds with large different  $\delta$  are completely miscible. The Hildebrand's solubility parameters provide an easy solubility prediction at a first glance. The work of Hildebrand had been developed by additional corrections that it is capable to predict solubility of highly non-ideal compounds such as electrolytes.

Hansen's solubility parameter was one of the solubility parameters developed based on Hildebrand's solubility parameter by considering more detail molecular forces: dispersion ( $\delta_D$ ), intra-permanent dipole forces ( $\delta_P$ ) and forces due to electron exchange: hydrogen bonding ( $\delta_H$ ) into a correlation [35]:

$$\delta^2 \approx \delta_D^2 + \delta_P^2 + \delta_H^2 \quad (13)$$

Another alternate approach for predicting mutual solubility of compounds is M-number (range 1-31), which is a measure of lipophilicity. Any pairs of compounds with M-number differ less than 15 units are miscible in all proportions at 25 °C [59]. Hansen solubility parameter is used later in investigation of inert solvent for extractive regeneration in this work.

As solubility of compounds related to their polarity, a useful empirical parameter for solvent polarity called polarity parameter ( $Z$ ) can be used. Polarity parameters are determined spectroscopically and furthermore it is normalized ( $E_T^n$ ) for a wider application. Their values range from 0-1 with water as most polar solvent being 1 and non-polar tetramethylsilane being 0 [59]. Extensive data sets of polarity parameter provide a good rough prediction of solubility.

Additional to the temperature dependent solution solubility, the reaction of CO<sub>2</sub> with amine is the decisive process for its industrial application.

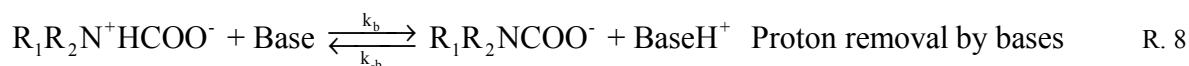
Absorption of CO<sub>2</sub> in amine solutions involves complex parallel reactions. The tertiary amine reacts according to base catalysed reactions with the presence of water [29] with the reaction R. 4:



The rate of reactions is given as:

$$R_{CO_2} = -k_2 [R_1R_2R_3N] [CO_2] \quad (14)$$

Several reaction mechanisms were proposed to describe reaction of CO<sub>2</sub> with primary and secondary amine solutions. Danckwerts [25] and Caplow [17] introduced zwitterions mechanism which involves two steps reactions:



Rate expression based on zwitterions mechanism is as follow:

$$R_{\text{CO}_2} = \frac{[\text{CO}_2][\text{R}_1\text{R}_2\text{NH}]}{\frac{1}{k_2} + \frac{k_{-1}}{k_2 \sum k_b [\text{B}]}} \quad (15)$$

Crooks and Donnellan [21] proposed termolecular (bases, amine and CO<sub>2</sub>) mechanism in single step where the rate of reaction is given as follow:

$$R_{\text{CO}_2} = (k_{\text{amine}} [\text{R}_1\text{R}_2\text{NH}] + k_{\text{H}_2\text{O}} [\text{H}_2\text{O}]) [\text{R}_1\text{R}_2\text{NH}] [\text{CO}_2] \quad (16)$$

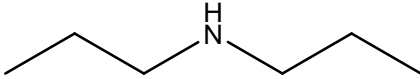
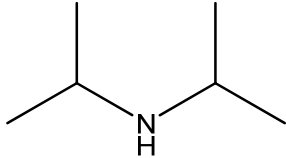
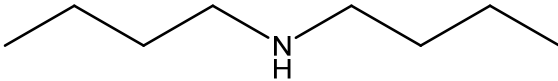
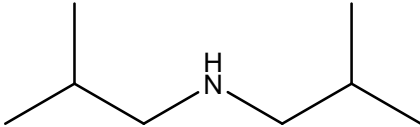
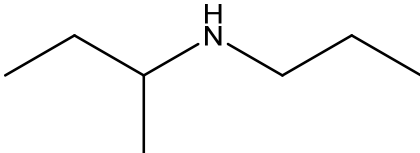
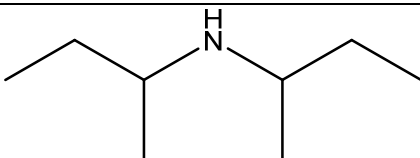
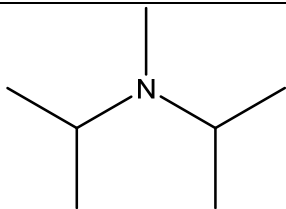
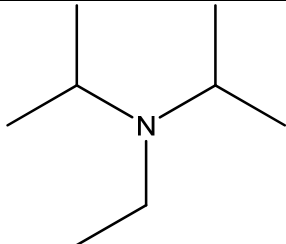
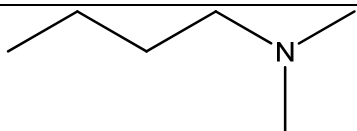
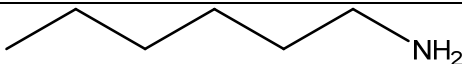
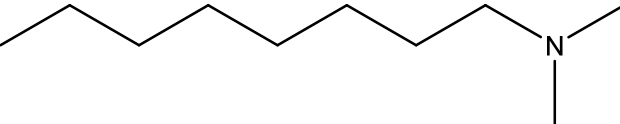
However the termolecular mechanism is unable to explain broken order of kinetics in non-aqueous solutions [81].

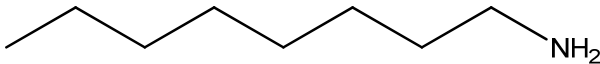
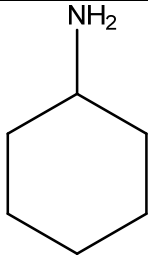
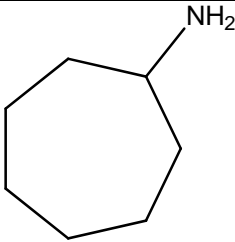
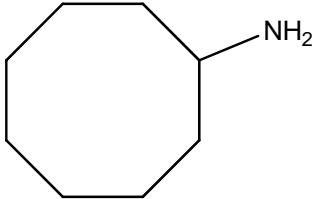
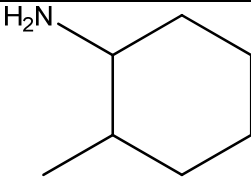
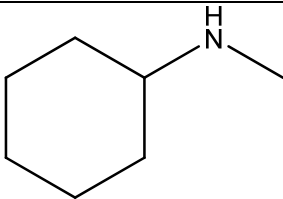
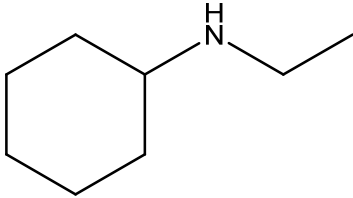
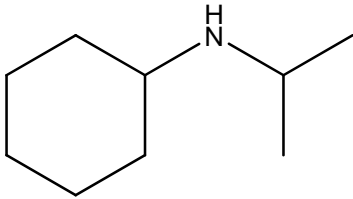
Additionally when the CO<sub>2</sub> reacts in aqueous amine solutions, reactions such as formation of carbonate, bicarbonate along with physical absorption of CO<sub>2</sub> occur.

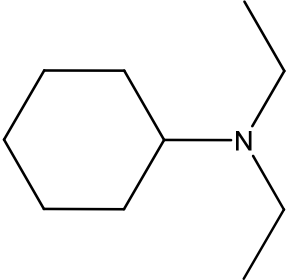
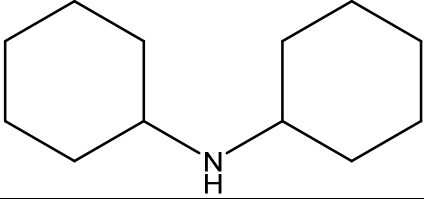
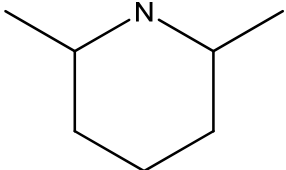
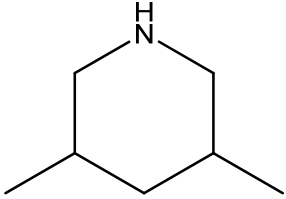
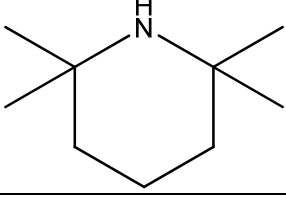
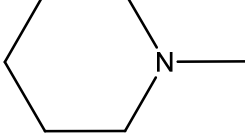
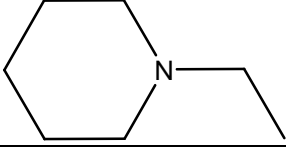
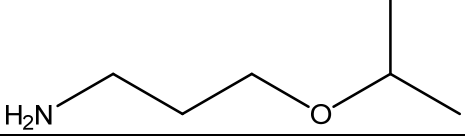
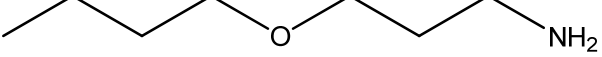
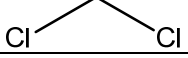
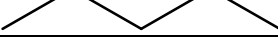
As the amine reacts with soluble CO<sub>2</sub>, all of these parallel complex reactions form reactive species in the solutions whose concentrations can not be determined in-situ. For determination of kinetic constants by numerical fitting of the integrated mass balances over all reactive species, the knowledge of the distribution of the chemical species is indispensable.

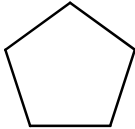
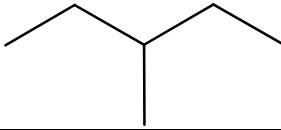
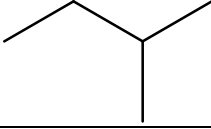
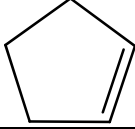
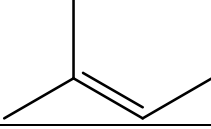
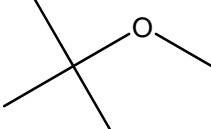
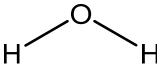
### 3 Experimental technique, chemicals and apparatuses

#### 3.1 Chemicals

Chemicals	CAS	Structure
Dipropylamine	142-84-7	
Diisopropylamine	108-18-9	
Dibutylamine	111-92-2	
Diisobutylamine	110-96-3	
Sec-butyl-n-propylamine	39190-67-5	
Di-sec-butylamine	626-23-3	
Di-isopropyl-methylamine	10342-97-9	
Di-isopropyl-ethylamine	7087-68-5	
Dimethylbutylamine	927-62-8	
Hexylamine	111-26-2	
Dimethyloctylamine	7378-99-6	

Chemicals	CAS	Structure
Octylamine	111-86-4	
Cyclohexylamine	108-91-8	
Cycloheptylamine	5452-35-7	
Cyclooctylamine	5452-37-9	
2-methyl-cyclohexylamine	7003-32-9	
Methyl-cyclohexylamine	100-60-7	
Ethyl-cyclohexylamine	5459-93-8	
Isopropyl-cyclohexylamine	1195-42-2	

Chemicals	CAS	Structure
Diethylcyclohexylamine	91-65-6	
Di-cyclohexylamine	101-83-7	
2,6-dimethylpiperidine	504-03-0	
3,5-dimethylpiperidine	35794-11-7	
Tetramethylpiperidine	768-66-1	
Methylpiperidine	626-67-5	
1-ethylpiperidine	766-09-6	
Isopropoxy-propylamine	2906-12-9	
Butoxy-propylamine	16499-88-0	
Dichlormethane	75-09-2	
Hexane	110-54-3	
Pentane	109-66-0	

Chemicals	CAS	Structure
Cyclopentane	287-92-3	
3-methylpentane	96-14-0	
2-methylbutane	78-78-4	
Cyclopentene	142-29-0	
2-methyl-2-butene	513-35-9	
Methyl-tert-butyl-ether	1634-04-4	
Carbon dioxide	124-38-9	$O=C=O$
Water	7732-18-5	

## 3.2 Apparatuses

Various apparatuses were used for experimental purposes. Here only the main apparatuses will be presented in detail.

### 3.2.1 Double stirred cell reactor

For determination of gas-liquid reactions kinetics parameters, vapour-liquid equilibrium, vapour-liquid-solid equilibrium and calorimetric data, the double stirred-cell reactor was used. The apparatus enables flexible and robust operation with good accuracy. Before conducting the reaction, the entire system was evacuated. Furthermore pure gas was kept at the same temperature as the desired reaction temperature and it was routed into the reactor once the solution is equilibrated.

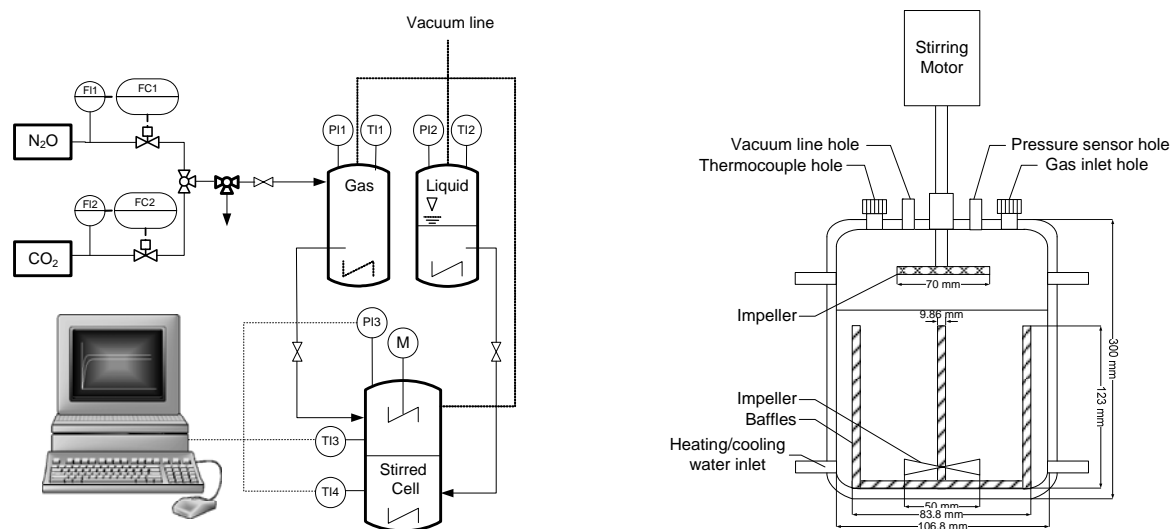


Fig. 10: Double stirred-cell unit

The pressure in the reactor was monitored and recorded using Labview<sup>TM</sup> software along with temperature of the reactor and fluid reservoir until equilibrium was achieved. The absorption rate could be calculated by solving mass balance of the gas phase to yield equation (17).

$$R_{\text{CO}_2} = -\frac{dP}{dt} \frac{V^{\text{gas}}}{RT} \quad (17)$$

### 3.2.2 Absorption unit

The absorption unit was used in vapour liquid equilibrium experiment. Carbon dioxide was mixed with nitrogen to provide exact partial pressure required. The flow of both gases was controlled by Bronkhorst<sup>TM</sup> precision valve up to one tenth mLN decimal precision. The mixed gas was routed into saturator which was kept at the same temperature as the absorption temperature. The wet mixed gas is introduced into 150 mL bubble column and the outgoing gas is analysed by gas chromatograph HP6890.

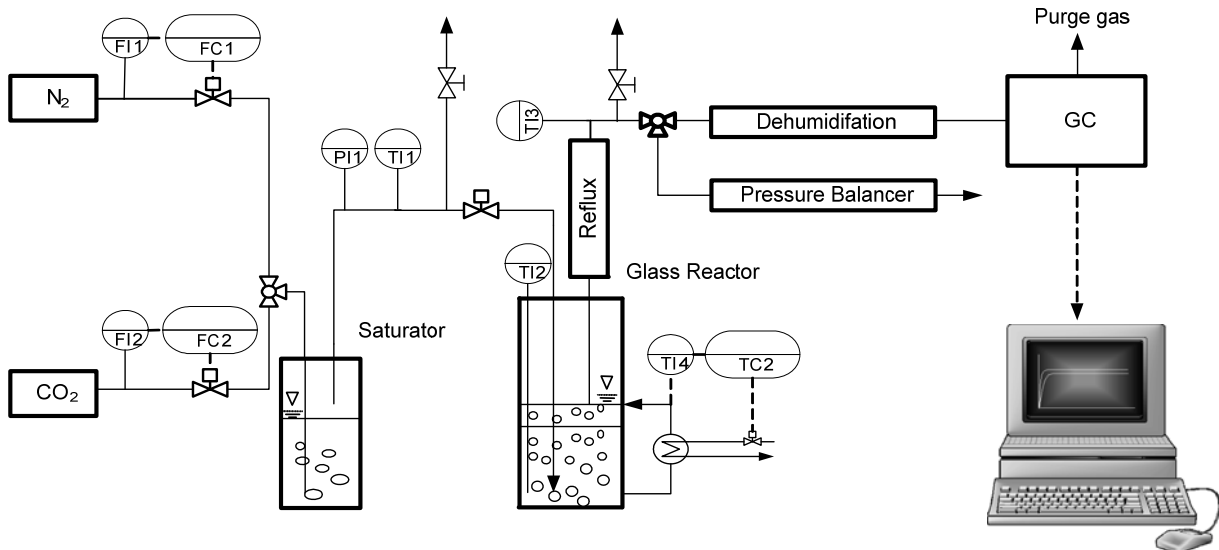


Fig. 11: Absorption unit

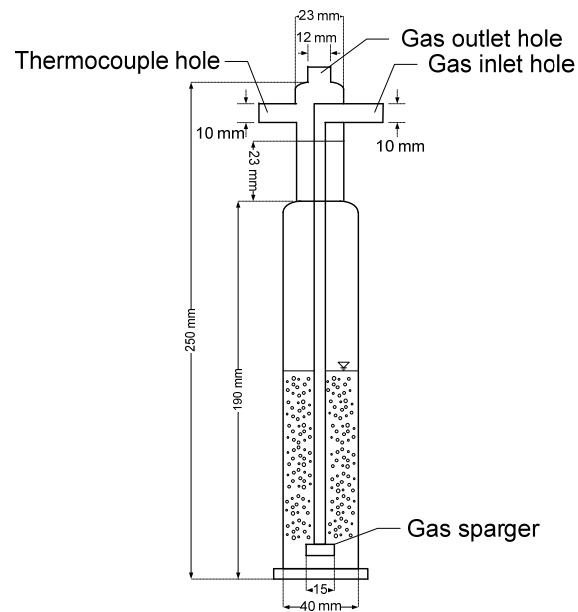


Fig. 12: Absorption bubble column

The absorption rate and liquid loading was obtained by solving the mass balance of the gas phase based on equation (18) and the liquid phase was analysed using gravimetric and titrimetric methods.

$$\frac{n_{\text{CO}_2 \text{ absorbed}}(t)}{n_{\text{amine}}} = \frac{\dot{n}_{\text{N}_2}}{n_{\text{amine}}} \int (Y_{\text{CO}_2 \text{ in}} - Y_{\text{CO}_2}(t)) dt \quad (18)$$

### 3.2.3 Capillary reactor

The glass milli-capillary reactor shown in Fig. 13 was used to investigate the gas-liquid-liquid absorption rate. It consists of 12 glass capillary segments which can be detached to fit the desired fluid residence time. The organic and aqueous liquid phases of the amine were introduced into the reaction by means of peristaltic pumps Reglo Digital MS-4/6-100 with flow rate range 0.002-43 mL/min.

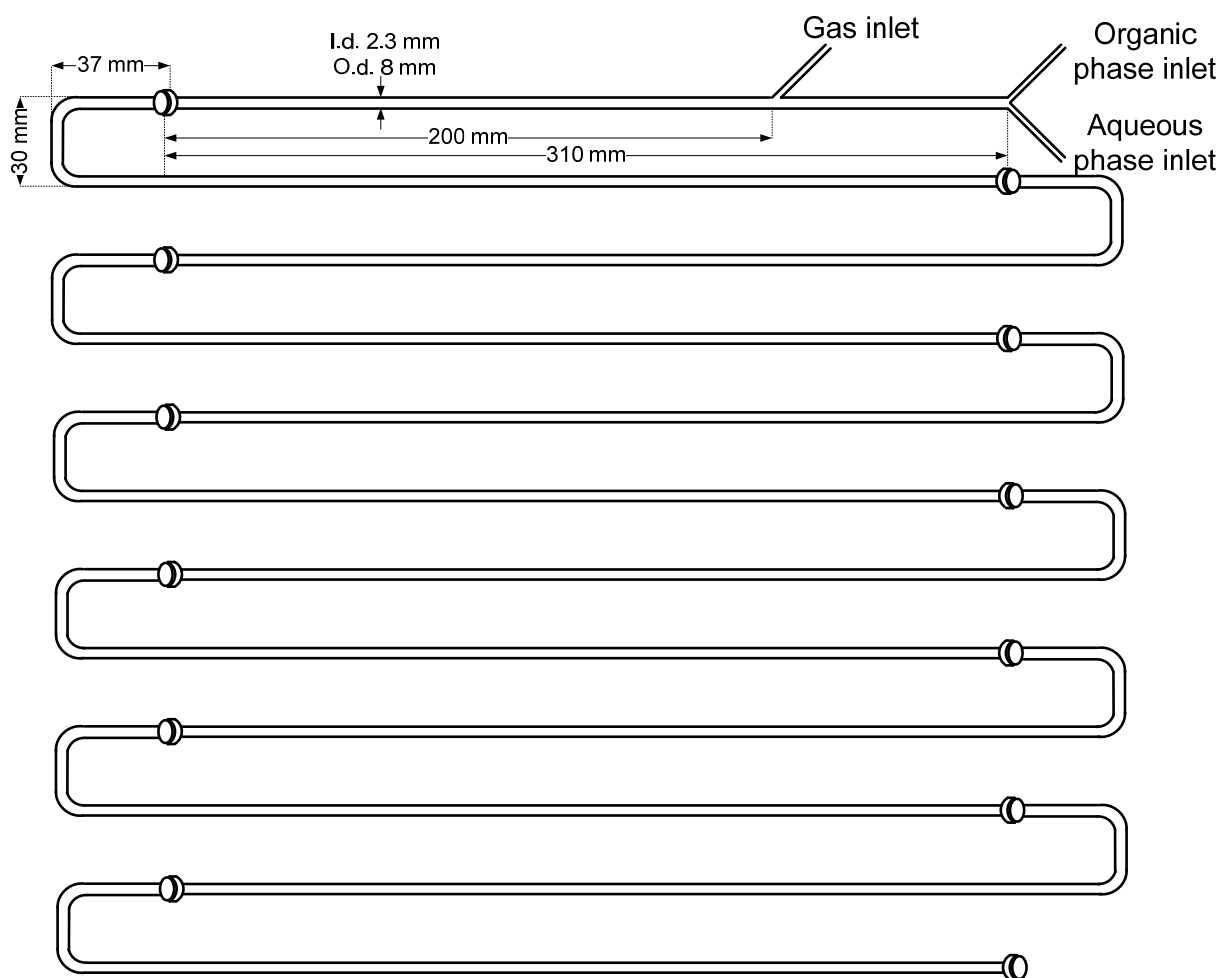


Fig. 13: Capillary reactor

The gas flow rate was controlled by Bronkhorst<sup>TM</sup> precision gas valve up to maximum 100mLN/min flowrate. The liquid aliquot was immediately separated from the remaining gas by flashing and it is immediately analysed for the amine concentration and CO<sub>2</sub> loading.

### 3.2.4 Gas-liquid reactor

The gas-liquid reactor was used in determining gas solubility in the amine solutions. Due to the relatively small reactor volume, the temperature of the reactor could be maintained homogeneous throughout the absorption process.

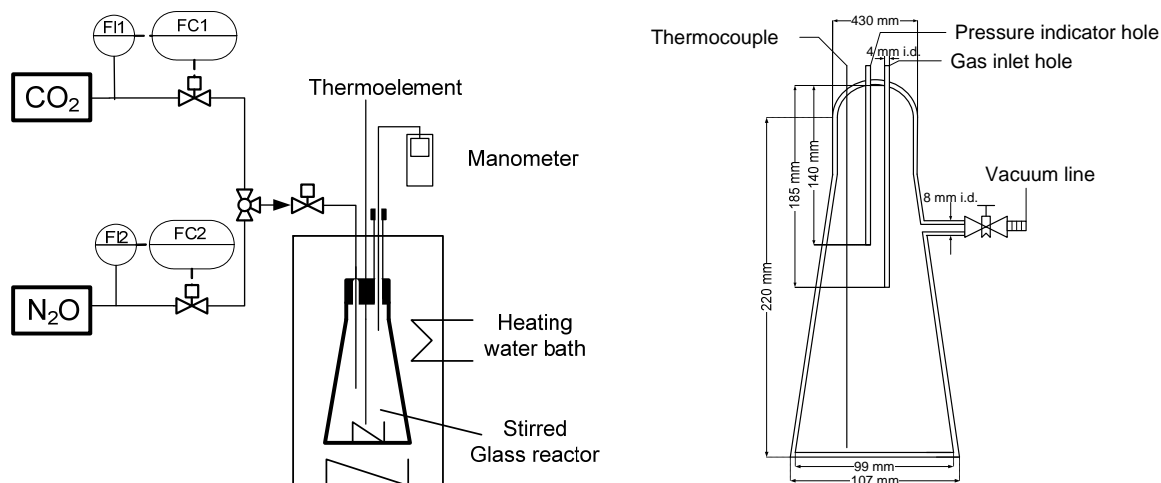


Fig. 14: Gas-liquid reactor

The glass reactor has 626.3 mL volume. The volume of the reactor occupied by gas phase was calibrated by experiments of solubility of CO<sub>2</sub> in water at temperature range 25-40°C [82]. Known amount of solution was charged into the glass reactor and vacuumed. The reactor was heated until vapour liquid equilibrium was achieved (indicated by constant values of pressure and temperature) and pure N<sub>2</sub>O was introduced slowly and absorption could be measured by decrease of pressure. Once the equilibrium pressure achieved, the nitrous oxide physical solubility could be calculated by solving mass balance to yield equation (19).

$$H_{\text{N}_2\text{O-Amine}} = \frac{(P^{\text{initial}} - P^{\text{equilibrium}})}{P^{\text{equilibrium}} RT} \frac{V_{\text{gas}}}{V_{\text{liquid}}} \quad (19)$$

### 3.2.5 Viscometer unit

Viscosities of the conjugate solutions were measured with capillary ubbelohde viscometer-I obtained from Schott<sup>TM</sup> as shown in Fig. 15. The temperature of the solutions was kept constant with a water bath. Additionally a light attenuation detector connected to the digital timer was applied to detect accurately the time elapsed for the surface of solutions to cross two measurement points.

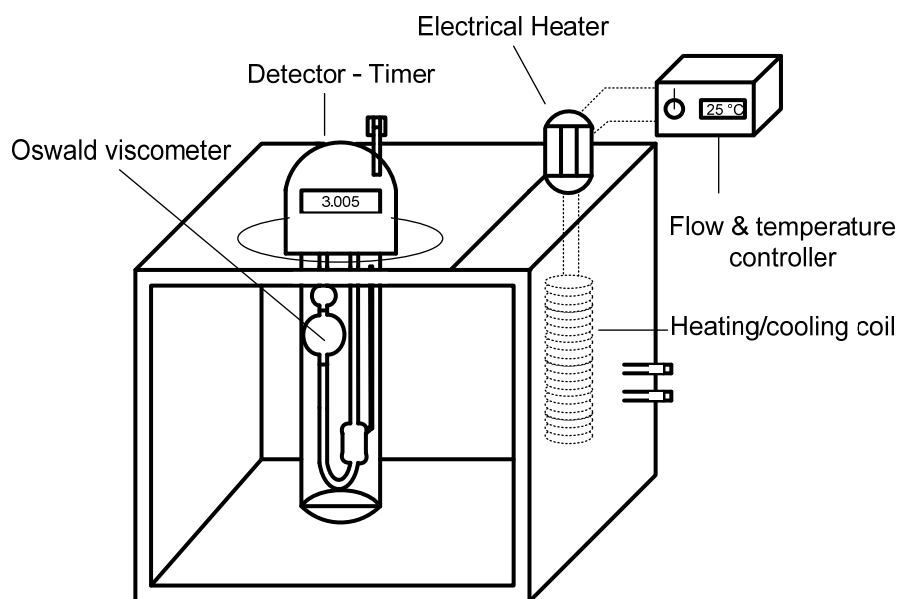


Fig. 15: Viscometer unit

Up to two decimals accuracy was expected from the detector. The viscometer was calibrated using bi-distilled water ranges from 25-80°C.

### 3.2.6 Extraction reactor

The extractor schema is given in Fig. 16. The extractor was made of double-wall glass and the temperature of the extraction was controlled using external thermostat. During extraction process the solution was stirred using external magnetic stirrer.

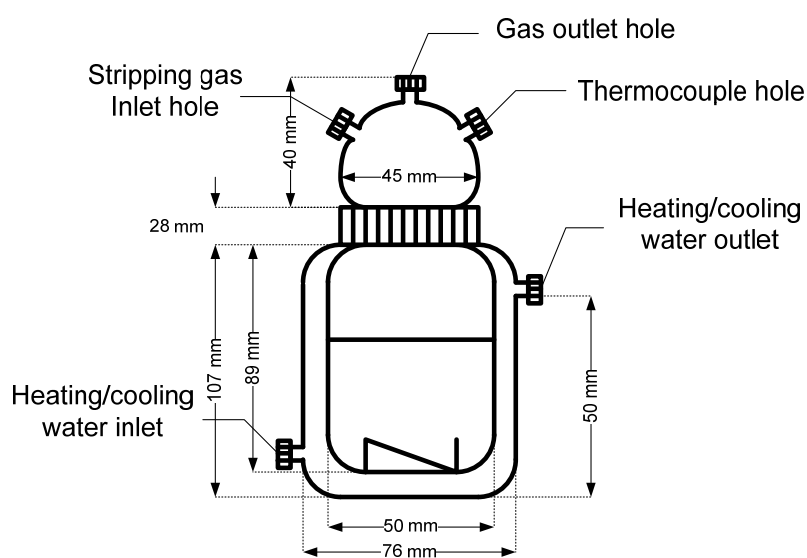


Fig. 16: Extraction reactor

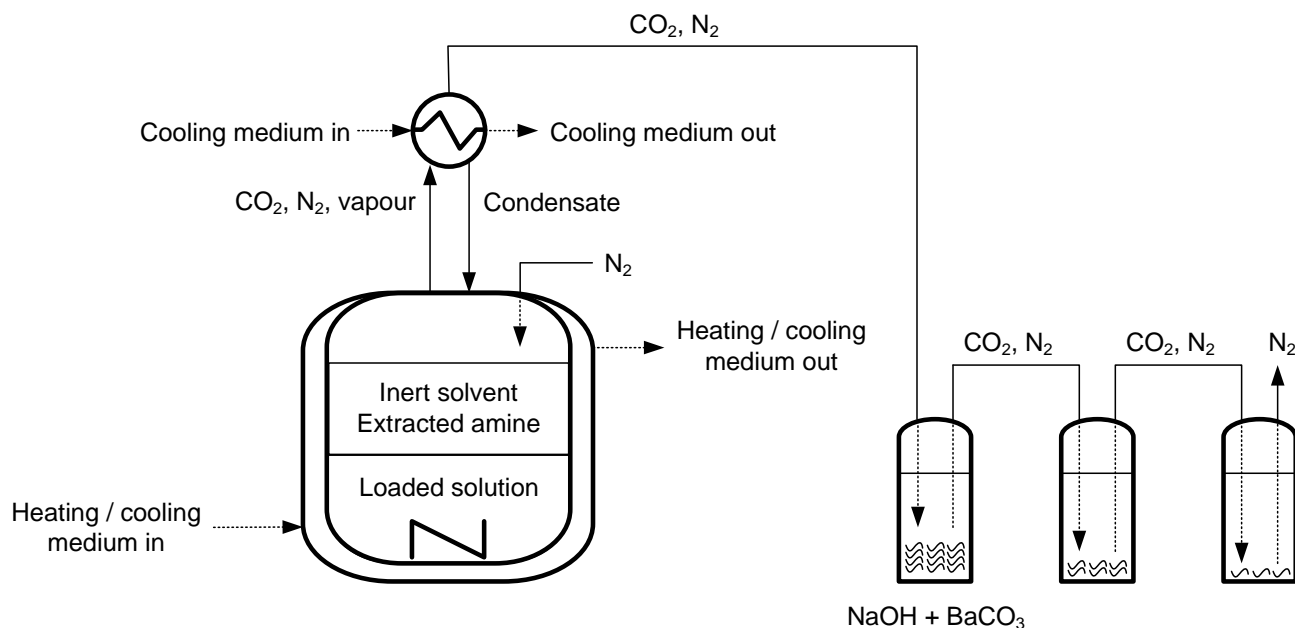


Fig. 17: Extraction unit

As shown in Fig. 17, the extraction reaction was equipped with CO<sub>2</sub> trap unit. The gas released during the reaction was stripped with inert nitrogen introduced above the surface of the liquid. The gas was routed into excess amount of NaOH and BaCl<sub>2</sub> mixture. The precipitated CO<sub>2</sub> as BaCO<sub>3</sub> were furthermore filtered and analysed using titrimetric method.

### 3.2.7 Amine screening unit

The amine screening unit is used for small scale absorption regeneration process. For absorption purpose, GL18 test tubes from Schott™ serves as the reactor and CO<sub>2</sub> was introduced into the reaction using 0.04 inch inner diameter PTFE capillary pipe. The absorption was carried out at 25°C using 20mLN/min CO<sub>2</sub> at atmospheric pressure. The amount of CO<sub>2</sub> absorbed was determined gravimetrically at an exact interval.

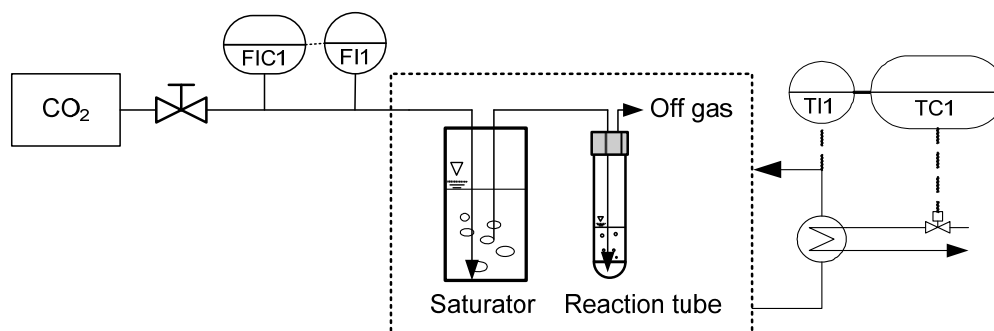


Fig. 18: Amine screening unit

Regeneration was done by heating the loaded solution from 40-90°C with 10°C interval. Upon heating the desorbed CO<sub>2</sub> was released in 10 and 5 minutes interval after the desired temperature in the solution was achieved. The amount of the desorbed CO<sub>2</sub> was determined gravimetrically. In order to avoid vapour loss, a porous cotton piece was placed on the top of each test tube as a drift eliminator. Control experiment using water-CO<sub>2</sub> system confirms the vapour loss problem could be overcome in this experiment.

### 3.2.8 Liquid phase analysis

Liquid aliquot of loaded solution is analysed to determine the CO<sub>2</sub> loading as well as amine concentration in the liquid. The total amine concentration of low concentration amine (aqueous phase of conjugate solution) was carried out by direct titration with 1N HCl up to the end point with methyl orange indicator. For high amine concentration, the amine concentration could not be determined by direct titration with HCl. This is due to the insolubility of amine in HCl before the end point of titration achieved. Thus a back-titration method was used. Excess amount of 1N HCl was introduced to neutralise aliquot having high amine concentration, resulting in homogeneous liquid phase. The mixture was then titrated with methyl orange indicator up to the end point. The amine concentration determination by titration method was validated using various amine solutions as well as pure amines. The results given in Table 3 were compared to the theoretical values, which are calculated assuming ideal solution.

Table 3: Standardisation of amine concentration determination

<b>Amines</b>	<b>MEA<sub>(aq)</sub></b>	<b>DPA<sub>(aq)</sub></b>	<b>DPA pure</b>	<b>DMCA pure</b>	<b>DSBA<sub>(aq)</sub></b>	<b>MCA<sub>(aq)</sub></b>	<b>MCA:DSBA 1:3<sub>(aq)</sub></b>
Theoretical [mol L <sup>-1</sup> ]	3.05	3.01	7.2	6.68	2.99	3.02	2.98
Titrimetric [mol L <sup>-1</sup> ]	3.03	3.02	7.2	6.68	3.02	3.03	3.01

A good agreement between theoretical and experimental values was obtained with various amines as well as pure DPA and DMCA amines. Thus the method was applied for determination of lipophilic amine concentration in the further study.

The amount of CO<sub>2</sub> in the liquid aliquot was also determined using standard precipitation as BaCO<sub>3</sub> method [40]. The aliquot was first treated with excess amount of 1N NaOH to convert all the CO<sub>2</sub> as bicarbonate and carbonate (R. 9). Under basic condition, the bicarbonate is converted to carbonate ion (R. 10).



Addition of BaCl<sub>2</sub> will precipitate the carbonate ion as BaCO<sub>3</sub> (R. 11).



Due to multiple steps including precipitation were taking place in the liquid sample analysis process, both reactions and precipitation process are checked to ensure the validity of the method. Moreover since the lipophilic amine DPA and DMCA are relatively strong base compare to conventional alkanolamines, the validity experiment is important. First, to ensure no error due to limitation of carbamate conversion to carbonate in NaOH-aliquot mixture, CO<sub>2</sub> from the treated aliquots were released by introducing high concentration HCl (37%wt.). The gas released was stripped with nitrogen into excess 1N NaOH – 0.1N BaCl<sub>2</sub> solutions. The BaCO<sub>3</sub> precipitate formed was analysed both gravimetrically and titrimetrically. This way, the CO<sub>2</sub> loading could be determined without carrying out the precipitation inside the aliquot itself. Both methods always give good agreement with deviation less than 3%.

The validity of sample precipitation as BaCO<sub>3</sub> by using mixture of 1N NaOH and excess 0.1N BaCl<sub>2</sub> was also checked using pure NaCO<sub>3</sub> and NaHCO<sub>3</sub>. Combined with the titrimetric method discussed above, the experiment shows a good agreement between experimental and theoretical values (calculated assuming all carbonate and bicarbonate are precipitated as BaCO<sub>3</sub>). The results are given in Table 4.

Table 4: Standardisation of BaCO<sub>3</sub> precipitation

<b>Samples</b>	<b>Theoretical mass of BaCO<sub>3</sub> [g]</b>	<b>Experimental mass of BaCO<sub>3</sub> in this work [g]</b>
1	0.020	0.020
2	0.050	0.049
3	0.121	0.099
4	0.297	0.296
5	0.499	0.493

Moreover the overall method applied in the experiment to determine CO<sub>2</sub> loading in amine solutions was validated with standard data in literature [77]. The obtained data for AMP system are given in Table 5.

Table 5: Standardisation of CO<sub>2</sub> loading in amine solutions

<b>AMP solutions</b>	<b>2 M</b>	<b>3 M</b>
CO <sub>2</sub> loading literature (20°C, 98.93 kPa CO <sub>2</sub> )	0.96	0.90
CO <sub>2</sub> loading in this work (20°C, 98.93 kPa CO <sub>2</sub> )	0.95	0.93

Thus the CO<sub>2</sub> loading determination in the further study was carried out with the method discussed above.

## 4 Results and discussion

### 4.1 Concept

The concept of CO<sub>2</sub> absorption by applying lipophilic amine solutions was developed by evaluating the solution characteristics in the absorption process. The mixture of lipophilic amine was found to have the characteristics of LCST (low critical solution temperature). Thus the amine solubility in water decreases upon temperature increase and liquid-liquid phase separation could be obtained upon heating. Several phenomena occurred in the absorption process, such as liquid-liquid phase transition and precipitation govern the conceptual absorption process.

#### 4.1.1 Absorption: homogeneous – regeneration: biphasic

The initial concept of aqueous lipophilic amine utilisation to absorb CO<sub>2</sub> starts from utilisation of homogeneous amine solution. As a test system, the mixture of hexylamine-water at the composition correspond to point S in Fig. 19 was applied for CO<sub>2</sub> absorption. The liquid mixture was initially homogeneous before absorption. However during the absorption process as depicted in Fig. 20, the solvent became biphasic as the liquid composition cross the miscibility gap in Fig. 19. Once the miscibility gap was crossed, the solution became homogeneous. It should be noted that the solubility equilibrium line in Fig. 19 corresponds to the hexylamine-water system without the presence of CO<sub>2</sub>. Thus it is only an approximation to explain the liquid-liquid phase transition during CO<sub>2</sub> absorption. The literal solubility equilibrium deviates from the hexylamine-water system due to the presence of amine reaction products with CO<sub>2</sub>.

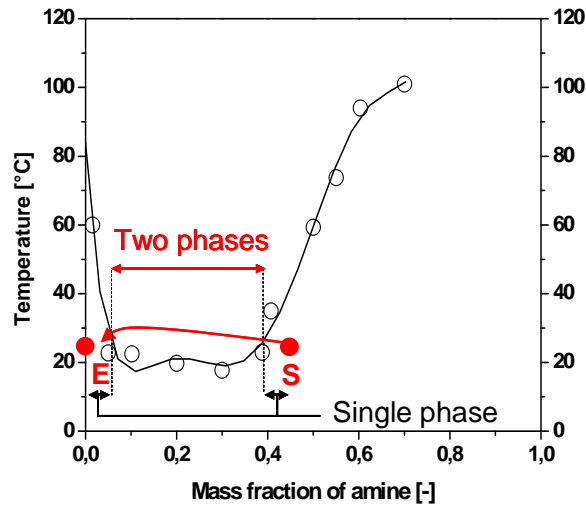
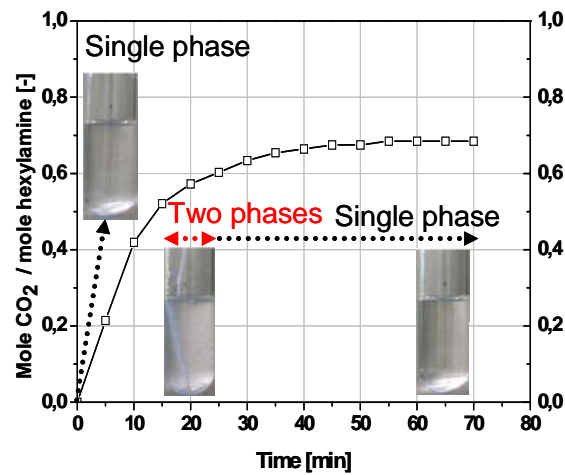


Fig. 19: Hexylamine-water solubility equilibrium

Fig. 20: CO<sub>2</sub> absorption curve into hexylamine-water solvent

Thus liquid-liquid phase transition from homogeneous to biphasic and vice versa took place despite the solution was initially homogeneous. Several disadvantages in application of homogeneous solutions are as follow:

- Complicated absorption process due to presence of two liquid-liquid phase transition
- High viscosity solution due to high amine concentration
- Precipitation due to high amine to water ratio
- Low driving force for thermomorphic liquid-liquid phase separation during regeneration

Precipitation is the most critical disadvantage in the homogeneous lipophilic amine solution. In extreme case, the reaction product with CO<sub>2</sub> formed stable precipitate. Thus the initial idea, which uses homogeneous solvent, was modified to direct usage of biphasic solvent.

#### 4.1.2 Absorption: heterogeneous – regeneration: biphasic

The practice of administering secondary liquid into a solvent in absorption process has been carried out for research and commercial purpose. Sharma studied the influence of presence of insoluble organic compound (2-ethyl hexanol) in bubble column during late 1960 [71]. In biological processes the addition of secondary organic liquid inside fermentors was also carried out. Since the rate of oxygen uptake for microbial fermentation is often the overall limiting step, the addition of secondary liquid, which has higher affinity towards oxygen than the affinity of medium-oxygen enhances the fermentation process [85].

Due to the addition of secondary liquid (organic), physical properties of liquid mixture such as density, viscosity, gas solubility and gas diffusivity change [30]. Moreover the mass transfer rate of dissolved gas across the boundary layer could be influenced. The outcome of addition the secondary liquid to the absorption process is contradictively varied in both reactive on non-reactive absorption system.

Three main mechanisms proposed for the change in mass transfer rates are as follow [30]:

- Formation of “gas-organic” complex

The components in the gas phase contact directly the secondary liquid (organic) phase to form “gas-organic” complex. The absorption process might be enhanced or altered dependent on the “gas-organic” interaction [14].

- Presence of “shuttle effect”

The components in the gas phase have higher affinity towards the secondary liquid (organic) and its droplets carry soluble gas components from the gas-liquid interface to the liquid bulk phase.

- Increase of turbulence or mixing in the gas-liquid boundary layer

The dynamic interaction of the organic droplet with the concentration boundary layer influences the turbulence in the boundary layer.

In terms of mass transfer at the boundary layer, two pathways are proposed [30]:

- Transfer in series: gas-aqueous phase transfer without direct gas-oil contact
- Transfer in parallel: both gas-oil and gas-aqueous phase transfer

Due to the complexity of the multiphase mass transfer involved in gas-liquid-liquid system, the attempts to quantify the effect of secondary liquid addition are done by analysing the overall liquid phase mass transfer ( $k_L$  and  $k_{L,a}$ ) and interfacial properties of the gas-organic-aqueous liquid system. The interfacial properties of the gas-organic-aqueous system

is expressed as spreading coefficient (S), which is interaction between phases in terms of surface tension defined in equation (20).

$$S_{OA} = \sigma_{AG} - (\sigma_{OG} + \sigma_{OA}) \quad (20)$$

The  $\sigma$  stands for surface tension, while the subscript G,O,A are gas, organic and aqueous phase respectively. The S value provides prediction whether the organic liquid forms droplets ( $S < 0$ ) or thin film ( $S > 0$ ) upon addition to aqueous phase.

The summary of the effects in terms of liquid phase mass transfer by considering the fraction of organic phase in the liquid ( $\Phi_{disp}$ ) and spreading coefficient are given in Table 6.

Table 6: Influence of secondary liquids presence in absorption processes [30]

Parameters	$k_L a$	a	$k_L$	System	Ref.
Presence of oil (global) $\Phi_{disp} \nearrow$	$\searrow$	$\nearrow$	$\searrow$	CO <sub>2</sub> – NaOH + 2-ethylhexanol	[71]
		$\nearrow$		CO <sub>2</sub> – NaOH + 2-ethylhexanol	[54]
		$\nearrow \searrow$		CO <sub>2</sub> – NaOH + toluene	[27]
	$\searrow$			O <sub>2</sub> – H <sub>2</sub> O + PFC40/77	[41]
	$\rightarrow$			O <sub>2</sub> – H <sub>2</sub> O + n-octane	[78]
$\Phi_{disp} \nearrow$	$\nearrow \searrow$			H <sub>2</sub> – H <sub>2</sub> O + n-octene	[46]
	$\searrow \nearrow$			CO <sub>2</sub> – K <sub>2</sub> CO <sub>3</sub> /KHCO <sub>3</sub> + toluene/n-dodecane/n-heptane/1-octanol	[19]
	$\searrow \nearrow$			O <sub>2</sub> – H <sub>2</sub> O + kerosene/paraffin/toluene/oleic acid	[85]
$S > 0$		$\nearrow$	$\searrow \nearrow$	O <sub>2</sub> – Na <sub>2</sub> SO <sub>3</sub> + n-alkanes/oleic acid	[49]
$\Phi_{disp} \nearrow$		$\rightarrow$		O <sub>2</sub> – H <sub>2</sub> O + PFC40	[52]
	$\nearrow \searrow$			O <sub>2</sub> – H <sub>2</sub> O + n-dodecane	[64]
$S < 0$	$\searrow$			O <sub>2</sub> – H <sub>2</sub> O + kerosene/paraffin/toluene/oleic acid	[85]
		$\searrow$	$\rightarrow$	O <sub>2</sub> – Na <sub>2</sub> SO <sub>3</sub> + n-alkanes/oleic acid	[49]
	$\Phi_{disp} \nearrow$	$\nearrow \rightarrow$			O <sub>2</sub> – Na <sub>2</sub> SO <sub>4</sub> + n-dodecane/n-hexadecane
$\searrow \nearrow \rightarrow$					

In the biphasic amine solvent, the organic phase containing high concentration of amine has higher affinity towards CO<sub>2</sub> than aqueous phase-CO<sub>2</sub> affinity. This can be deduced from the non-polar nature of CO<sub>2</sub>. In the further investigation, the CO<sub>2</sub> solubility in both organic and aqueous phase proved this prevalence.

In brief the biphasic liquid solvent was proposed for CO<sub>2</sub> absorption due to several reasons as follow:

- High absorption rate due to presence of high concentration amine in the organic phase
- High driving force for thermomorphic liquid-liquid phase separation during regeneration
- Avoidance of precipitation by providing sufficient amount of amine to water ratio

The concept applied in this study is to employ initially biphasic amine solution as depicted in Fig. 21. After CO<sub>2</sub> absorption the solution transform to homogeneous phase and upon heating in regeneration, the homogeneous loaded lipophilic amine solutions undergoes liquid-liquid phase separation. The thermally-induced liquid-liquid phase separation is designated thermomorphic liquid phase separation and it is due to the nature of lipophilic amine-water mixture whose solubility lower upon temperature increase.

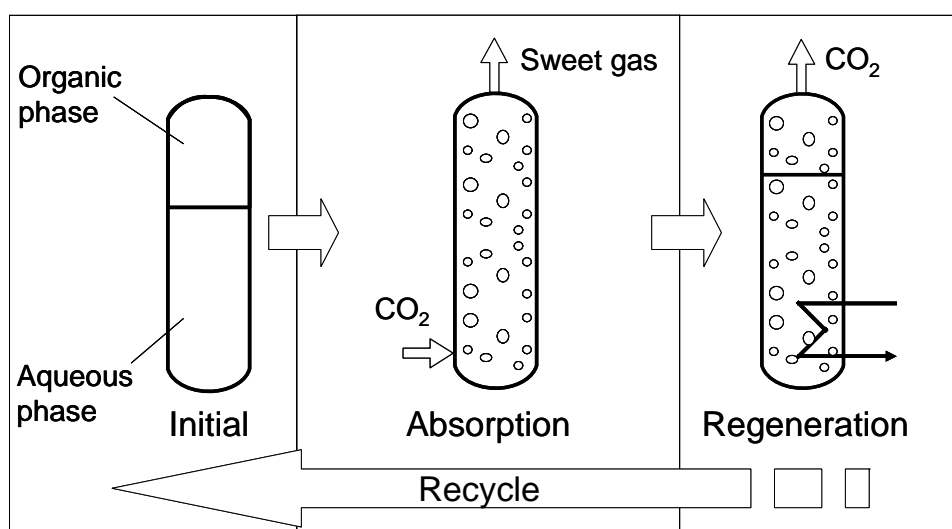


Fig. 21: Concept of biphasic amine solution application for CO<sub>2</sub> absorption

The solubility characteristics of amine in water at increase of temperature are depicted in Fig. 22. Literally the solubility of amine in water stabilised by hydrogen bonds formed upon mixing of amine with water ( $T_1$ ). The thermomorphic liquid phase separation is caused by breakage of of inter- and intra-molecular hydrogen bonds in amine-water solutions ( $T_2$ ). Once

the hydrogen bonds are broken, the self associate nature of water will push water out of the solution and the overall solution becomes biphasic (T<sub>3</sub>) [75],[86].

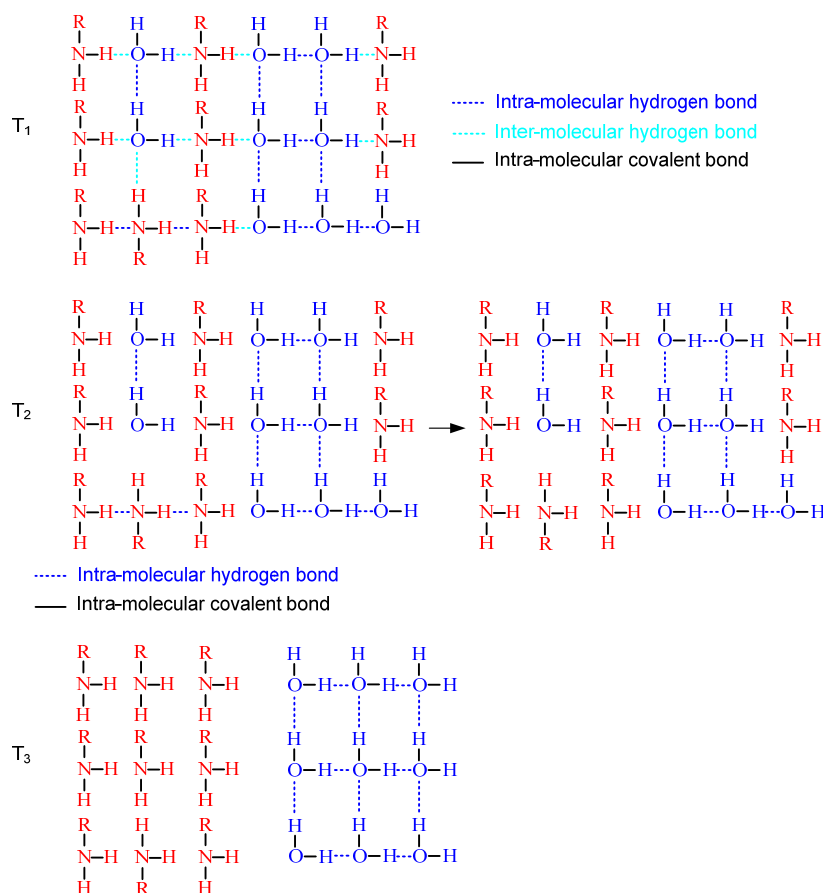


Fig. 22: Thermomorphic liquid phase separation phenomena ( $T_1 < T_2 < T_3$ )

The driving force for thermomorphic liquid phase separation could be maintained high with usage of initially biphasic amine solution and tertiary lipophilic amines, which are less soluble in water.

Added to the thermomorphic liquid separation, precipitation issue is crucial in the application of biphasic lipophilic amine solutions for CO<sub>2</sub> absorption. It was found during the amine screening process that even there's reasonable amount of amine to water ratio, precipitation still occurred in some lipophilic amines-water system. As an example, in the extreme case, the CO<sub>2</sub> absorption into mixture of 2-methylcyclohexylamine-water was followed by severe precipitation as depicted in Fig. 23.

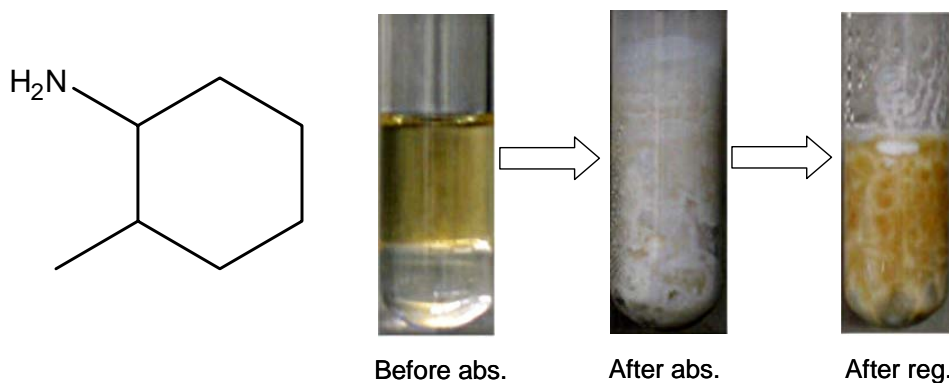
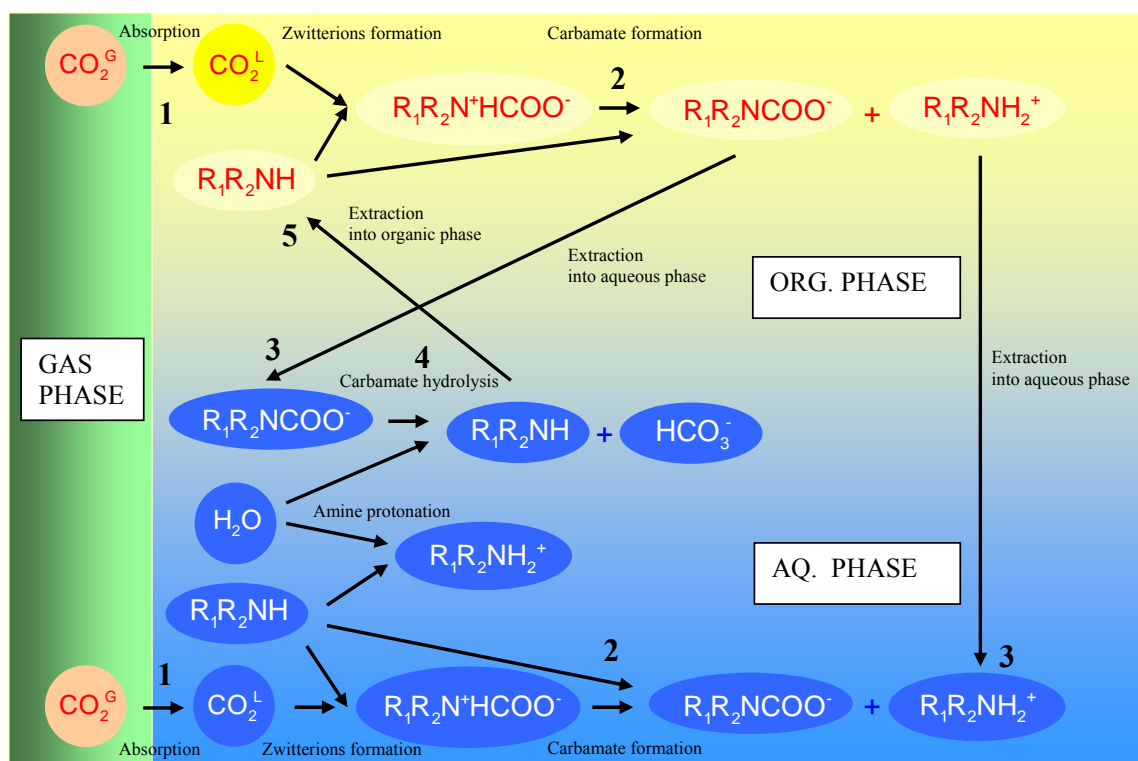


Fig. 23: 2-methylcyclohexylamine precipitation (4.3M)

Even upon heating up to 90°C, minor amount of the precipitate dissolved as liquid with very low degree of regeneration. Moreover once the temperature was brought down to room temperature, the precipitate remained solid. Thus selection of appropriate lipophilic amines for CO<sub>2</sub> absorption is very crucial.

#### 4.1.3 CO<sub>2</sub> absorption mechanism in biphasic amine solution

The schematic diagram of proposed absorption mechanism, which was validated in the experiment later, is given in Fig. 24. In this study both aqueous and organic phase are reactive.

Fig. 24: CO<sub>2</sub> – biphasic amine absorption mechanism

The CO<sub>2</sub> from gas phase will dissolve in both organic and aqueous phase (1) and react with amine in the respective phase to form carbamate and ammonium ions (2). As discussed before, due to the presence of high amine concentration in organic phase, the CO<sub>2</sub> absorption rate in organic phase is significantly higher than that in aqueous phase. The carbamate formed in organic phase as ionic species is extracted into aqueous phase along with the ammonium ion (3). The extracted carbamate is hydrolysed in aqueous phase due to the presence of high concentration water, leaving bicarbonate and free amine in water (4). The free amine which is nonpolar will be re-extracted back to the organic phase (5). The process occurs until the biphasic solvent transform to homogeneous solvent. In homogeneous solvent, only step (3) and (5) will be absent.

Regeneration process is simply reversal of the absorption process, which starts from homogeneous CO<sub>2</sub> loaded solution until it transform to biphasic solution. The regeneration temperature is highly dependent on the lipophilic amine used.

#### 4.1.4 Comparison of biphasic and homogeneous solvent for CO<sub>2</sub> absorption

An attempt to compare the performance of biphasic and homogeneous solution was done with N,N-dipropylamine solution. Dipropylamine was chosen to minimise the influence of water in the absorption process as the reaction of CO<sub>2</sub> with secondary and primary amine takes place even under water absence. For this purpose 90 mmol dipropylamine (correspond to 25 mL 3.6 M dipropylamine) was used. As solubilisation agent the 1,4-butanediol was used as it was found to be able to solve the solution at minimum amount compare to other alcohols. Moreover it is chemically inert and its CO<sub>2</sub> solubility under experimental condition is low. The volume of both solutions was kept the same to minimise the error due to volumetric effect because physical absorption takes place along with chemical absorption and physical absorption is highly volume dependent. The absorption result carried out with 20% CO<sub>2</sub>, 300 mLN/min is shown in Fig. 25.

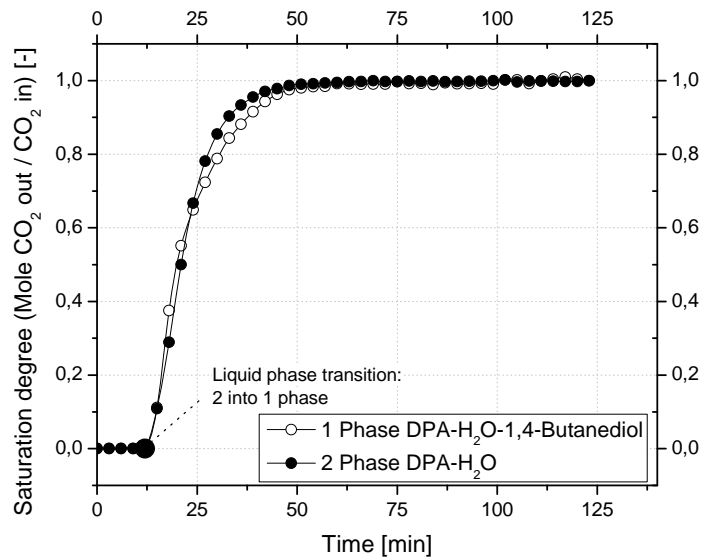


Fig. 25: CO<sub>2</sub> absorption into homogeneous and biphasic dipropylamine solutions

Comparable CO<sub>2</sub> absorption rate and capacity were observed in both homogeneous and biphasic solutions. During absorption the biphasic solvent transform to homogeneous liquid. Thus both loaded solution were initially homogeneous during regeneration.

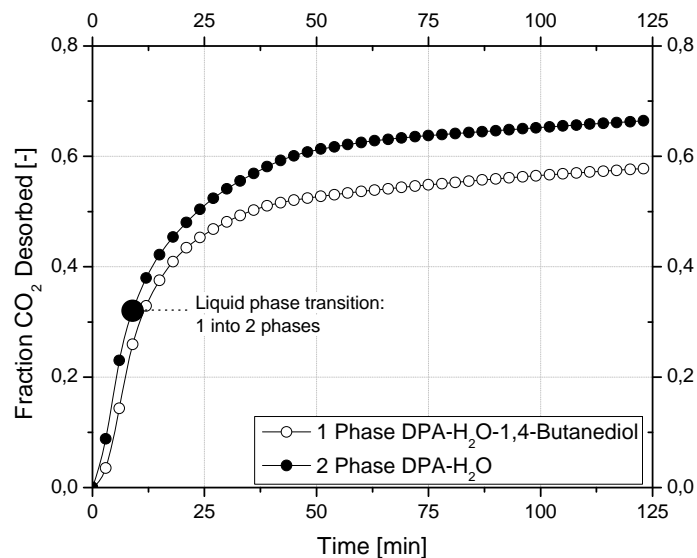


Fig. 26: Regeneration of homogeneous and biphasic dipropylamine solutions

During regeneration at 80°C with 300 mLN/min N<sub>2</sub> as a strip gas, the solution which was biphasic before absorption (2 Phase) had thermomorphic liquid phase separation at 30-

40% degree of regeneration. The regeneration curve depicted in Fig. 26 shown considerably higher regeneration rate and regeneration degree in initially biphasic (2 Phase) compare to initially homogeneous solution. In brief application of biphasic amine solvent improves the more significantly the amine regeneration than the CO<sub>2</sub> absorption characteristic.

## 4.2 Influence of lipophilic amine structure to its properties

In the industrial processes involving amine scrubber to remove CO<sub>2</sub>, cost of energy used in regeneration process as well as the investment cost are decisive factors. Thus sorbents with good kinetics and high degree of regeneration are sought. The amine-CO<sub>2</sub> reactions are acid-base neutralisation reaction in which base strength plays an important role in the absorption and regeneration process. Moreover specific to our biphasic lipophilic system, the aqueous solubility of the amine is substantial in both absorption and regeneration process. The influences of both parameters will be discussed in the following section. Some other parameters such as viscosity will be discussed briefly.

Lipophilic amines which comprise hydrocarbon substituents are divided into aliphatic and aromatic amines (arylamine). The aromatic ring in the arylamine strongly decreases the base strength of the overall amine molecule [83]. Thus the arylamine was not considered in the further investigation.

### 4.2.1 Influence of amine structure to molecule base strength

In the molecular level, three main factors which influence the basicity of the amine molecule will be discussed in the following section. Each of the factors influences the basicity in a different way.

#### 4.2.1.1 Inductive effect

The alkyl groups in the aliphatic amine are able to release electrons, which increase the electronegativity of nitrogen atom and stabilization of the positively charged nitrogen atom. Thus, with addition of more alkyl substituents the base strength of the overall amine molecule should increase. Therefore, in a gas phase the overall amine base strength is influenced mainly by the electronegativity of central nitrogen atom in the order of: R<sub>3</sub>N >

$R_2NH > RNH_2 > NH_3$ . However in aqueous solution, the overall basicity of the amine molecule is also influenced by solubilisation and steric effect. As the result of all effects, in aqueous solutions basicity of aliphatic amines is usually in the order of:  $R_2NH > RNH_2 > R_3N > NH_3$  [83]. The inductive effect provides information about the range of carbon atom attached to central nitrogen atom in a molecule, which influences the electronegativity of the overall molecule. Studies conclude the inductive effect caused by alkyl group decreases rapidly upon increase of distance from central basic atom. Moreover alkyl group was found to have weak inductive effect to the central nitrogen atom [57]. Only molecular modification near to the central basic atom (up to three atoms distance), within the inductive range, influences the base strength of the overall molecule. The highest influence typically could be resulted upon modification to three carbon atom nearby the central nitrogen atom.

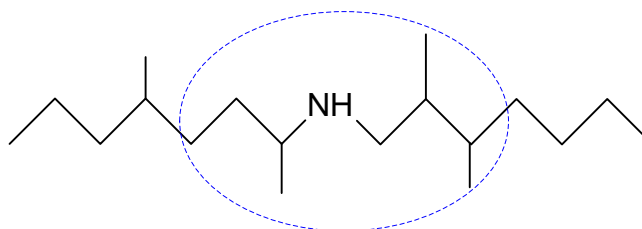


Fig. 27: Inductive effect range in an amine molecule

The hypothesis was confirmed by the data presented in

Table 7.

Table 7:  $pK_b$  values of amines in water at 25 °C ( $pK_b, NH_3 = 4.79$ ) [57]

Alkyl substituent (R)	$RNH_2$	$R_2NH$	$R_3N$
Methyl	3.38	3.29	4.24
Ethyl	3.37	3.02	3.35
Octyl	3.35	3.00	-
Octadecyl	3.40	3.00	-

The  $pK_b$  of the primary amines shows low influence of inductive effect due to alkyl group length to the basic strength of the overall amine molecule. In case of primary amine, the steric effect does not influence the basic strength as the amino group is always accessible. In both secondary and tertiary amines the steric and solubilisation effect exhibits stronger influence to the basic strength.

Amine molecule's basic strength can be enhanced by increasing electron density of the nitrogen atom. For this purpose, the electron density can be increased by attaching electron donor group near the base central (nitrogen atom) or by conjugating the nitrogen atom with

other electron donor group. The base strength of amine is predicted to decrease under the following circumstances [24].

- The nitrogen atom is attached to electron-withdrawing groups.
- The lone pair of electron on the nitrogen atom is in an sp or sp<sup>2</sup> hybridized orbital.
- The lone pair of electron on the nitrogen atom is conjugated with an electron-withdrawing group.
- The lone pair of electron on the nitrogen atom is involved in maintaining aromaticity of the molecule.

Relative inductive effect is measured with reference to hydrogen as depicted in Fig. 28:

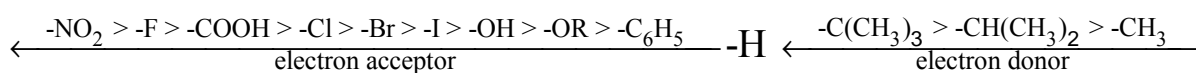


Fig. 28: Electronegativity of substituents groups

The inductive effect is responsible for the decrease of alkanolamines' basic strength upon addition of more hydroxyl group in the molecule. Moreover hydroxyl group in hydrocarbon molecule is identified as weak acid [15]. Solvents with high base strength give high absorption rate with the expense of low equilibrium CO<sub>2</sub> partial pressure upon regeneration.

#### 4.2.1.2 Solubilisation effect

Unlike in the gas phase, the amine base strength in the aqueous solutions is affected by its solubilisation in water. Upon amine-water mixing, protonated amine (ammonium ion) and hydroxyl ion (strongest base) are formed. The stabilisation of the positively charged nitrogen atom as well as base strength favours more hydrogen atoms on the nitrogen atom. Thus theoretically base strength favour good aqueous solubility.

The solubilisation of aliphatic amine is mainly due to hydrogen bonding upon amine-water mixing. More hydrogen atom attached to nitrogen atom will increase solubility in water. Even though the amine molecules are randomly distributed, their interactions with water form intermolecular hydrogen bond. This indicates that they are not freely moving in the continuum. This hydrogen bonding interaction is weak (13-42 kJ/mol) compare to single

covalent bond strength (210-420 kJ/mol), however they are approximately ten times stronger than van der waals forces [59].

With increase of alkyl chain group size, the aqueous solubility decreases. The alkyl substituent having linear chain has lowest solubility compare to the branched or cyclic structure alkyl substituent. As the sphericity of the molecule increase, its hydrophobic influence decreases.

#### 4.2.1.3 Steric effect

Steric effect occurs in combination with the solubility effect to influence the basic strength. Aliphatic amine molecules having large alkyl substituent obstruct the attachment of center nitrogen atom with proton. This reduces the basicity as well as the reaction rate. 2-amino-2-methyl-1-propanol (AMP), which is sterically hindered amine version of ethanolamine (MEA) has significantly lower reaction rate than MEA.

The base strength expressed in terms of  $pK_b$  is given in Table 8.

Table 8: Base strength of amine with various alkyl structures

<b>Primary amines</b>	<b><math>pK_b</math></b>	<b>Secondary amines</b>	<b><math>pK_b</math></b>	<b>Tertiary amines</b>	<b><math>pK_b</math></b>
Propylamine	3.8	Dipropylamine	3.2	Triethylamine	3.8
Isopropylamine	3.6	Diisopropylamine	3.1	Tripropylamine	3.2
Butylamine	3.8	Dibutylamine	3.2	Tributylamine	3.2
Isobutylamine	3.7	Piperidine	3	Methylpiperidine	3.8
sec-Butylamine	3.6	2,6Dimethylpiperidine	2.8	Ethylpiperidine	3.5
Hexylamine	3.8	Dihexylamine	3.3	Dimethylhexylamine	4
Cyclohexylamine	3.4	Dicyclohexylamine	2.9	Dimethylcyclohexylamine	3.6

The influence of steric effect is more pronounce in the secondary and tertiary amines where the  $pK_b$  decreases as the alkyl group size increase. In secondary amine, the  $pK_b$  is higher than primary and tertiary amine, which is contributed by the inductive effect rather than solubility and steric effect. In tertiary amine, the combination of solubility and steric effect is dominant to determine the overall base strength of the amine.

The combination of induction, solubilisation and steric effects decide the overall base strength of the amine. Perrin et.al. has developed the correlation for prediction of aliphatic amines' pK<sub>a</sub> values as function of the alkyl group length (n = number of methyl chain) as follow [57]:

$$\text{Primary amine} \quad : \quad \text{pK}_a = 10.6 \pm 0.2 \quad (21)$$

$$\text{Secondary amine} \quad : \quad \text{pK}_a = 11.1 \pm 0.1 - n \times 0.2 \quad (22)$$

$$\text{Tertiary amine} \quad : \quad \text{pK}_a = 10.5 \pm 0.2 - n \times 0.2 \quad (23)$$

The correlation indicates the secondary amines are expected to have highest K<sub>b</sub> than primary and tertiary amines.

#### 4.2.1.4 Influence of amine structure to viscosity

The viscosity of hydrocarbon molecule at various temperatures depends on the molecular size. The larger the molecular size, the higher the viscosity. Similar to other quantities in mixing thermodynamic, the viscosity of lipophilic amine solution deviates from the ideal condition non-linearly dependent on composition upon mixing with water. The increase of viscosity is quantified by increase of solution's activity coefficient. Saleh et.al. has determined the positive deviation from ideality by quantifying the excess free energy (activity), enthalpy as well as entropy of water-butylamine, water-sec-butylamine and water-tert-butylamine systems [66].

Previous study shows linear lipophilic amines comprising more than 6 carbon atoms forms gel during mixing in water. It might be caused by structure increase associated with solution of hydrocarbon in water. The viscosity increase is less pronounced with secondary or tertiary amine – water system. In the industrial application, the viscosity of the amine solution under CO<sub>2</sub> atmosphere is more important. Thitakamol and Veawab found the viscosity and density of MEA solution increase significantly depending on degree of CO<sub>2</sub> loading [76]. Added with the decrease of surface tension, foaming occurs. The viscosity increase is also contributed from the amine degradation product, addition of corrosion inhibitor and also surfactant. In extreme case, in the later investigation, some of the lipophilic amine solutions form gel during absorption process.

#### 4.2.2 Exploration for suitable lipophilic amines

Based on the studied parameter above the screening was carried out. Additionally volatility issue might limit the usage of lipophilic amine in absorption process. Table 9 summarise the boiling point of primary amines at increasing linear alkyl chain length. Any isomers with branching in the alkyl group will result in reduction of boiling point compare to that of linear chain amine. Based on volatility, among primary and secondary aliphatic lipophilic amines, the ones with alkyl group starting from six carbon atoms could be applied for CO<sub>2</sub> absorption.

Table 9: Primary amines' boiling points [48]

<b>Primary amines</b>	<b>N-boiling point [°C]</b>	<b>Condition (25°C, 1atm)</b>
Methylamine	-6.33	Gas soluble in water
Ethylamine	16.58	Low boiling point liquid soluble in water
n-propylamine	48.5	Low boiling point liquid soluble in water
n-butylamine	77.4	Liquid soluble in water
n-pentylamine	104.5	Liquid soluble in water
n-hexylamine	132.7	Liquid partially soluble in water
n-heptylamine	156.9	Liquid partially soluble in water
n-octylamine	179.6	Liquid partially soluble in water
n-nonylamine	202.2	Liquid partially soluble in water
n-decylamine	220.5	Liquid partially soluble in water
Cyclohexylamine	134	Liquid soluble in water

Table 10: Secondary amines' boiling points [48]

<b>Secondary amines</b>	<b>N-boiling point [°C]</b>	<b>Condition (25°C, 1atm)</b>
Diethylamine	55	Low boiling point liquid soluble in water
Dipropylamine	110	Liquid partially soluble in water
Dibutylamine	159	Liquid with limited solubility in water
Di-sec-butylamine	134	Liquid with limited solubility in water
Di-isobutylamine	137	Liquid with limited solubility in water
Dicyclohexylamine	256	Liquid slightly soluble in water

Among tertiary aliphatic lipophilic amines, the ones with alkyl group having total number of carbon atom more than six carbon atoms were considered.

Table 11: Secondary amines' boiling points [48]

<b>Tertiary amines</b>	<b>N-boiling point [°C]</b>	<b>Condition (25°C, 1atm)</b>
Trimethylamine	2.9	Vapour soluble in water
Triethylamine	89	Liquid with limited solubility in water
Tripopylamine	155-158	Liquid with limited solubility in water
Dimethylcyclohexylamine	159	Liquid with limited solubility in water
Diethylcyclohexylamine	193.52	Liquid with limited solubility in water

From the solubility-viscosity criteria, the lipophilic amines having certain length of alkyl chain form immediately gel upon mixing with water. The effect is various dependent on types of amine.

For primary amines, the alkyl length shouldn't achieve more than six carbon atoms. The isomers from the linear primary amine have fewer tendencies to form gel upon mixing with water, however they are economically infeasible.

For secondary amines, longer alkyl chain can be applied without drawback of gel formation. Alkyl chain up to total 10 carbon atoms in secondary amine molecule could be applied for absorption. Further study reveals as the alkyl group size increase in secondary amine, the absorption rate decreases due to both sterically hindered effect and mass transfer resistance related to solution viscosity.

For tertiary amine, the gel formation is less pronounced compare to both primary and secondary amines. The solubility issue in tertiary amine is related to solubility hindered effect. The lipophilic tertiary amines can only be utilised properly if its ammonium species resulted from reaction with CO<sub>2</sub> can be dissolved in aqueous phase. In this case, strong non-polar tertiary lipophilic amines could not be applied for CO<sub>2</sub> absorption. Since the polarity criterion varies significantly influence by the solvent-amine interaction, the criteria for tertiary amine could not be defined very accurately. Frequently unexpected outcomes were found after testing the particular amine. However one can propose to apply tertiary amines with minimum molecular size while keeping its boiling point and base strength at reasonable values. The limited solubility of tertiary amines in water serves as auto-extractive agent to extract the lipophilic amine from the loaded aqueous phase and enhance the regeneration.

From base strength criteria, secondary amines are expected to be more suitable as activator for CO<sub>2</sub> absorption than primary amines. This is proposed based on the base strength deduced from study by Perrin et.al. (22) [57]. In tertiary lipophilic amine, the steric effect is more dominant than base strength for CO<sub>2</sub> absorption process because of the solubility hindered effect. Moreover it serves to provide absorption capacity rather than absorption rate.

### 4.3 Lipophilic amines applied in CO<sub>2</sub> absorption

In this work, the investigation was carried out with two lipophilic amines, i.e. N,N-dipropylamine (DPA) and N,N-dimethylcyclohexylamine (DMCA). Both lipophilic amines were selected from the first screening process [75], [86]. Their aqueous solubility characteristics are given in Fig. 29.

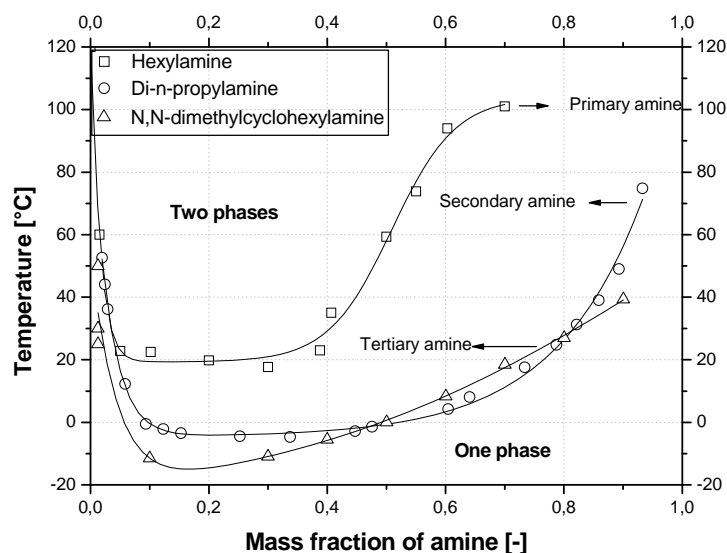


Fig. 29: DPA-H<sub>2</sub>O and DMCA-H<sub>2</sub>O solubility curves

In general, at room temperature lipophilic amines have a very low solubility (<5%wt.) in water however they have significant ability to dissolve water dependent on types of amines. The solubility of amine in water as well as water in amine is in the order of primary amines > secondary amines > tertiary amines.

The ternary solubility of lipophilic amine mixtures in water, represented by 3.6M DPA-DMCA-H<sub>2</sub>O system, is relatively constant as depicted in Fig. 30. Above the solubility temperature, the solutions remained biphasic.

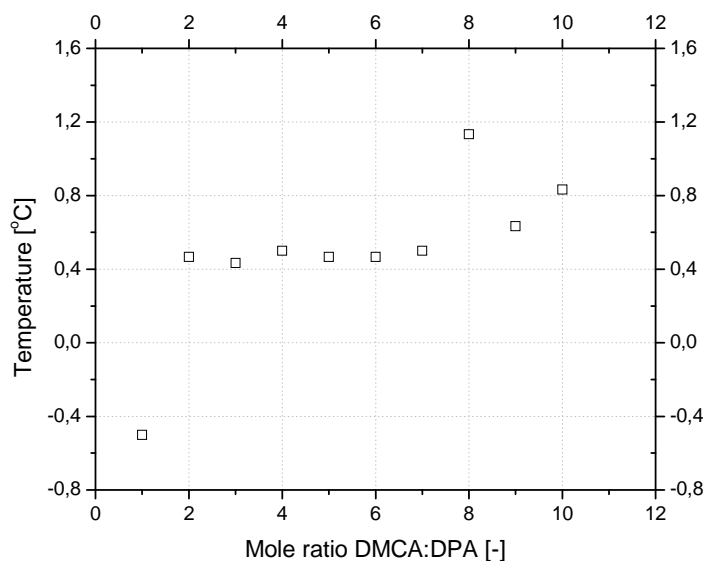


Fig. 30: Solubility curve of ternary system DPA-DMCA-H<sub>2</sub>O (3.6 M amine)

At high concentration of DPA, the nonpolar amine-amine interaction is considerably higher than the amine-water interaction. This is indicated by the low solubility temperature anomaly at low mole ratio of DMCA:DPA.

The liquid-liquid phase separation rate of lipophilic amine solutions, which were preloaded with CO<sub>2</sub>, depends mainly on the temperature.

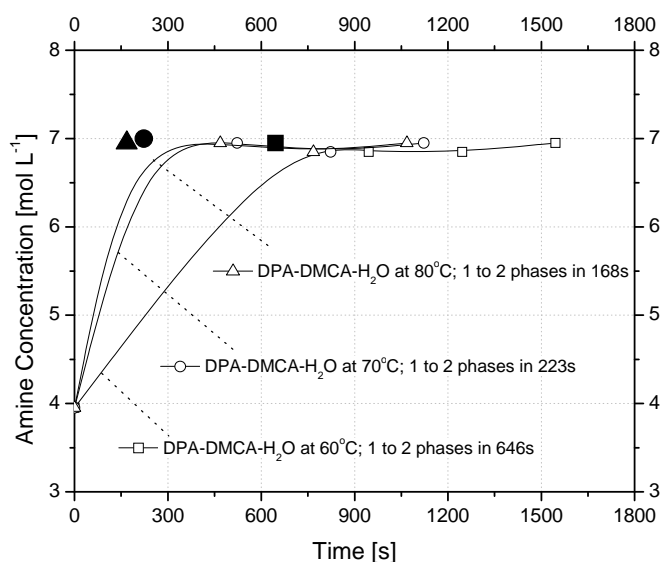


Fig. 31: Thermomorphic liquid-liquid phase separation of CO<sub>2</sub>-loaded 3.6 M 1:2-DPA:DMCA

Moreover the loaded solutions, which were initially homogeneous phase, would turn to biphasic solutions with constant organic phase concentration. This characteristic is very

important in amine regeneration, because the regenerated amine is isolated in organic phase, leaving the concentration of regenerated amine in aqueous phase low and provides more driving force for further amine regeneration reaction.

### 4.3.1 N,N-dipropylamine (DPA)

The N,N-dipropylamine (DPA) was used as an activator due to its high absorption and reaction rate with CO<sub>2</sub>. Moreover the biphasic DPA-H<sub>2</sub>O solution transform to homogeneous phase upon CO<sub>2</sub> absorption at considerably shorter time than any other tested lipophilic amines during the screening experiment as depicted in Fig. 32.

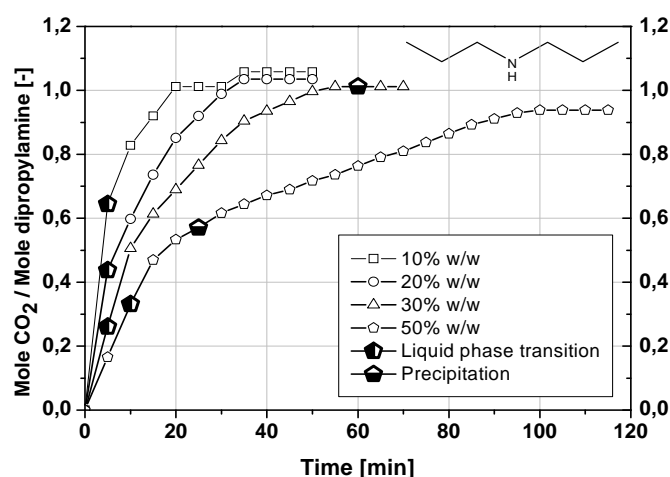


Fig. 32: CO<sub>2</sub> absorption into dipropylamine (DPA) (20mlN/min, 1atm CO<sub>2</sub> at 25°C)

At high DPA concentration starting from 30%wt. (2.7M), the DPA-H<sub>2</sub>O mixture precipitates during CO<sub>2</sub> absorption. Severe precipitation occurs especially at solution with composition 50%wt. DPA (4.3M) as shown in Fig. 33.

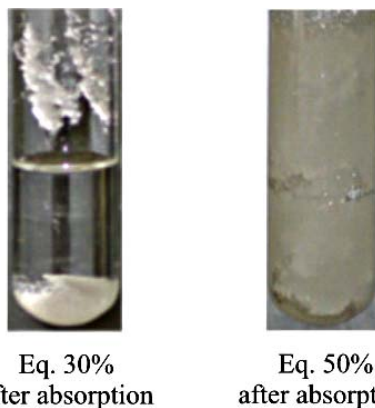


Fig. 33: Dipropylamine (DPA) precipitation

The DPA regeneration characteristics shown in Fig. 34 indicate that the precipitate dissolved at 40°C and reasonable degree of regeneration could be expected from DPA-H<sub>2</sub>O system.

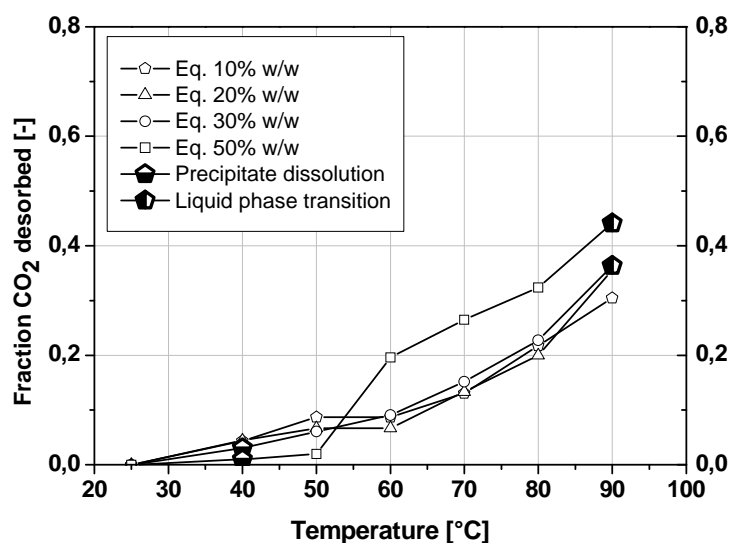


Fig. 34: Dipropylamine (DPA) regeneration characteristics

Due to its application as activator, high concentration of DPA will not be employed in the CO<sub>2</sub> absorption. In chapter 4.7, the precipitation phenomena of DPA are discussed furthermore.

#### 4.3.2 N,N-dimethylcyclohexylamine (DMCA)

DMCA is tertiary amine with relatively strong base strength ( $pK_b=3.6$ ) but low solubility in water. Its low solubility in water is exploited in this work to promote thermomorphic liquid phase separation upon heating in regeneration process. As tertiary amine, DMCA has high CO<sub>2</sub> absorption capacity with CO<sub>2</sub> loading in solution approaching 1:1 mole CO<sub>2</sub> absorbed/mole DMCA. Its absorption characteristics are given in Fig. 35.

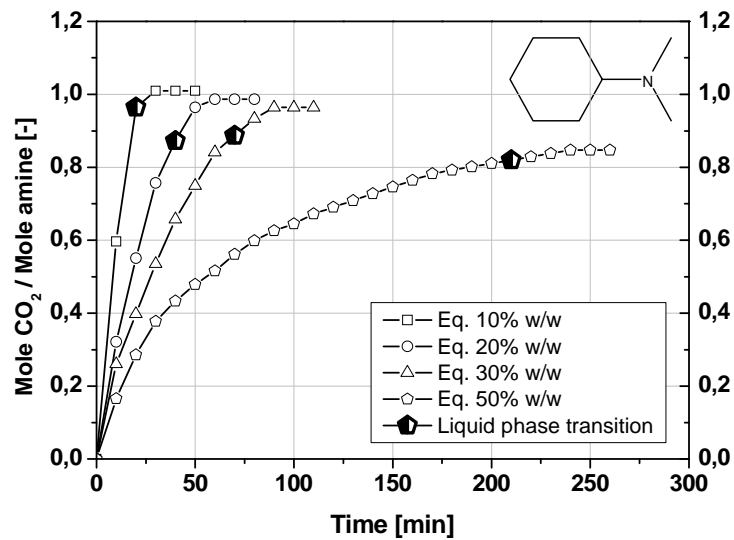


Fig. 35: CO<sub>2</sub> absorption into dimethylcyclohexylamine (DMCA) (20mlN/min, 1atm CO<sub>2</sub> at 25°C)

The liquid phase transition from biphasic to homogeneous phase requires significant CO<sub>2</sub> loading and absorption time, however when DMCA is mixed with DPA, this drawback can be overcome. As mentioned before, the tertiary amine's most important characteristic is to promote thermomorphic liquid phase separation at low temperature. These characteristics enable the regeneration to be taken place at low temperature as indicated in Fig. 36.

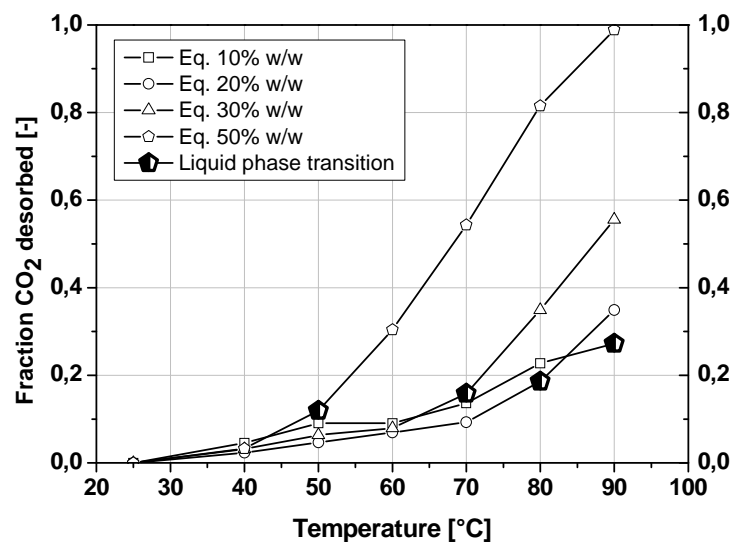


Fig. 36: Dimethylcyclohexylamine (DMCA) regeneration characteristics

The regeneration temperature depends on the lipophilic amines and its composition. The self-associate characteristic of water is more pronounced with increase of amine concentration in water. As a rule of thumb, lipophilic amines with lower solubility in water can be regenerated also at lower temperature. Thus in general the order of regeneration temperature is primary > secondary > tertiary amines. However there is anomaly to this rule which is caused by unique combination of inductive – solubility – steric effect in amine molecule. This will be discussed in the second screening process discussed in chapter 4.11.

#### 4.4 Physicochemical properties: DPA-H<sub>2</sub>O and DMCA-H<sub>2</sub>O

DPA and DMCA are not widely applied in CO<sub>2</sub> absorption process. The availability of DPA and DMCA aqueous solution data was scarce that most of the physicochemical data was measured during this work.

##### 4.4.1 Density

The density of the solutions was measured with 10 and 50 mL Gay-Lussac pycnometer and the temperature during the experiment was maintained using Haake cryostat bath type F3 – C3 with the temperature precision up to 1 decimal. The volume of the pycnometer at various temperatures was also calibrated with degassed demineralised water and it gave good agreement with the manufacturer's data. The conjugate organic and aqueous solutions of DPA and DMC were prepared by mixing of each amine with the water. Due to the solubility limit, the organic and aqueous phases were formed. The solutions were heated under constant temperature until the solutions appeared clear to eye, approximately 1-2 hours for each temperature and they were separated for further analysis.

The measured density was correlated with the correlation (24) with  $R^2 > 0.99$ .

$$\rho = c_1 + c_2 \cdot T + c_3 \cdot T^2 \quad (24)$$

Density of the conjugate solutions was measured from 25-60°C. The conjugate solutions of DPA and DMCA have unique characteristics which can be observed even from their density. As the temperature increase, the properties of the organic phase are significantly influenced than the aqueous phase. The profile of the density is depicted in Fig. 37.

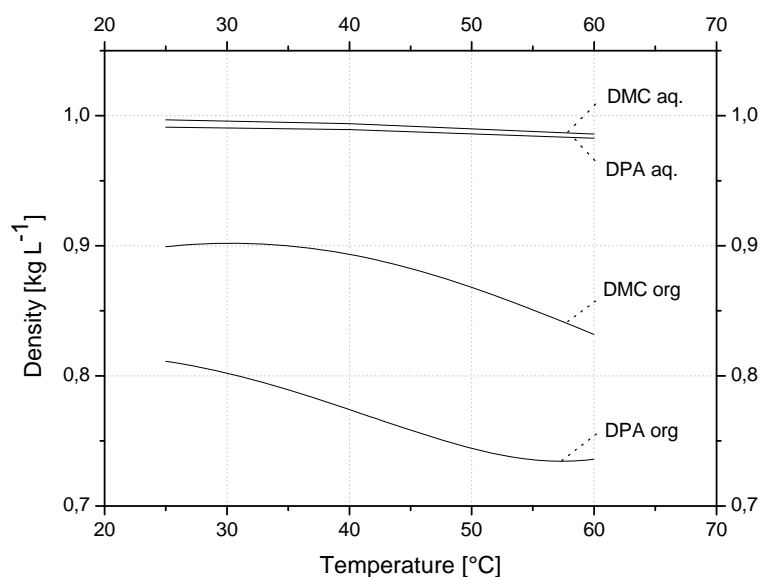
Fig. 37: Density of DPA-H<sub>2</sub>O and DMCA-H<sub>2</sub>O conjugate solutions

Table 12: Density parameter constants refer to equation (24)

Solutions	$c_1$	$c_2$	$c_3$
DPA organic phase	3.07	-0.012	$2 \cdot 10^{-5}$
DPA aqueous phase	0.439	0.004	$-6 \cdot 10^{-6}$
DMCA organic phase	-6.162	0.047	$-8 \cdot 10^{-5}$
DMCA aqueous phase	0.467	0.004	$-6 \cdot 10^{-6}$

At elevated temperature, density of aqueous phase decreases linearly similar to that of homogeneous solutions while the organic phase decrease with non-linear behaviour. This characteristic is also observed with other properties discussed later.

#### 4.4.2 Viscosity

Kinematic viscosity of conjugate solutions was measured from 25-60°C. The viscosity of the organic phase is highly influenced by increase of temperature. The sensitivity is even higher than that of density, where from 25-50°C, the density of organic phase decreases less than 30% while the viscosity decreases approximately 70%. Thus the momentum diffusivity of organic phase is highly sensitive towards temperature change. This characteristic can be

observed in Fig. 38. The kinematic viscosity is calculated with additional kinetic correction with the equation (25).

$$\nu = K \cdot (t - c_k) \quad (25)$$

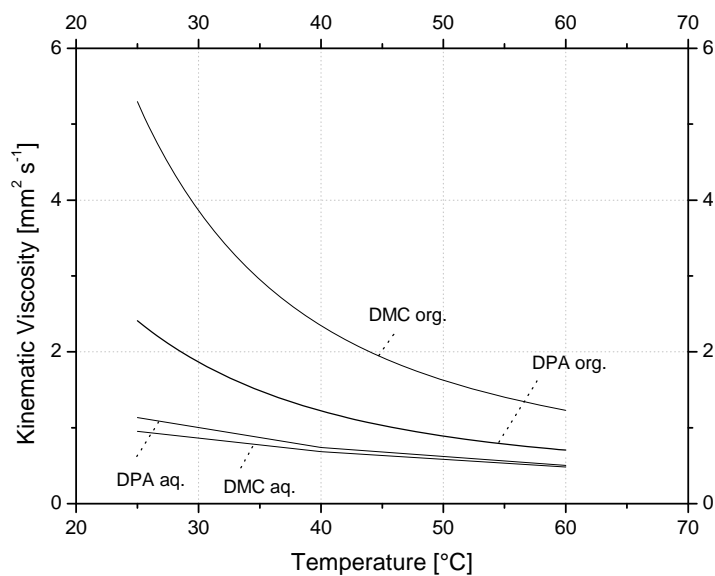


Fig. 38: Kinematic viscosity of DPA-H<sub>2</sub>O and DMCA-H<sub>2</sub>O conjugate solutions

Table 13: Kinematic viscosity parameter constants refer to equation (25)

Solutions	$c_1$	$c_2$
DPA organic phase	$1.978 \cdot 10^{-5}$	3478.40
DPA aqueous phase	0.0005	2308.40
DMCA organic phase	$4.877 \cdot 10^{-6}$	4127.80
DMCA aqueous phase	0.0015	1924.50

#### 4.4.3 Gas physical solubility

The physical solubility of CO<sub>2</sub> was measured indirectly using nitrous oxide analogy due to its reactivity with amine solution. Due to similarity in molecular weight and electronic structure of CO<sub>2</sub> and N<sub>2</sub>O, the N<sub>2</sub>O analogy can be applied. Thus the Henry constant for CO<sub>2</sub> – amine system was obtained from N<sub>2</sub>O analogy with the following relation [2],[45]:

$$\frac{H_{\text{CO}_2\text{-amine}}}{H_{\text{N}_2\text{O-amine}}} = \frac{H_{\text{CO}_2\text{-H}_2\text{O}}}{H_{\text{N}_2\text{O-H}_2\text{O}}} \quad (26)$$

The physical solubility of CO<sub>2</sub> and N<sub>2</sub>O in water was measured by Versteeg et.al [82]. The obtained Henry constant was correlated in equation (27).

$$H_{\text{CO}_2\text{-amine}} = c_1 \cdot e^{\left(\frac{c_2}{T}\right)} \quad (27)$$

The parameter retrieved was from correlated data with  $R^2 > 0.99$ .

The gas physical solubility was measured from 25-60°C. As the temperature reached 50°C, significant amount of vapour presented in the reactor. Thus experiment with temperature above 60°C is not suggested as it might lead to error due to condensation of vapour. The characteristic of the physical solubility is presented as Henry constant in Fig. 39 and the parameters for the estimation are given in Table 14.

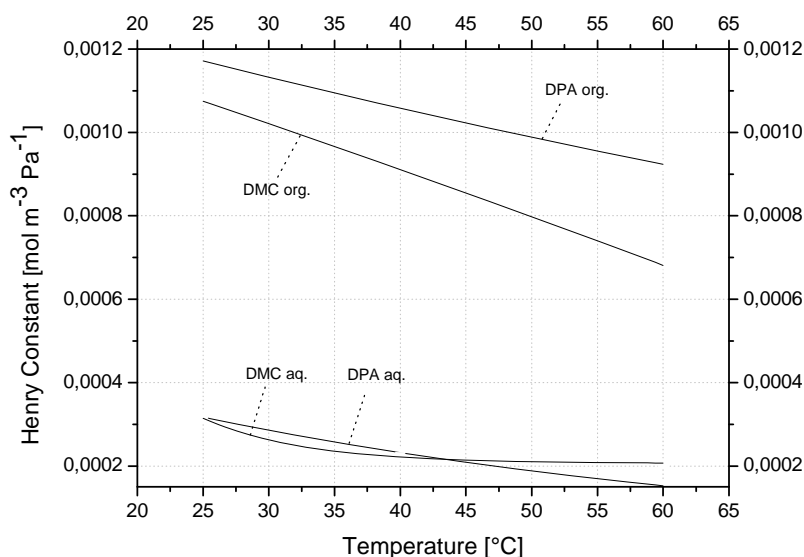


Fig. 39: CO<sub>2</sub> physical solubility into DPA-H<sub>2</sub>O and DMCA-H<sub>2</sub>O conjugate solutions

Table 14: Physical solubility parameter constants refer to equation (26)

Solutions	$c_1$	$c_2$
DPA organic phase	$1.21 \cdot 10^{-4}$	678.61
DPA aqueous phase	$3.14 \cdot 10^{-7}$	2064.31
DMCA organic phase	$1.39 \cdot 10^{-5}$	1300.80
DMCA aqueous phase	$5.82 \cdot 10^{-6}$	1172.76

For aqueous phase, the physical solubility of the DMCA reaches its tangential value at temperature 40°C while the DPA has not. This is due to the influence of aqueous solubility of the conjugate solution, in which the amount of DMCA in the aqueous phase is very minor starting from 40°C. Once the tangential value achieved, the solution will behave similar to that of water.

#### 4.4.4 Diffusivity of CO<sub>2</sub> in amine solutions

The diffusivity of CO<sub>2</sub> into the solution using double stirred cell reactor was measured indirectly using dimensionless correlation. Unlike conventional absorption apparatus where the diffusion coefficient can be measured directly according to the mass transfer theories [26],[47], the diffusivity measured by stirred cell reactors was obtained from mass transfer-hydrodynamic-properties dimensionless Sherwood, Reynolds, Schmidt numbers. The specific parameters for the double stirred cell used in this study were determined experimentally using CO<sub>2</sub>-water absorption system [80].

$$\text{Sh}=0.583 \text{Re}^{0.8124} \text{Sc}^{0.4425} \quad (28)$$

Once the gas-liquid equilibrium achieved, the liquid mass transfer coefficient ( $k_L$ ) can be calculated from mass balance (29) combined with N<sub>2</sub>O analogy.

$$\ln \left( \frac{P(t)-P^{\text{equilibrium}}}{P^{\text{initial}}-P^{\text{equilibrium}}} \right) = -k_L \cdot A \cdot \left( \frac{P^{\text{initial}}}{P^{\text{equilibrium}} \cdot V_L} \right) \cdot t \quad (29)$$

The CO<sub>2</sub> diffusivities in amine solutions were measured at specific amine concentrations which were used to study the CO<sub>2</sub>-amine reaction kinetics constant.

### 4.5 Thermodynamic modelling

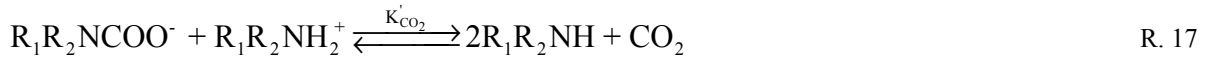
Several thermodynamic models were developed to describe the composition of the chemical species. Kent and Eisenberg introduce the thermodynamic model by fitting of equilibrium constant to the experimental data [42]. All of the non-idealities are summed up into the apparent equilibrium constant. The model was proven to correlate the data well while retaining computational simplicity [51],[72],[77]. Moreover the model was widely applied with modifications by Hu and Chakma [38], Kritpiphat and Tontiwachwuthikul [44], Sulaiman [72]. The reactions involved are given as follow:



$$P_{\text{CO}_2} = h_{\text{CO}_2} \text{CO}_2 \quad (30)$$

Deshmukh and Mather [28] introduced activity and fugacity coefficients based on Debye-Hückel theory to describe the non-ideality. Extensive work with electrolyte NRTL model was done by Austgen and Rochelle [4]. An approach to include equation of states into reactive gas-liquid equilibrium was also carried out [23].

All of the models given above are complex and highly nonlinear which require high computation effort. Thus attempts were done to reduce their complexity. Gabrielsen [34] reduced the equations substantially into only one explicit equation providing low partial pressure of CO<sub>2</sub> thus low loading of CO<sub>2</sub> in the solution. Thus the reactions can be simplified for primary/secondary amines and tertiary amine respectively into R. 17 and R. 18.



This simplification is applicable up to loading of CO<sub>2</sub> lower than 0.48 for MEA system where the formation of carbamate reaction has the major influence on the system.

#### 4.5.1 Mathematical modelling

The modified Kent-Eisenberg model was applied in this work to determine the concentration of reactive species in the amine solutions during absorption due to its simplicity and accuracy at every CO<sub>2</sub> loading range. The reactions R. 12 - R. 16 are taken into account into the model. Physical solubility of CO<sub>2</sub> in respective amine solutions, not in water, was applied in the model. The equilibrium equations for R. 12 - R. 16 are given as follow:

$$K_1 = \frac{[\text{R}_1\text{R}_2\text{NH}][\text{HCO}_3^-]}{[\text{R}_1\text{R}_2\text{NCOO}^-]} \quad (31)$$

$$K_2 = \frac{[R_1R_2NH][H_3O^+]}{[R_1R_2NH_2^+]} \quad (32)$$

$$K_3 = \frac{[H_3O^+][HCO_3^-]}{[CO_2]} \quad (33)$$

$$K_4 = [OH^-][H_3O^+] \quad (34)$$

$$K_5 = \frac{[H_3O^+][CO_3^{2-}]}{[HCO_3^-]} \quad (35)$$

Investigation of the reactions R. 14, R. 15 and R. 16 was done by Kent and Eisenberg [42] and the correlations in SI units [77], are given as follow:

$$K_3 = \exp(-241.818 + 298.253 \times 10^3 T^{-1} - 148.528 \times 10^6 T^{-2} + 332.648 \times 10^8 T^{-3} - 282.394 \times 10^{10} T^{-4}) \quad (36)$$

$$K_4 = \exp(39.5554 - 987.9 \times 10^2 T^{-1} + 568.828 \times 10^5 T^{-2} - 146.451 \times 10^8 T^{-3} + 136.146 \times 10^{10} T^{-4}) \quad (37)$$

$$K_5 = \exp(-294.74 + 364.385 \times 10^3 T^{-1} - 184.158 \times 10^6 T^{-2} + 415.793 \times 10^8 T^{-3} - 354.291 \times 10^{10} T^{-4}) \quad (38)$$

For CO<sub>2</sub> physical solubility in amine solution, the correlation developed by Kent-Eisenberg for CO<sub>2</sub>-water was not used. Instead, the correlation measured for CO<sub>2</sub>-DPA and CO<sub>2</sub>-DMCA given in Table 14 was used.

Moreover the amine balance (39), carbon balance (40), and charge balance (41) are taken into account:

$$[R_1R_2NH]_0 = [R_1R_2NH] + [R_1R_2NCOO^-] + [R_1R_2NH_2^+] \quad (39)$$

$$[CO_2]_{\text{absorbed}} = \alpha [R_1R_2NH]_0 = [R_1R_2NCOO^-] + [HCO_3^-] + [CO_2] + [CO_3^{2-}] \quad (40)$$

$$[HCO_3^-] + [R_1R_2NCOO^-] + [OH^-] + 2[CO_3^{2-}] = [R_1R_2NH_2^+] + [H_3O^+] \quad (41)$$

The parameter K<sub>1</sub> and K<sub>2</sub> are determined by fitting to the experiment values and the concentration of reactive chemical species in amine solutions during absorption can be obtained by solving equations (30)-(41) with the given K<sub>1</sub> and K<sub>2</sub> values.

#### 4.5.2 CO<sub>2</sub>-aqueous phase DPA model

The absorption of CO<sub>2</sub> into DPA solution comprises complex parallel reactions from R. 7 - R. 16. Not all of the reactions are dominant in every degree of CO<sub>2</sub> loading in solution and it can be analysed from the result depicted in Fig. 40.

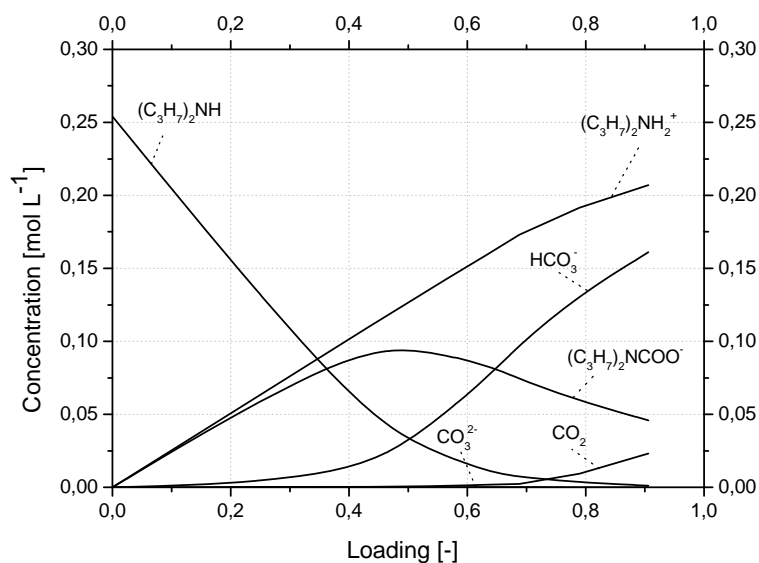
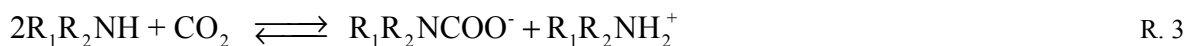


Fig. 40: CO<sub>2</sub>-aqueous DPA concentration profile (254 mol m<sup>-3</sup> DPA at 40°C)

The reaction of CO<sub>2</sub> in aqueous N,N-dipropylamine and also primary and secondary amines consists of two reaction regions which indicate the domination of one or more reactions dependent on the loading of CO<sub>2</sub> in the solution. When CO<sub>2</sub> loading is below 0.5, the carbamate formation reaction which is a fast reaction, dominates the absorption process that the reaction could be simplified into reaction R. 3 which is the reversion of R. 17 [3],[33].



This region is characterised by fast absorption kinetics (steep decrease of concentration of free amine in liquid phase) where carbamate and protonated amine are continuously formed. Minor amount of bicarbonate is formed mainly contributes to the reaction of CO<sub>2</sub> with hydroxyl ion owes to basicity of the amine. Due to this effect, only very small amount of soluble CO<sub>2</sub> present in the liquid solutions. Additionally the reaction of hydroxyl ion with CO<sub>2</sub> can't be neglected for the determination of absorption kinetics as it enhances mass transfer despite low concentration of hydroxyl ion [73].

The second region with CO<sub>2</sub> loading above 0.5 is characterised with pronounced carbamate hydrolysis reactions, exhaustion of the free amine and decrease of basicity. The main capacity of CO<sub>2</sub> storage is in the form of bicarbonate ions contributed from carbamate hydrolysis. Moreover increase amount of soluble CO<sub>2</sub> is observed as a result from decrease of basicity along with saturation of solution with CO<sub>2</sub>. The equilibrium constants K<sub>1</sub>

(deprotonation constant) and  $K_2$  (carbamate hydrolysis constant) with refer to equations (31) and (32) are determined and correlated with the equation (42).

$$K(\alpha) = \exp(c_1 + c_2\alpha + c_3\alpha^2 + c_4\alpha^3 + c_5\alpha^4 + c_6\alpha^5 + c_7\alpha^6) \quad (42)$$

The parameters are given in Table 15 based on the equilibrium data given in Table 16.

Table 15: DPA equilibrium constant correlation refer to equation (42)

Parameters	$c_1$	$c_2$	$c_3$	$c_4$	$c_5$	$c_6$	$c_7$
$K_1$	-4.64297	-210.974	1558.34	-5811.68	11063	-10320.8	3730.68
$K_2$	-4.53131	-4.32184	32.7246	-106.984	172.998	-132.247	35.7181

Table 16: Loading of CO<sub>2</sub> in 0.254 M Aqueous DPA at 40°C

Loading [-]	CO <sub>2</sub> partial pressure [kPa]
0.21	0.63
0.34	1.01
0.42	1.19
0.5	2.46
0.69	10.13
0.91	101.33

The predicted data is compared with experimental data and it gives a good agreement with deviation less than 1% as shown in Fig. 41.

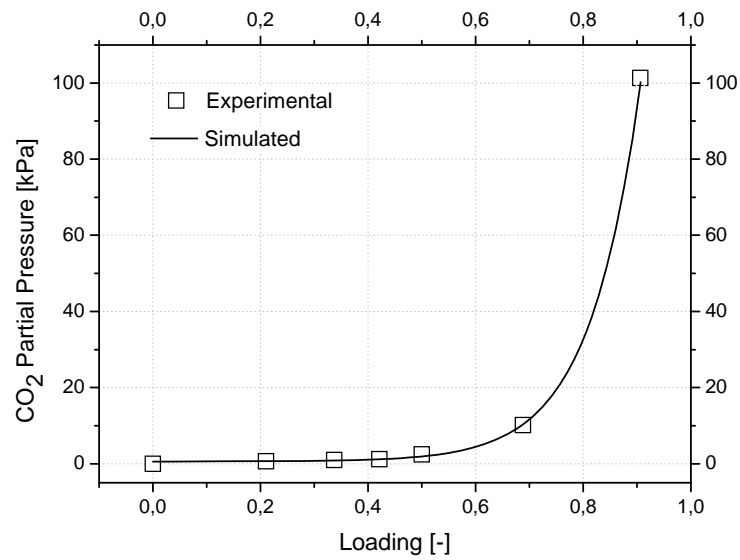


Fig. 41: CO<sub>2</sub>-aqueous DPA loading curve (254 mol m<sup>-3</sup> DPA at 40°C)

### 4.5.3 CO<sub>2</sub>-aqueous MEA model

As a comparison with commercial alkanolamine, the modelling is also carried out for ethanolamine (MEA) and the result is depicted in Fig. 42.

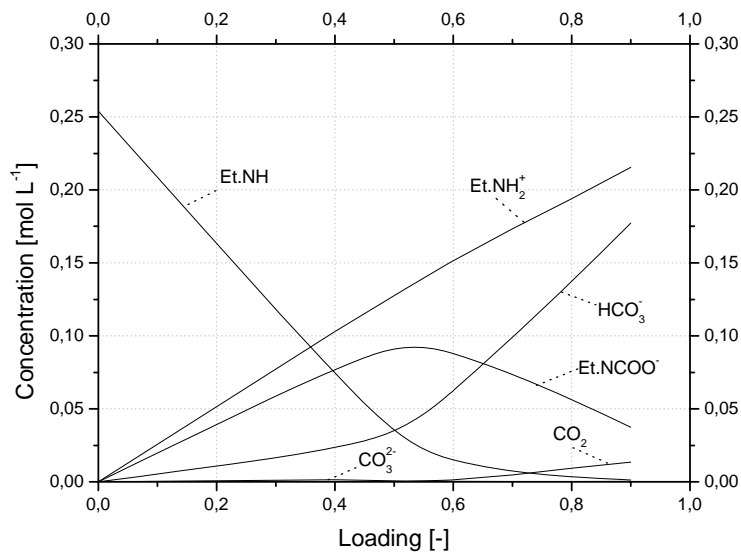


Fig. 42: CO<sub>2</sub>-aqueous MEA concentration profile (254 mol m<sup>-3</sup> MEA at 40°C)

MEA has a weaker base strength compare to DPA ( $pK_{b\text{-MEA}}=4.48$ ,  $pK_{b\text{-DPA}}=3.2$ ) due to presence of a hydroxyl substituent, which is an electron withdrawing substituent. This influences significantly the prevalence of reactions during CO<sub>2</sub> absorption. Strong bases in the amine solution available to react with CO<sub>2</sub> (acid) are mainly amine and hydroxyl ion. Both bases react competitively with CO<sub>2</sub>. In case of amine as strong base, the reaction yields carbamate and ammonium (stoichiometric 1:1). In case of amine as weak base, the reaction yields bicarbonate. Comparing the MEA profile (Fig. 42) with DPA profile (Fig. 40) with the same absorption condition, at CO<sub>2</sub> loading range below 0.3, lower amount of carbamate is observed in MEA than DPA solutions. Thus the reaction of CO<sub>2</sub> with hydroxyl ion to form bicarbonate is significant even at low CO<sub>2</sub> loading in MEA solution and lower absorption rate than DPA could be expected.

#### 4.5.4 CO<sub>2</sub>-aqueous DMCA model

The tertiary amine reacts with CO<sub>2</sub> only with the presence of water according to base catalysed of CO<sub>2</sub> hydration mechanism.

Theoretically, 1:1 mole ratio of tertiary amine to CO<sub>2</sub> is expecting to react according to R. 4.

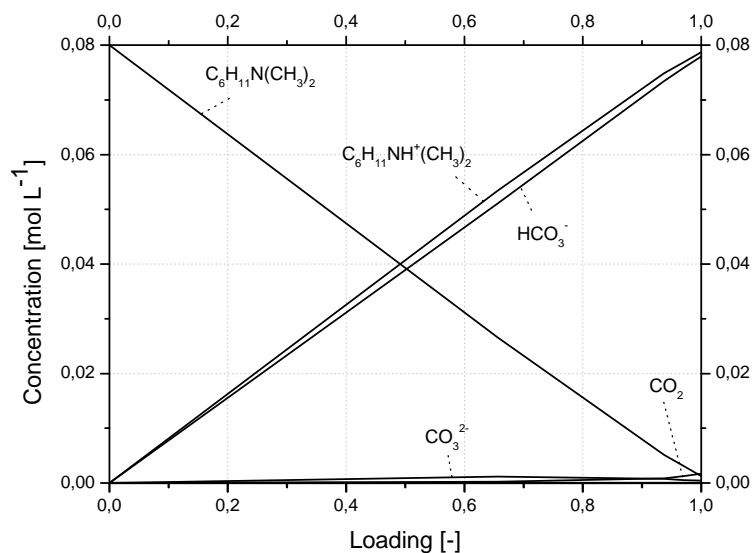


Fig. 43: CO<sub>2</sub>-aqueous DMCA concentration profile (80 mol m<sup>-3</sup> DMCA at 40°C)

The simulated concentration of the liquid phase depicted in Fig. 43 indicates consistency with the base-catalysed reaction mechanism for CO<sub>2</sub>-tertiary amine. Approximately ratio 1:1 decrease of DMCA concentration to increase of protonated DMCA and bicarbonate can be observed. In aqueous tertiary amine solutions, the main capacity of CO<sub>2</sub> is stored as bicarbonate while some of the bicarbonate is also converted as carbonate. Unlike DPA or other primary or secondary amine, the reaction of DMCA is slower and tends to be constant independent on the degree of CO<sub>2</sub> saturation in the solution. The DMCA protonation constants are also correlated based on the data in Table 17 with the correlation in equation (43).

$$K(\alpha, T) = \exp(c_1 + c_2/T + c_3/T^3 + c_4\alpha + c_5/\alpha + c_6/\alpha^2 + c_7 \ln(RRRN_0)) \quad (43)$$

Table 17: DMCA equilibrium constant correlation refer to equation (43)

Parameters	c <sub>1</sub>	c <sub>2</sub>	c <sub>3</sub>	c <sub>4</sub>	c <sub>5</sub>	c <sub>6</sub>	c <sub>7</sub>
K <sub>1</sub>	243.026	-3672.4	-1,03×10 <sup>8</sup>	-857.793	-1843.64	508.944	-768.937

Table 18: Loading of CO<sub>2</sub> in 80 mol m<sup>-3</sup> aqueous DMC at 40°C

Loading [-]	CO <sub>2</sub> Partial Pressure [kPa]
0.66	1.01
0.94	3.38
0.97	5.07
1	6.76

Similar to DPA, the predicted equilibrium partial pressure from the DMC model fits the experimental data. The plot is depicted in Fig. 44.

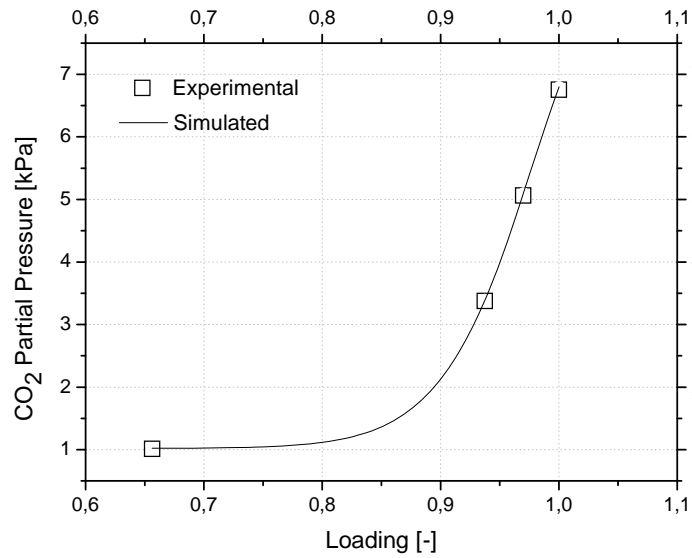


Fig. 44: CO<sub>2</sub>-aqueous DPA loading curve (254 mol m<sup>-3</sup> DPA at 40°C)

#### 4.5.5 CO<sub>2</sub>-aqueous MDEA model

As a comparison with commercial alkanolamine, the modelling is also carried out for methyldiethanolamine (MDEA) and the result is depicted in Fig. 45.

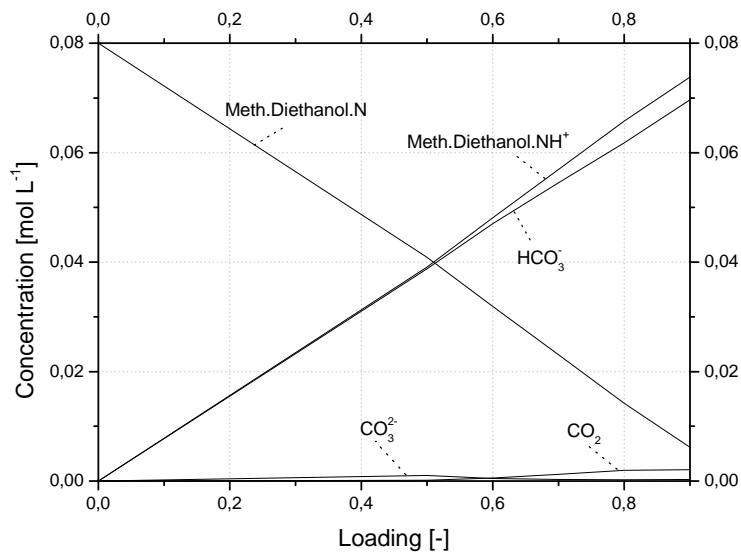


Fig. 45: CO<sub>2</sub>-aqueous MDEA concentration profile (80 mol m<sup>-3</sup> MDEA at 40°C)

A similar profile to that of DMCA is observed also in MDEA system and both profiles agree with the base-catalysed reaction mechanism, in which the tertiary amine reacts with CO<sub>2</sub> with ratio 1:1 stoichiometrically.

#### 4.5.6 CO<sub>2</sub> - 3 M DPA model

For industrial application, amine solutions applied reasonably have high concentration. The solvent composition used dependent on the gas composition as well as economic consideration. Solvents with high amine concentration have high gas absorption capacity with the expense of economic feasibility. For lipophilic amine system, precipitation due to application of highly concentrated amine solution is crucial. Thus the DPA with amine concentration up to 3M was applied for this study. The simulated result is depicted in Fig. 46.

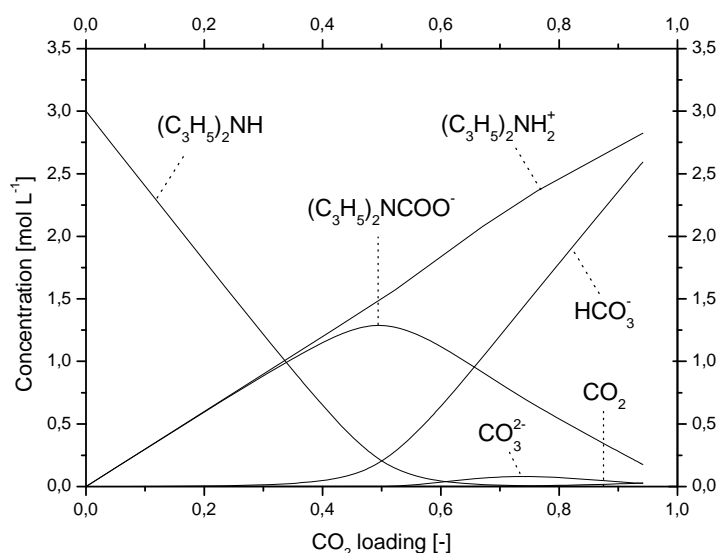


Fig. 46: CO<sub>2</sub>-DPA concentration profile (3000 mol m<sup>-3</sup> DPA at 40°C)

The DPA which was initially biphasic transformed to homogeneous phase at equilibrium CO<sub>2</sub> partial pressure below 15 mbar, which is out of the experimental apparatus accuracy. Moreover it is 10 fold lower than CO<sub>2</sub> partial pressure in industrial process. Thus investigation was carried out at the reasonable CO<sub>2</sub> partial pressure while maintaining the accuracy of the measurement.

As discussed before, the reaction of CO<sub>2</sub> in DPA comprises two reaction regions which indicate the domination of one or more reactions dependent on the loading of CO<sub>2</sub> in the solution.

#### Region I:

In the CO<sub>2</sub> loading region lower than 0.4, the carbamate formation, which is a fast reaction, is dominant. Different from the concentration profile in the aqueous phase (Fig. 40), at high DPA concentration the role of DPA as proton removal agent from zwitterions is dominant. This can be interpreted from Fig. 46, where the ammonium ion concentration is exactly proportional to carbamate concentration at loading below 0.4 and almost no CO<sub>2</sub> is absorbed as bicarbonate. Due to DPA base strength and high concentration in the solution, the ammonium is primarily formed in stoichiometric amount to carbamate ion as by-product of the DPA-CO<sub>2</sub> reaction.

#### Region II:

In the CO<sub>2</sub> loading region above 0.4 the solution which is saturated with carbamate ion undergoes hydrolysis to form bicarbonate and carbonate. Due to this reason, the regeneration of loaded solvent is done only partially in industrial process. The energy spent to regenerate the highly loaded solution in region II is less than the energy spent to regenerate region I.

The result of the simulation was furthermore validated with the experimental values and the result is depicted in Fig. 47.

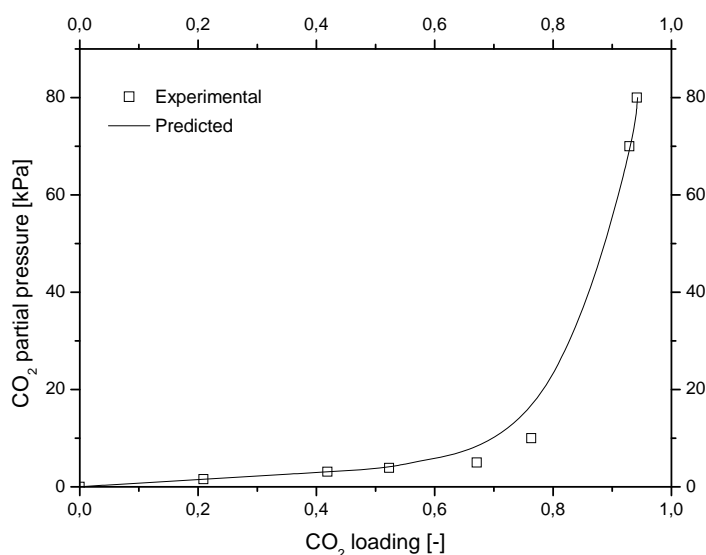


Fig. 47: Loading of CO<sub>2</sub> in 3000 mol m<sup>-3</sup> aqueous DPA at 40°C

To avoid precipitation the CO<sub>2</sub> partial pressure used was limited up to 80 kPa. The DPA protonation constant ( $K_1$ ) as well as carbamate stability constant ( $1/K_2$ ) of the system was given in Table 19.

Table 19: CO<sub>2</sub> - 3M DPA equilibrium constant correlation refer to equation (43)

Parameters	$c_1$	$c_2$	$c_3$	$c_4$	$c_5$	$c_6$	$c_7$
$K_1$	-40.482	-10.098	-10	31.923	33.430	-4.074	-43.488
$K_2$	-0.017	-317.522	4.38E+06	-1.758	-1.249	0.138	-0.820

#### 4.5.7 CO<sub>2</sub> - biphasic 3 M DMCA model

In DMCA-CO<sub>2</sub> system, the liquid-liquid phase transition can be observed clearly in the loading curve depicted in Fig. 48.

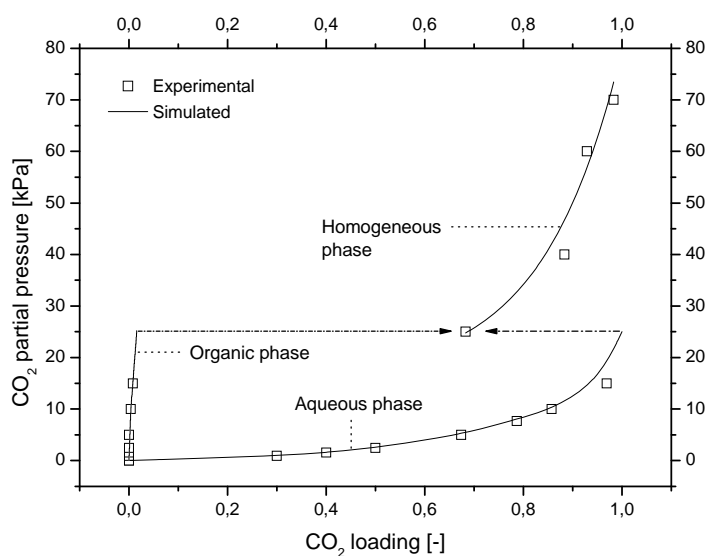


Fig. 48: Loading of CO<sub>2</sub> in 3000 mol m<sup>-3</sup> aqueous DMCA at 40°C

At CO<sub>2</sub> partial pressure below 25 kPa, the solution remained biphasic during CO<sub>2</sub> absorption. It was found that during absorption the organic phase behaves correspondingly to physical solvent, in which the CO<sub>2</sub> loading increases linearly at elevated CO<sub>2</sub> partial pressure. The importance of aqueous phase in the absorption system is more pronounced in Fig. 48 and it explain more clearly the solubility hindered effect discussed previously. The aqueous phase serves as storage for the ionic reaction product of CO<sub>2</sub> with DMCA due to their affinity to

polar solvent. Once the aqueous phase is saturated, there will be no further absorption taking place. Due to the nature of tertiary amine, the main CO<sub>2</sub>-amine reaction takes place at the interface between organic and aqueous solutions. Fig. 48 also shows the agreement of predicted with experimental values.

In the simulation part the analysis was divided into three parts:

Regime I: Aqueous phase,  $P_{\text{CO}_2} < 25\text{kPa}$

The simulated result depicted in Fig. 49 indicates the extraction of ionic reaction product of DMCA-CO<sub>2</sub> into aqueous phase.

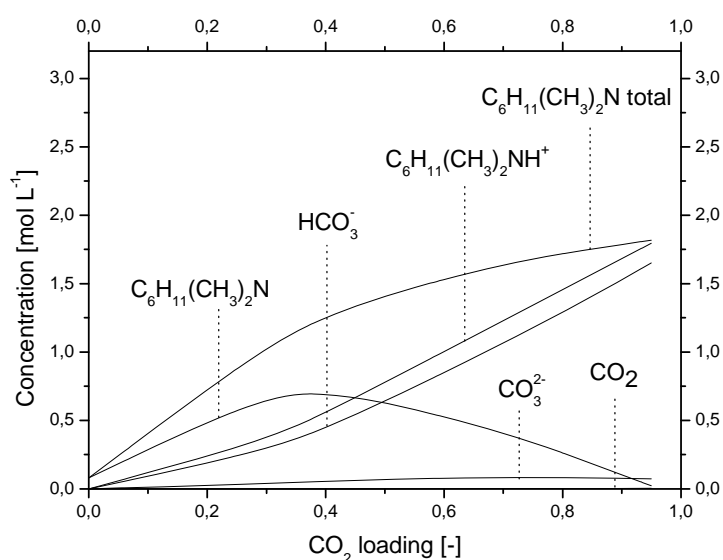


Fig. 49: Concentration profile in bulk phase aqueous phase DMCA ( $P_{\text{CO}_2} < 25\text{kPa}$ )

This can be observed by increase of the total amount of amine with increase of CO<sub>2</sub> partial pressure. At low CO<sub>2</sub> loading where minor amount of amine exist in aqueous phase, some of the extracted amines remain as free amines. However as the extraction proceeds furthermore, the solution was saturated with more amine and the free amine start to be converted to ammonium ion by water. The amine extraction is also in parallel with bicarbonate extraction. The bicarbonate in the aqueous phase was obtained by the CO<sub>2</sub> reaction in both organic and aqueous phase. Therefore the aqueous phase has a very distinctively high CO<sub>2</sub> loading compare to organic phase.

### Regime II: Organic phase, $P_{\text{CO}_2} < 25\text{kPa}$

The concentration profile of components in organic phase can be observed in Fig. 50. In organic phase, only the amount of organic phase (amine) decreases during absorption. The amine concentration in organic phase remains constant. The concentration of the ionic species is significantly lower than non-ionic species due to non-polarity nature of organic phase. However negligible amount of ammonium and bicarbonate (below 0.1M) were formed in the presence of minor amount of water.

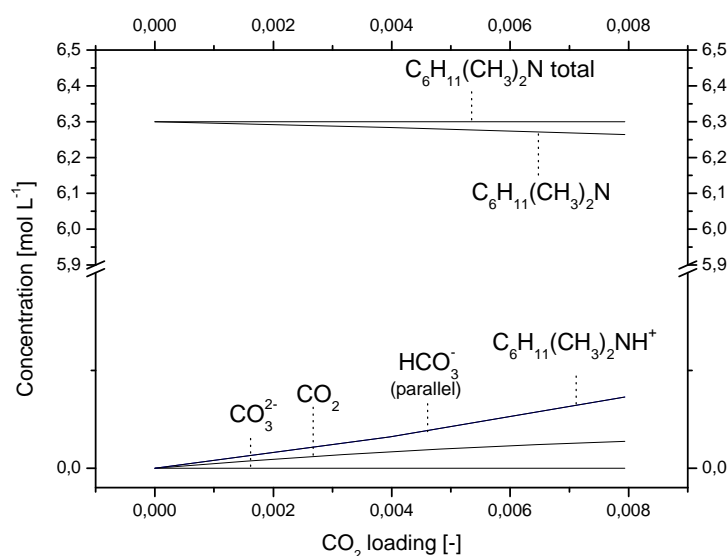


Fig. 50: Concentration profile in bulk phase organic phase DMCA ( $P_{\text{CO}_2} < 25\text{kPa}$ )

### Region III: Homogeneous phase, $P_{\text{CO}_2} > 25\text{kPa}$

The homogeneous phase was observed visually at CO<sub>2</sub> partial pressure above 25kPa. The liquid-liquid phase transition process takes place instantaneously from cloudy solutions to clear homogeneous solution. After the formation of homogeneous phase, the exhausted aqueous phase was invigorated with free amine, which is initially present in organic phase. This explains the additional absorption capability and capacity of the DMCA solutions right after the homogeneous phase is achieved, as depicted in Fig. 48 in between CO<sub>2</sub> partial pressure 25 to 40 kPa. In a deeper observation depicted in Fig. 51, once the homogeneous solution is formed, the DMCA reacts with CO<sub>2</sub> stoichiometrically based on base catalysed mechanism [29].

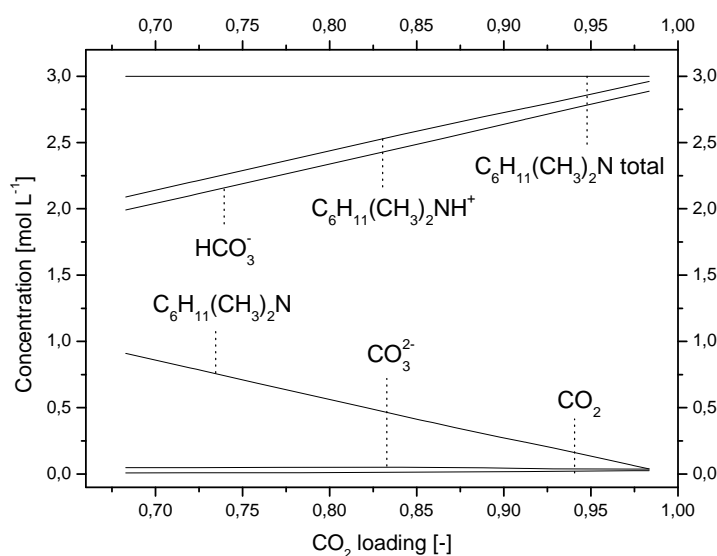


Fig. 51: Concentration profile in bulk phase homogeneous DMCA solutions ( $P_{\text{CO}_2} > 25\text{kPa}$ )

Thus ammonium as well as bicarbonate is formed and free amines are consumed in stoichiometric proportion. The amine deprotonation constants obtained from the simulation are given in Table 20. The predicted data are compared with the experimental values and it is depicted in Fig. 48.

Table 20: CO<sub>2</sub> – biphasic 3M DMCA equilibrium constant correlation refer to equation (43)

Parameters	a <sub>1</sub>	a <sub>2</sub>	a <sub>3</sub>	a <sub>4</sub>	a <sub>5</sub>	a <sub>6</sub>	a <sub>7</sub>
$K_{1 \text{ Aq. ph. (} P_{\text{CO}_2} < 25 \text{ kPa)}}$	-13,318	-2096,6	-1,25E+08	-1,696	2,146	-0,199	1,571
$K_{1 \text{ Org. ph. (} P_{\text{CO}_2} < 25 \text{ kPa)}}$	-4,218	-2085,75	-1,29E+08	-6,88	0,044	-2,53E-04	-0,569
$K_{1 \text{ Hmg. (} P_{\text{CO}_2} > 25 \text{ kPa)}}$	3033,95	-1115,4	-1,07E+08	-2493,48	-6021	1801,07	3333,17

#### 4.6 Kinetics of CO<sub>2</sub>-DPA and CO<sub>2</sub>-DMCA

The zwitterions mechanism was applied for the determination of kinetics. The kinetics expression is given in (15).

$$R_{\text{CO}_2} = \frac{[\text{CO}_2][\text{R}_1\text{R}_2\text{NH}]}{\frac{1}{k_2} + \frac{k_{-1}}{k_2 \sum k_b [\text{B}]}} \quad (15)$$

Assumptions were applied for the analysis providing occurrence of fast reaction of CO<sub>2</sub> with amine ( $k_2 \gg k_{-1}$ ):

$$\frac{1}{k_2} \gg \frac{k_{-1}}{k_2 \sum k_b [B]} \quad (44)$$

Thus the kinetic expression can be modified into second order rate equation (45).

$$R_{\text{CO}_2} = -k_2 [\text{CO}_2] [\text{R}_1 \text{R}_2 \text{NH}] \quad (45)$$

The Danckwerts plot technique was applied to determine the kinetics constants of the second order reactions of CO<sub>2</sub> with secondary amine according to reaction R. 7 in the Zwitterions mechanism. The method is applicable for fluid-fluid systems. For CO<sub>2</sub>-amine system, the technique is applicable if equation (46) and (47) hold where the Hatta number is defined in equation (48) with m and n stand for reaction order with respect to CO<sub>2</sub> and amine. Fast reaction is expected.

$$\sqrt{\text{Ha}} > 3 \quad (46)$$

$$\sqrt{\text{Ha}} \ll \frac{[\text{RRRNH}_0]}{[\text{CO}_2^*]} \quad (47)$$

$$\text{Ha} = \frac{\sqrt{\frac{2}{(m+1)} D k_{m,n} [\text{CO}_2^*]^{m-1} [\text{RRRNH}_0]^n}}{k_L^2} \quad (48)$$

Providing both the criteria are fulfilled, the Danckwerts plot equation for second order gas-liquid reaction is expressed in equation (49).

$$\frac{P_{\text{CO}_2}}{\text{Ra}} = \frac{1}{a} \left( \frac{1}{k_G} + \frac{h_{\text{CO}_2}}{\sqrt{D_{\text{CO}_2} k_2 [\text{RRRNH}_0]}} \right) \quad (49)$$

However, since the diffusivity of CO<sub>2</sub> in each amine solutions is unique and strong dependent on the composition of amine and also temperature, each experiment was done with both N<sub>2</sub>O and CO<sub>2</sub> which takes almost 5-6 hours each. Additionally, to validate the experiment, the kinetic parameter of well known MEA and DEA were determined.

#### 4.6.1 Kinetics of CO<sub>2</sub> – organic phase DPA and DMCA

For organic phase DPA, two systems are investigated, namely pure DPA-CO<sub>2</sub> (40°C) and DPA-water-CO<sub>2</sub> (40°C). For pure DPA direct absorption with CO<sub>2</sub> followed by the amine-CO<sub>2</sub> reaction is possible due to carbamate formation. In this case, based on the

zwitterions mechanism, which there's no species other than free amine itself can deprotonate the zwitterions, the concentration of the amine was assumed to decrease stoichiometrically in the reaction. The CO<sub>2</sub> absorption rate was measured in double stirred cell reactor and the typical profile of the pressure evolution are depicted in Fig. 52 and Fig. 53. Despite the difference of CO<sub>2</sub> fed to the reactor, from both figures one can observe clearly the CO<sub>2</sub> absorption and reaction rate with DPA are significantly higher than those of CO<sub>2</sub>-DMCA.

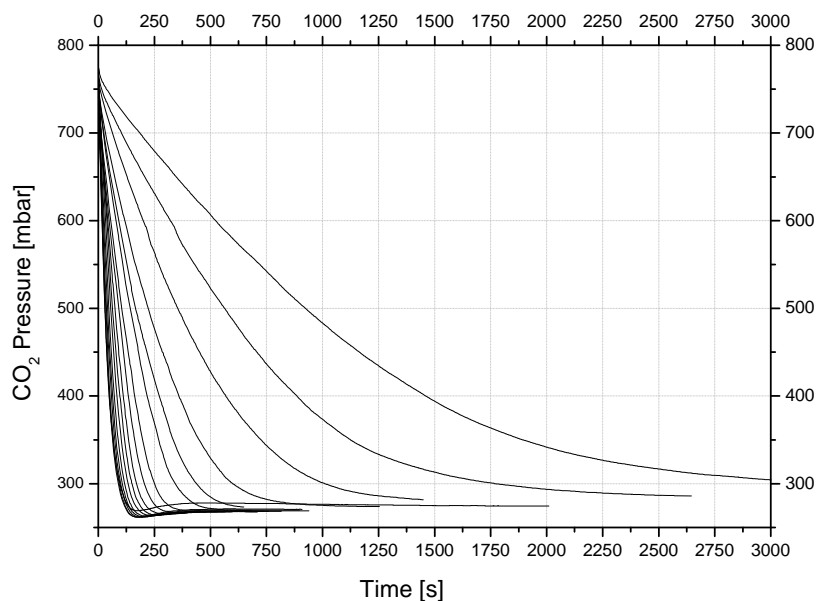


Fig. 52: Pressure profile of CO<sub>2</sub> – organic phase DPA

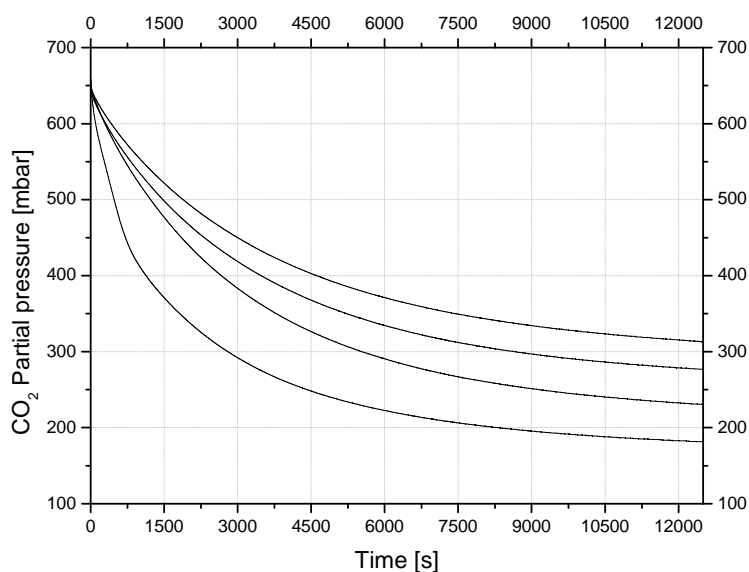


Fig. 53: Pressure profile of CO<sub>2</sub> – organic phase DMCA

The Danckwerts plots of system organic pure DPA, DPA-H<sub>2</sub>O and DMCA-H<sub>2</sub>O are depicted in Fig. 54, Fig. 55 and Fig. 56 respectively.

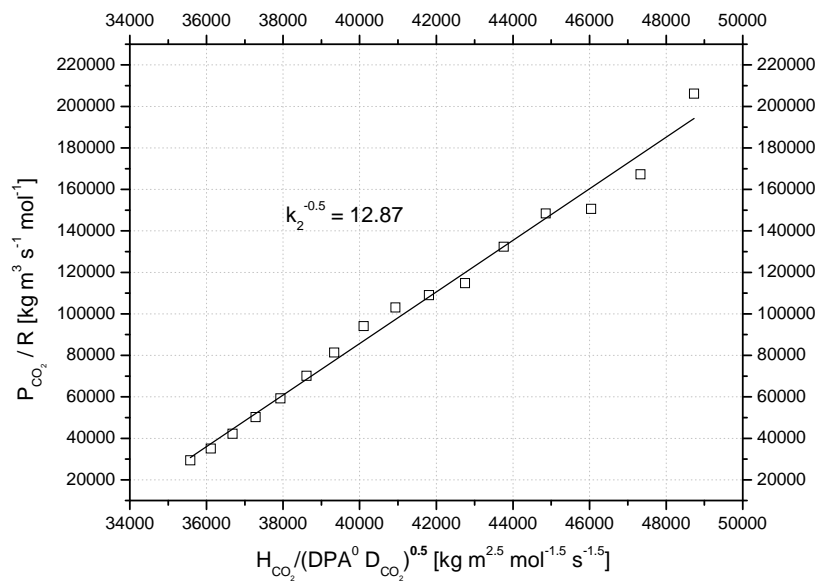


Fig. 54: Danckwerts plot of CO<sub>2</sub> – pure DPA system 3500-7500 mol/m<sup>3</sup> at 40°C

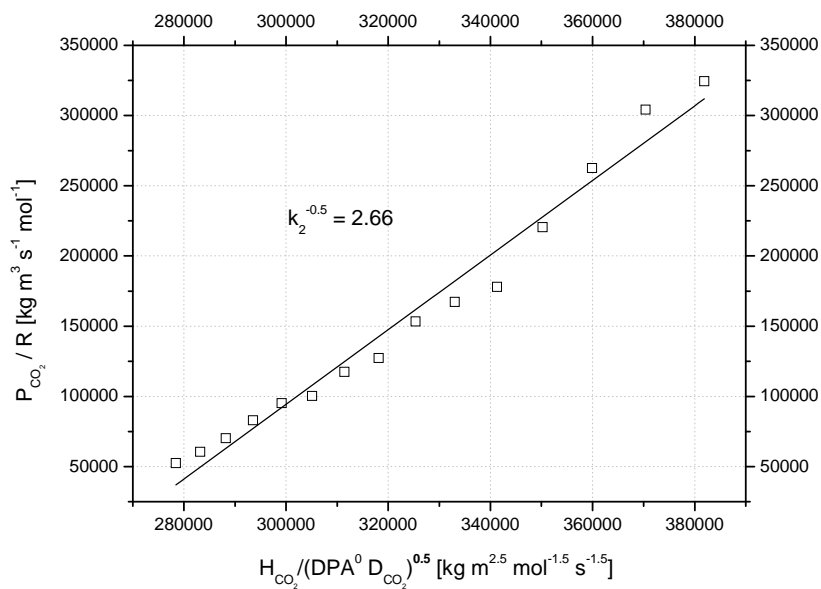


Fig. 55: Danckwerts plot of CO<sub>2</sub> – DPA-H<sub>2</sub>O system 3200-6500 mol/m<sup>3</sup> at 40°C

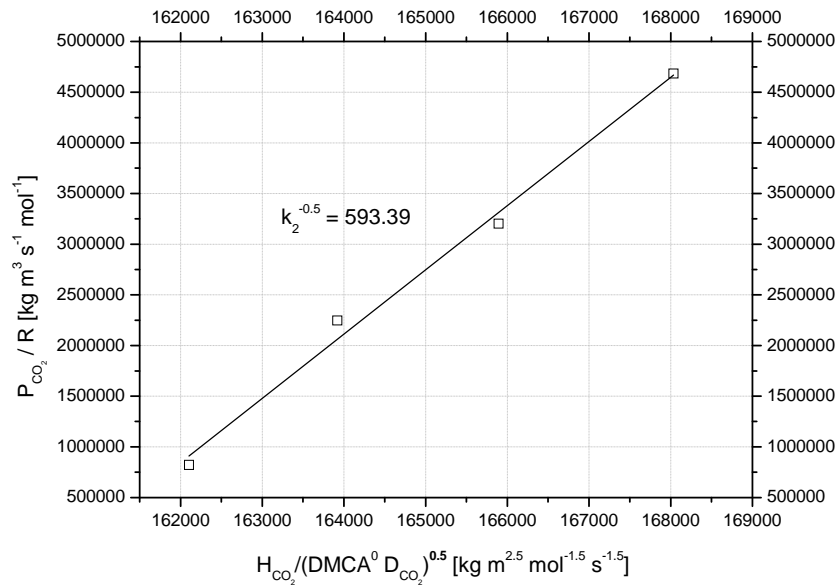


Fig. 56: Danckwerts plot of CO<sub>2</sub> – DMCA-H<sub>2</sub>O system 6200-6800 mol/m<sup>3</sup> at 40°C

For CO<sub>2</sub>-DMCA system, the investigation was carried out with DMCA-water-CO<sub>2</sub> system. Pure DMCA does not react with CO<sub>2</sub>, it absorb CO<sub>2</sub> only physically due to non-specific van der Waals interaction [29].

Table 21: Kinetics parameters of organic phase lipophilic amines

System	T [K]	Amine conc. [mol m <sup>-3</sup> ]	k <sub>2</sub> [m <sup>3</sup> mol <sup>-1</sup> s <sup>-1</sup> ]
Pure DPA	313	3500-7500*	6.04E-3
DPA-H <sub>2</sub> O	313	3200-6500	141.7E-3
DMCA-H <sub>2</sub> O	313	6200-6800	2.84E-6

\* concentration decrease was calculated stoichiometrically

#### 4.6.2 Kinetics of CO<sub>2</sub> – aqueous phase DPA and DMCA

As discussed before in chapter 4.5.7 that the CO<sub>2</sub>-amine reactions products are ionic compounds which are more stable to stay in aqueous phase. Thus the CO<sub>2</sub>-amine reactions favour polar medium. This could be observed in the kinetics constant obtained for the aqueous phase systems are higher than those obtained in organic phase. This however doesn't mean that the CO<sub>2</sub> absorption rate into aqueous phase DPA and DMCA is higher. It was

found in the experiments that the CO<sub>2</sub> absorption rates in organic phase are always higher than in aqueous phase and the rates are non-linearly dependent on the CO<sub>2</sub> partial pressure. The Danckwerts plot of system aqueous MEA, DEA and CO<sub>2</sub> are depicted in Fig. 59 and Fig. 60. The plot for aqueous phase DPA and DMCA are depicted in Fig. 57 and Fig. 58 respectively.

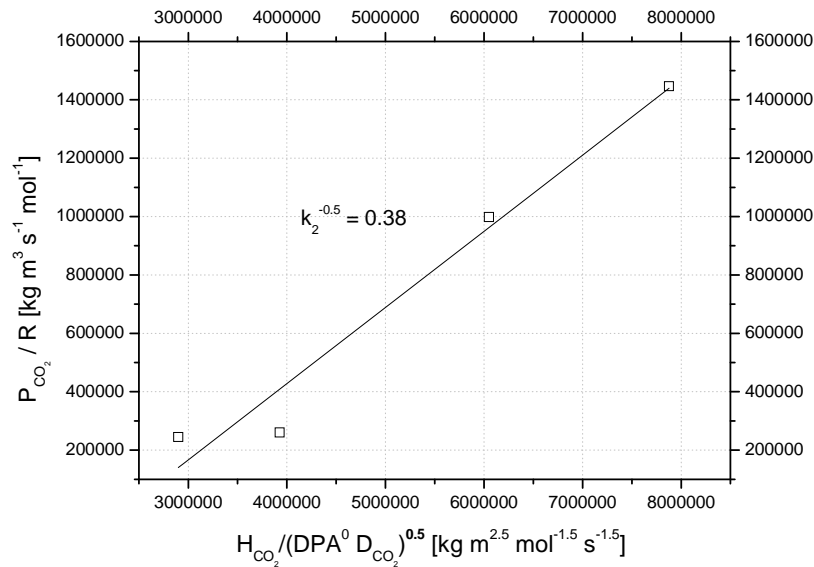


Fig. 57: Danckwerts plot of CO<sub>2</sub> – DPA system 0-300 mol/m<sup>3</sup> at 40°C

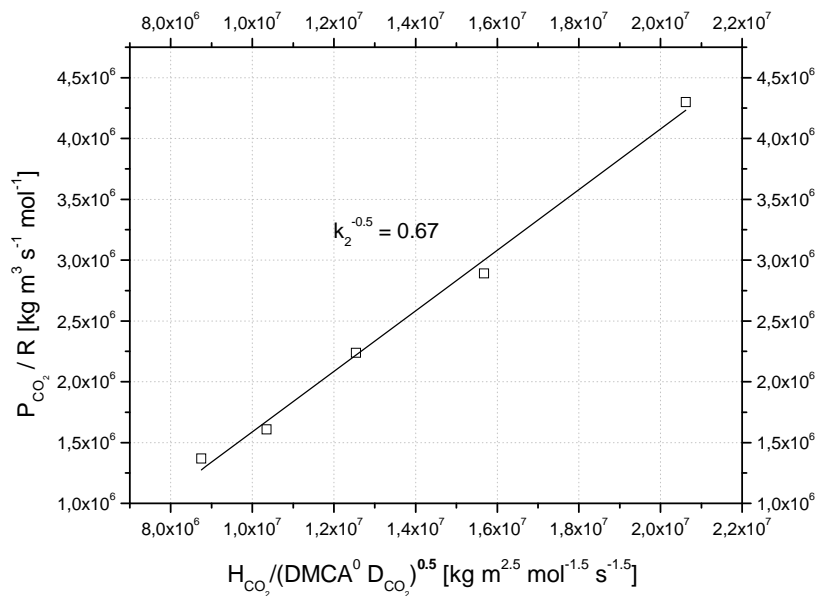
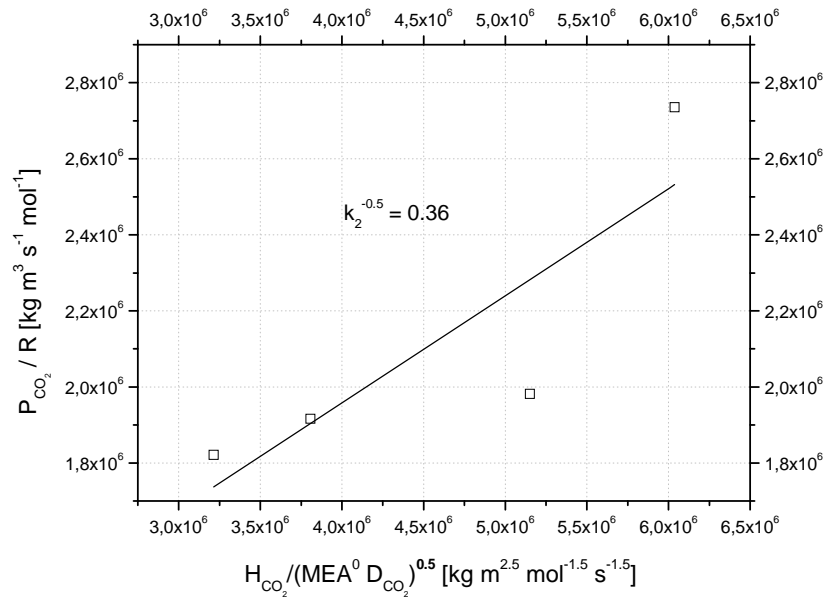
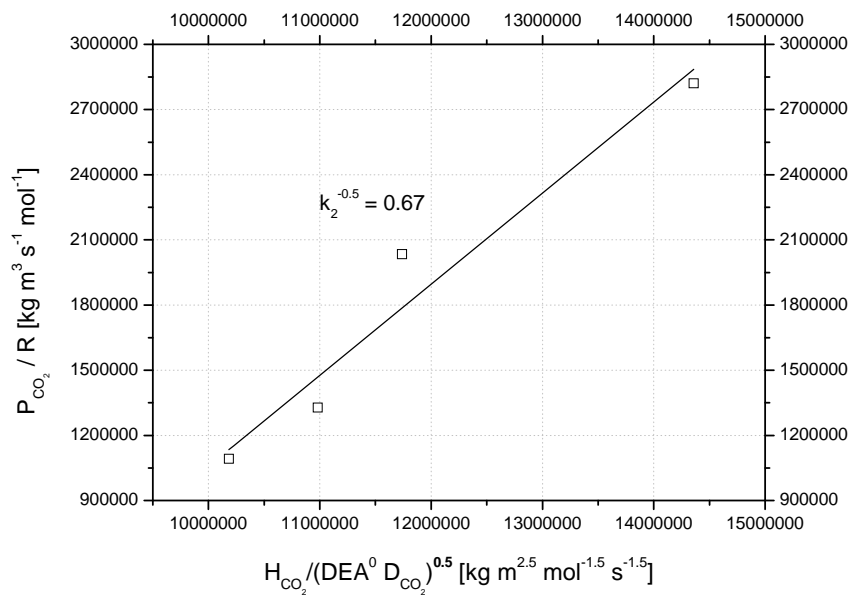


Fig. 58: Danckwerts plot of CO<sub>2</sub> – DMCA system 0-80 mol/m<sup>3</sup> at 40°C

Fig. 59: Danckwerts plot of CO<sub>2</sub> – MEA system 0-300 mol/m<sup>3</sup> at 40°CFig. 60: Danckwerts plot of CO<sub>2</sub> – DEA system 0-80 mol/m<sup>3</sup> at 40°C

The overall kinetics parameters of the aqueous phase system were given in Table 22.

Table 22: Kinetics parameters of aqueous lipophilic and alkanolamines

System	T [K]	Amine conc. [mol m <sup>-3</sup> ]	k <sub>2</sub> [m <sup>3</sup> mol <sup>-1</sup> s <sup>-1</sup> ]	T [K]	Amine conc. [mol m <sup>-3</sup> ]	k <sub>2 ref</sub> [m <sup>3</sup> mol <sup>-1</sup> s <sup>-1</sup> ]
MEA	313.15	0-300	7.72	318	0-3200	10.40 [50]
				303	0-2000	7.74 [65]
DEA	313.15	0-55	2.25	313	0-4000	1.53 [81]
				308	1000	2.5 [70]
				303	0-1500	1.10 [65]
DPA	313.15	0-300	6.84			
DMCA	313.15	0-80	2.24			

The DPA as secondary amine has comparably high reaction rate similar to that of primary alkanolamine MEA, while DMC as tertiary amine has high reaction rate comparable to secondary alkanolamine DEA.

#### 4.6.3 Kinetics of CO<sub>2</sub> – biphasic DPA and DMCA

In order to investigate the kinetics of reaction between CO<sub>2</sub> with DPA and DMCA at the interface of organic and aqueous liquid phase, a capillary reactor depicted in Fig. 13 was used. To enable better visualisation and adherence of aqueous phase on the wall of the capillary, glass was chosen as the material for capillary.

In order to obtain well-defined flow pattern of CO<sub>2</sub> – organic – aqueous phase DPA, a flow map was constructed. The flow map depicted in Fig. 61 was constructed with various flowrates of organic and aqueous DPA which give stable flow pattern within CO<sub>2</sub> flowrates 20-80 mLN/min at 25°C. The flow map is highly dependent on the liquid and gas involved as well as material and size of the capillary.

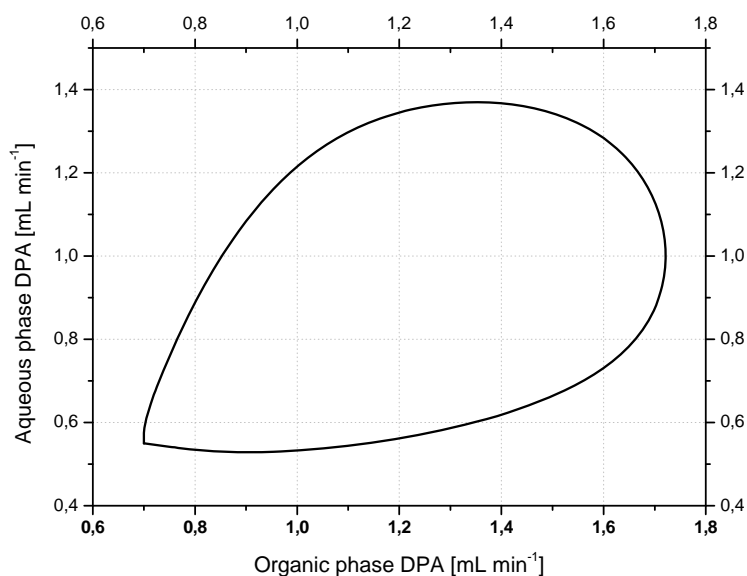


Fig. 61: Flow map of CO<sub>2</sub> – organic phase – aqueous phase DPA in 2.3 mm glass capillary

The area within the curve gives a stable flowrate. To give a better overview of the visualisation of flow pattern, the flow patterns resulted from flow configuration of 1 mL/min organic phase DPA and 0.7 mL/min aqueous phase DPA at 25-50 mLN/min CO<sub>2</sub> are depicted in Fig. 62. The continuous phase is aqueous phase DPA, while organic phase comes in contact with CO<sub>2</sub> at the top and base of gas slug cylinder. This way the solubility hindered effect could be avoided.

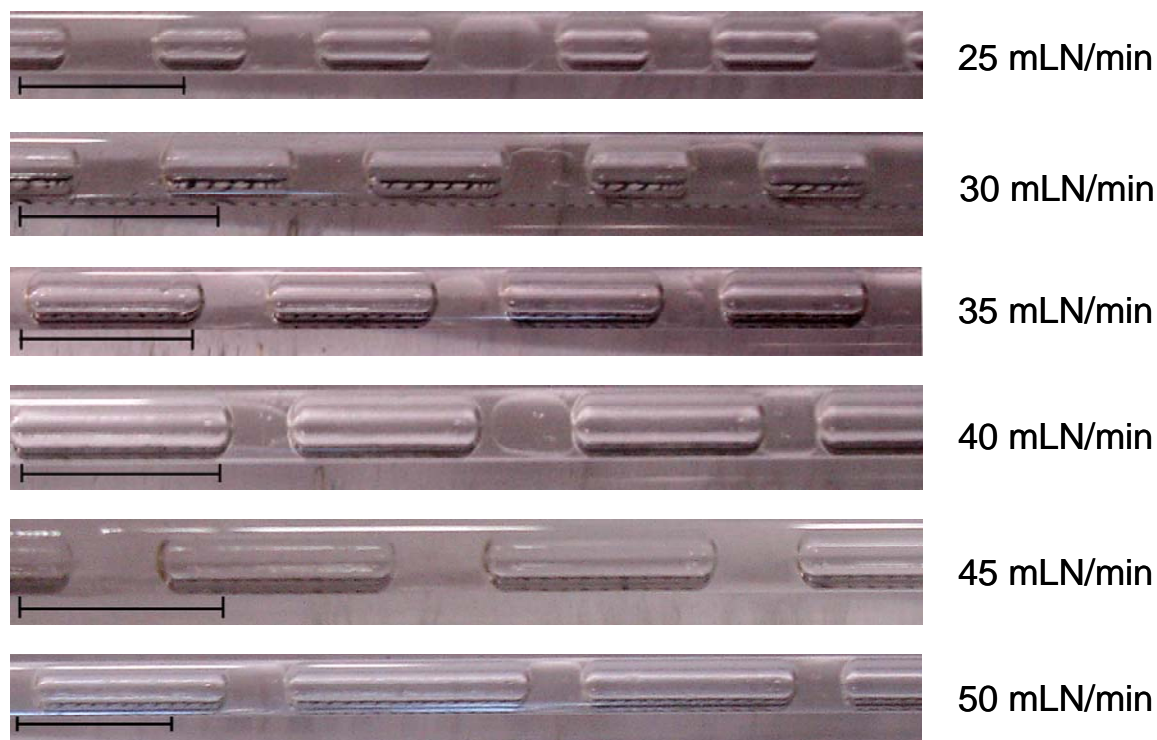


Fig. 62: Flow patterns of CO<sub>2</sub>-organic phase DPA-aqueous phase DPA (1 scale = 10 mm)

The usage of capillary reactor enables direct contact of CO<sub>2</sub> with organic and aqueous phase of DPA at the same time. However it also restricts the operating windows of the system only within the region, in which the flow of gas-liquid-liquid is stable. Result of absorption experiments with 40 mLN/min CO<sub>2</sub> at various organic and aqueous phase DPA solutions indicate possibility of additional mass transfer resistance between the organic phase DPA and gas phase CO<sub>2</sub>. This is shown by the results in Fig. 63, in which the absorption takes place mainly only within 70 cm of the capillary reactor and the total CO<sub>2</sub> loading in the liquid phase remains low (below 0.5) regardless the length of capillary as well as residence time.

This phenomenon is proposed to be caused by the presence of liquid-liquid-gas film at the interface of three phases. This can also be observed from Fig. 62, in which the organic phase DPA is floating surrounded by the aqueous phase DPA.

CO<sub>2</sub> in gas phase must be first transferred to the aqueous phase before achieving organic phase. The additional resistance by aqueous phase film resulted in CO<sub>2</sub> absorption mainly only into aqueous phase rather than organic phase. This is supported by the low total CO<sub>2</sub> loading in liquid phase because CO<sub>2</sub> did not reach the organic phase during absorption and the resistance from organic and aqueous phase does not enable CO<sub>2</sub> to contact directly the organic phase. This is also indicated by the result shown in Fig. 63.

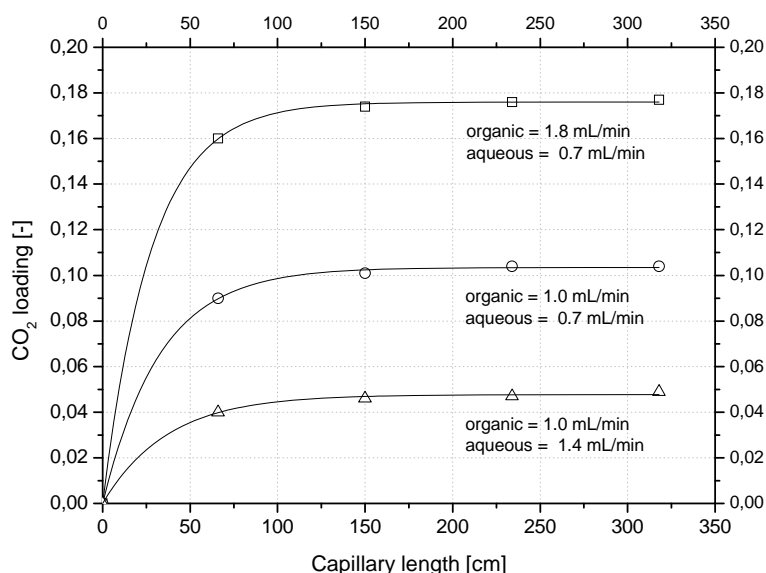


Fig. 63: CO<sub>2</sub> loading profile in liquid phases in a capillary reactor (40 mLN/min CO<sub>2</sub>)

With increase of aqueous phase's flowrate, the hold up of aqueous phase in the capillary increases and it hampers the direct contact of CO<sub>2</sub> with organic phase DPA. Further investigation with flow configuration 1.0 mL/min organic phase and 0.7 mL/min aqueous

phase DPA under various gas flowrates was carried out. With increase of gas holdup in capillary, a higher CO<sub>2</sub> loading was achieved.

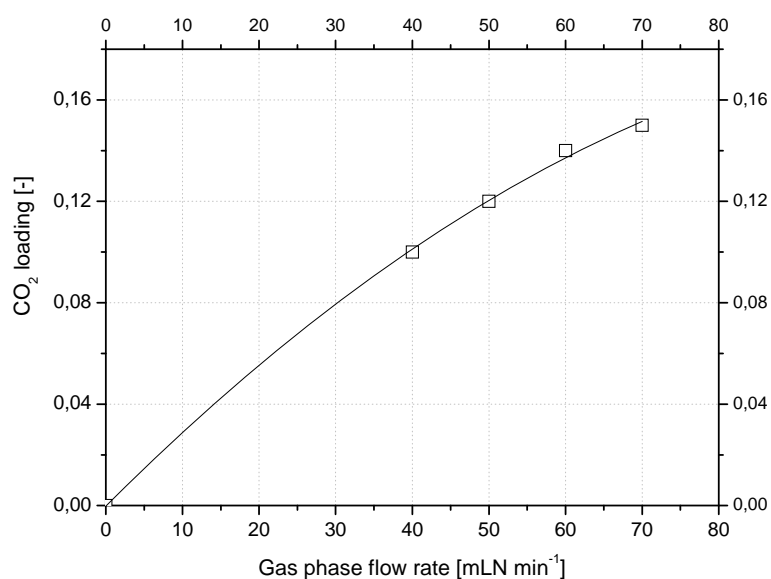


Fig. 64: CO<sub>2</sub> loading profile in liquid phases in a capillary reactor (elevated CO<sub>2</sub> flowrate)

This could be expected not only because of increase of interfacial area between gas-liquid phase, but also from higher probability of contact between organic phase with gaseous CO<sub>2</sub> as depicted in Fig. 62. With increase of gaseous CO<sub>2</sub> hold-up in the capillary reactor, the distance of organic phase DPA to gaseous CO<sub>2</sub> slug is reduced, leading to a better absorption. Due to the presence of the gas-liquid-liquid system, the kinetics measured in Table 23 corresponds to the kinetics of CO<sub>2</sub>-with aqueous phase.

Table 23: CO<sub>2</sub> absorption rate at various flowrates of organic and aqueous phase DPA

Process parameter			Absorption rate [mol CO <sub>2</sub> mol amine <sup>-1</sup> s <sup>-1</sup> ]
CO <sub>2</sub> [mLN min <sup>-1</sup> ]	Organic DPA [mL min <sup>-1</sup> ]	Aqueous DPA [mL min <sup>-1</sup> ]	
40	1	1.4	0.01
40	1	0.7	0.023
40	1.8	0.7	0.041

Changing the material of capillary reactor with other hydrophilic material might reverse the distribution of the liquids, in which organic phase DPA is the continuous phase, while

aqueous phase DPA is dispersed phase. However due to the presence of gas-liquid-liquid film, the kinetics measured will correspond to kinetics of organic phase DPA with gaseous CO<sub>2</sub>. Thus further research must be carried out to determine more suitable method for measuring the kinetics of three phases gas-liquid-liquid systems.

#### 4.7 DPA precipitation phenomena

DPA precipitation wasn't observed in kinetics determination experiment due to the relatively low amount of CO<sub>2</sub> gas applied. However precipitation occurs once high amount of CO<sub>2</sub> and its reaction products are formed in the DPA solution. The precipitates formed at high CO<sub>2</sub> loading are salts of protonated amine (ammonium) with carbonate, bicarbonate and carbamate ion. Even though the stability of the precipitates is relatively low (decompose starting from 40°C), its occurrence in absorption column will cause a serious problem. For the lipophilic amine DPA-water system, increasing temperature does not resolve the precipitation problem completely. As the volatility of amine increases at high temperature, the precipitation will take place also along the path passed by gas because the gas phase comprises amine and water vapor as well as CO<sub>2</sub>. These three components are the main reactants to form precipitates.

To resolve this problem, a water wash unit after the regeneration column will be required. In the experiment with initially high concentration DPA-H<sub>2</sub>O solution (~75% wt. DPA), less than 10% wt. CO<sub>2</sub> could be absorbed into the DPA-H<sub>2</sub>O solution without precipitation. The influence of water to avoid precipitation can be observed in Fig. 65.

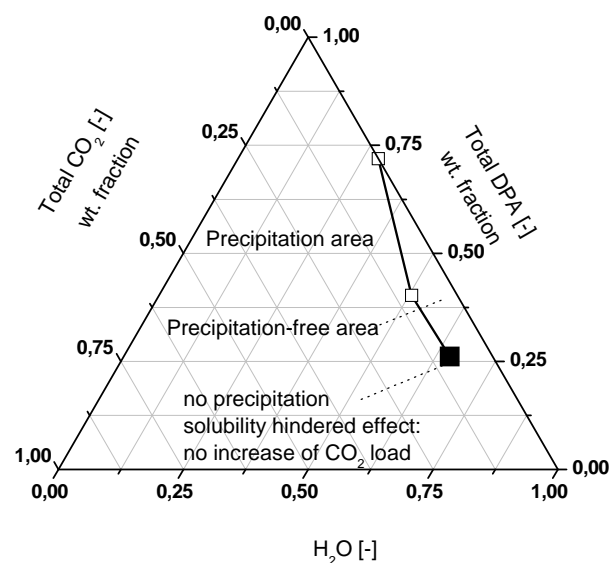


Fig. 65: DPA-H<sub>2</sub>O-CO<sub>2</sub> precipitation diagram

Addition of water into the DPA-H<sub>2</sub>O-CO<sub>2</sub> solution could avoid precipitation however since water is polar component, the CO<sub>2</sub> absorption capacity could not be enhanced.

Addition of 5% wt. tertiary amine DMCA into 75% wt. DPA in H<sub>2</sub>O solution, as depicted in Fig. 66, can both resolve the precipitation issue and increase the CO<sub>2</sub> absorption capacity in the solution.

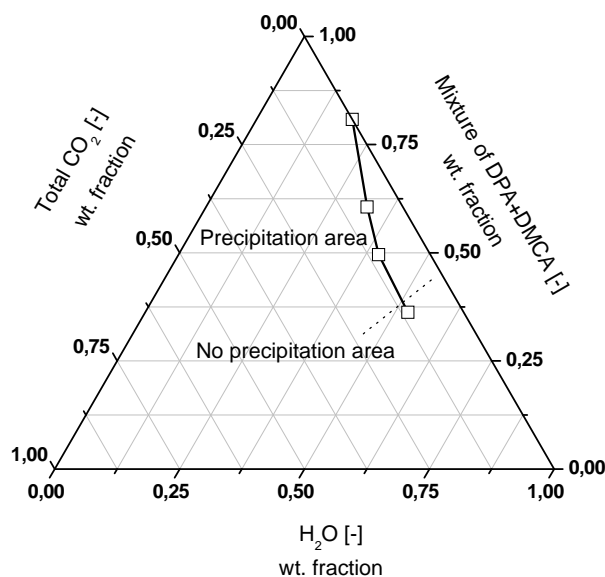


Fig. 66: DPA-DMCA-H<sub>2</sub>O-CO<sub>2</sub> precipitation diagram

Thus the tertiary amine in the lipophilic amine solution serves not only to provide more CO<sub>2</sub> absorption capacity but also to avoid precipitation. For this reason, investigation of the lipophilic amine mixtures is of an interest for commercial application. In chapter 4.9, investigation of the DPA-DMCA mixtures characteristic to meet practical application is discussed.

#### 4.8 Enthalpic study of DPA and DMCA solutions

The energy requirements to regenerate loaded amine solutions could be broken down to several purposes. Among the purposes discussed in the previous chapter, the absorption enthalpy represents the energy required to revert the reactions during absorption as well as the dissolved gas's liquefaction enthalpy. Thus it could be used to compare semi-quantitatively the approximate energy requirement. Two methods have been applied to measure the absorption enthalpy, namely by direct measurement using reaction calorimeter and by means

of van't Hoff thermodynamic equation. Only the data of the latter method are presented in this work. The influence of the temperature scanning to the CO<sub>2</sub> partial pressure for calorimetric measurement is depicted in Fig. 67.

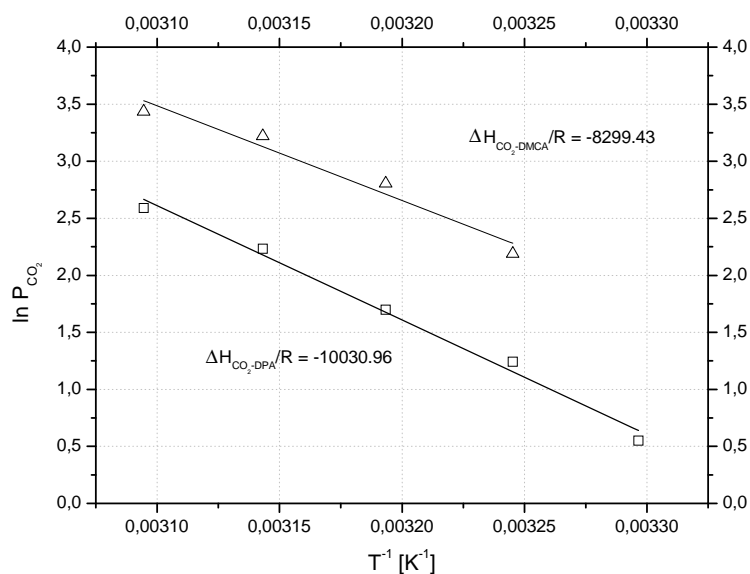


Fig. 67: CO<sub>2</sub> partial pressure at elevated temperature

Due to the higher base strength of lipophilic amines compare to alkanolamines, the absorption enthalpy of DPA (secondary amine) and DMCA (tertiary amine) are at the order of primary and secondary alkanolamine. The calculated absorption enthalpy along with the values of conventional alkanolamine solutions are given in Table 24.

Table 24: Absorption enthalpy of CO<sub>2</sub> - lipophilic and alkanolamines

Amine	Absorption enthalpy	
	[kJ mol <sup>-1</sup> ]	
MEA	-82	[18]
DEA	-69	[18]
MDEA	-49	[18]
DPA	-84.230	
DMCA	-68.997	

However the overall economic feasibility of the application of lipophilic amines for CO<sub>2</sub> absorption does not rely mainly on the absorption enthalpy, but also on the regeneration

temperature of lipophilic amines which is significantly lower than that of alkanolamines. This is discussed in the following chapter 4.9.

## 4.9 Mixtures of DPA and DMCA

In industrial application, primary or secondary amines are mixed with tertiary amines to combine their characteristics. Due to the fast reaction rate of primary and secondary amine with CO<sub>2</sub>, they are designated activator. On the other hand the tertiary amine provides high CO<sub>2</sub> absorption capacity.

The lipophilic amines have unique characteristics that their absorption is highly influenced by the presence of water. Without sufficient amount of water in the solutions, absorption of secondary amine could be followed by precipitation. For tertiary lipophilic amines, the full capacity of tertiary amine can not be exploited without sufficient amount of water. Thus, knowledge of the optimum composition of solution is indispensable.

Systematic experimental investigation was carried out not only on the concentration of the amine and also the ratio of activator to tertiary amine but also on the operating temperature to regeneration. The results were also compared with that of mixture of commercial alkanolamine.

### 4.9.1 Regeneration temperature

Systematic experimental investigation was carried out not only to determine the range of amine concentration and the ratio of activator to tertiary amine but also to determine the operating temperature for regeneration. For this purpose a standard test solution of 2.5 N binary mixture of N,N-Dipropylamine and water was used. The selection of the amine is based on the nature of secondary amines which are more difficult to be regenerated than tertiary amines.

For determining suitable regeneration temperature in the test, the initial solution was loaded with 300 mL/min 200 mbar CO<sub>2</sub> to ensure less influence of carbamate hydrolysis which might arise at high loading [1]. A loading 0.7 mole CO<sub>2</sub>/mole amine was achieved. Samples were regenerated at elevated temperature 70-90°C.

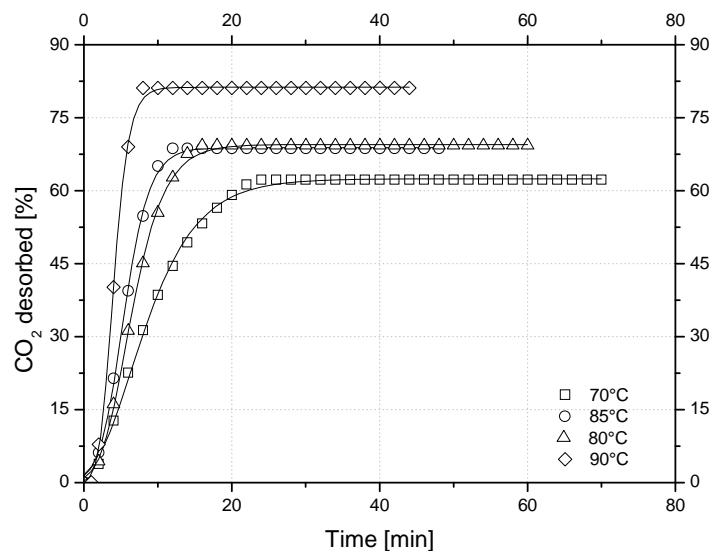


Fig. 68: Regeneration characteristics of 2.5N DPA solutions at elevated temperature

Results presented in Fig. 68 indicate the apparent optimum operating temperature for regeneration at the specified condition at 80°C. Increase of temperature up to 85°C does not affect the regeneration characteristic significantly. Temperature 90°C is not considered furthermore as the vapour pressure of solutions is significantly high at the respective temperature. It was also observed that the high regeneration effect at 90°C is contributed from the closure with boiling point of water. For further experiments, 80°C temperature is used for the entire desorption experiments.

#### 4.9.2 Influence of amine concentration

In industrial process the amine concentration applied is based on technical and economic consideration. High amine concentration solution is preferred since it has high absorption capacity with the expense of lower molecular efficiency in terms of mole CO<sub>2</sub>/mole amine and high cost. To determine the operating windows for applicable amine concentration, the solution with mole ratio 1:2 DPA:DMCA was used. This composition was selected as the upper margin due to the fact that high concentration of activator might lead to the most undesired properties: precipitation. CO<sub>2</sub> at flowrate 300 mLN/min and concentration 200 mbar was used. Tested under the given conditions, mixture of lipophilic amines' absorption-regeneration characteristics are depicted in Fig. 69 and Fig. 70.

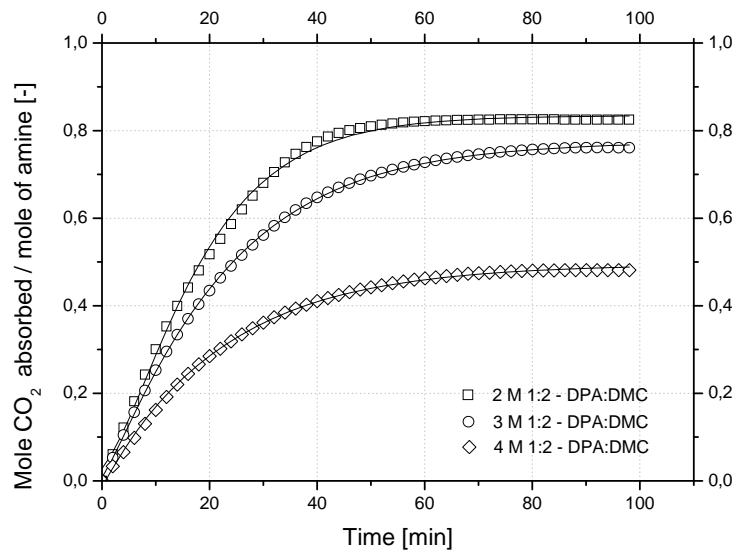


Fig. 69: DPA-DMCA absorption characteristics with concentration increase

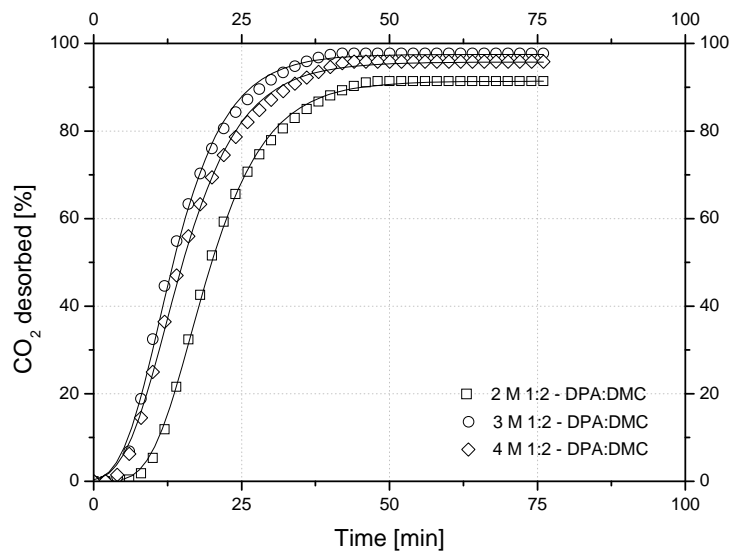


Fig. 70: DPA-DMCA regeneration characteristics of with concentration increase

With increase of amine concentration, absolute capacity will increase however with the expense of the loading (mole CO<sub>2</sub>/mole amine). It can be observed that mixtures of amine with concentration 4 M has significantly low absorption loading. This is more apparent in biphasic amine solution because of the ‘solubility hindered’ effect associates with the concentration of water in amine solution which does not present in water-soluble alkanolamine.

The influence of water to the absorption capacity is more significant with the presence of tertiary lipophilic amines in the solution. In absorption process, tertiary lipophilic amine similar to alkanolamine reacts with water according to base catalysed hydration of CO<sub>2</sub> mechanism. Dependent on the ratio of the mole of tertiary lipophilic amine to water, deficiency in the amount of water will lead to reduction of absorption capacity. This was observed especially when the high concentration solutions of tertiary lipophilic amines did not achieve homogeneous phase at the end of absorption. Thus the absorption capacity is limited by the composition in the solutions.

Additional increase of concentration of amine more than 4 molar is not beneficial due to the solubility effect. Moreover the viscosity of solutions increases significantly along with the increase of amine concentration. The comparison depicted in Fig. 71 indicates the concentration of amines up to 3 M to be the safe upper margin.

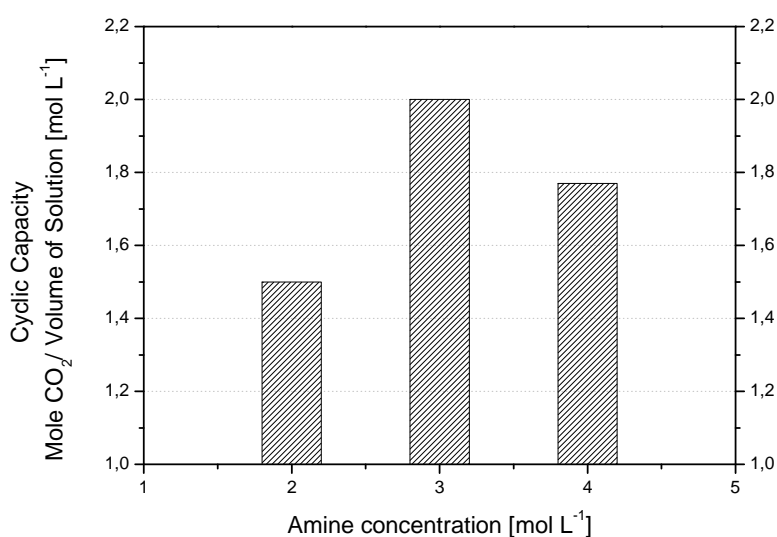


Fig. 71: Net capacity of 3 M - 1:2 DPA:DMCA with concentration increase

Thus the amine concentration up to 3 M enables full exploitation of solution's absorption capacity without precipitation issue even under high CO<sub>2</sub> partial pressure applied in industrial process (200 mbar).

#### 4.9.3 Influence of activator to tertiary amine ratio

Once the operating window for amine concentration was determined, the ratio of the the activator (DPA) to tertiary amine (DMCA) could be determined subsequently. For this

purpose the CO<sub>2</sub> at flowrate 300 mLN/min and concentration 200 mbar was used. The results are depicted in Fig. 72 and Fig. 73.

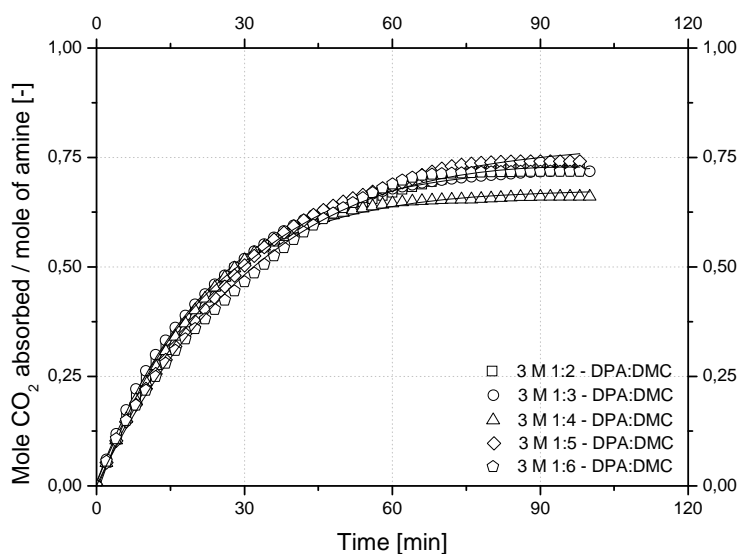


Fig. 72: DPA-DMCA absorption characteristics with amine ratio variation

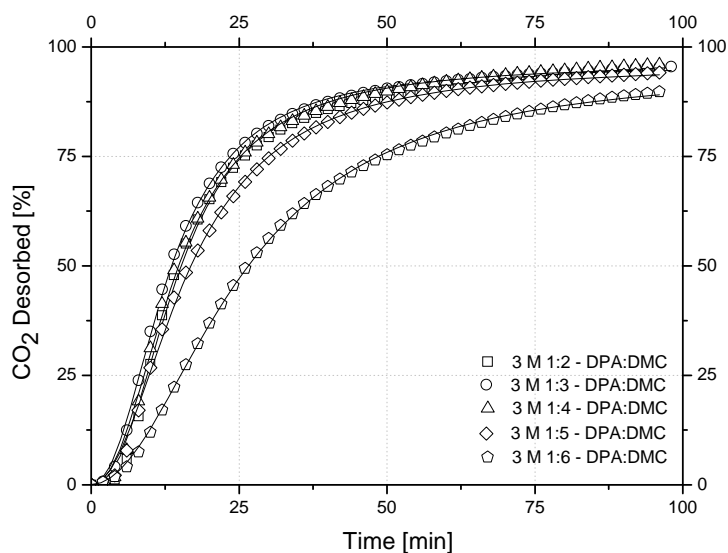


Fig. 73: DPA-DMCA regeneration characteristics with amine ratio variation

Similar absorption and regeneration rates were observed for solutions having mole ratio DPA to DMCA up to 1:4 and. All initial solutions were biphasic and only solutions with ratio DPA:DMCA up to 1:4 became homogeneous phase during absorption at the respective

highlighted point depicted in Fig. 72. Lower absorption rate was observed as the ratio of DPA:DMCA increase due to lower reaction of CO<sub>2</sub> with tertiary amine compare to secondary amine.

Result of one experiment of 3M 1:3 DPA:DMCA regeneration by heating from 40°C is given in Fig. 74. The maximum desorption rate was obtained also when the solution reached thermomorphic phase separation, which is the desired effect that is expected from biphasic solvent.

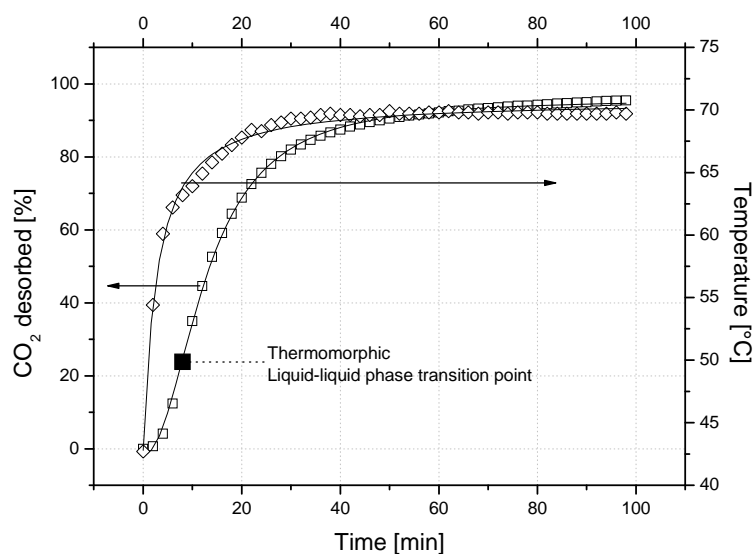


Fig. 74: 3 M 1:3 – DPA:DMCA regeneration process at 70°C

It is also observed that the loaded solutions which remained two phases after absorption, i.e. initially two phases during regeneration did not exhibit fast desorption kinetics. This is due to the fact that in these solutions due to the solubility limitation, most of the amine present in the organic phase and less amount of amine in aqueous phase does not provide large enough driving force to diffuse out of the aqueous phase. This phenomenon is similar to the phenomenon at the end phase of desorption when most of the amine presents in organic phase and it takes more effort for the small concentration of amine in the aqueous phase to diffuse to the organic phase.

The loading characteristic of the solvent described later indicates partial pressure of CO<sub>2</sub> at about 500-600 mbar would load the solution into its full capacity. In general the solutions exhibit characteristics similar to that of chemical absorbent with additional high capacity even at low partial pressure of CO<sub>2</sub>.

#### 4.9.4 Performance comparison with commercial mixed alkanolamine

The mixture of ethanolamine (MEA) with methyldiethanolamine (MDEA) and 2-amino-2-methyl-1-propanol (AMP) and MDEA served to compare the performance of lipophilic amine with commercial alkanolamine. Higher concentration of CO<sub>2</sub>, which is 400 mBar, provided by dilution with N<sub>2</sub> with total flow 300 mLN/min was used for this purpose. The result is depicted in Fig. 75.

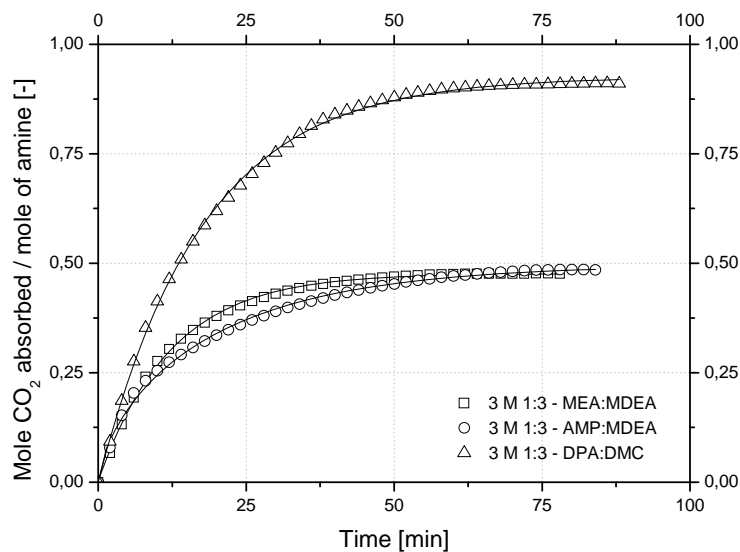


Fig. 75: Absorption comparison: DPA-DMCA mixture with alkanolamine mixtures

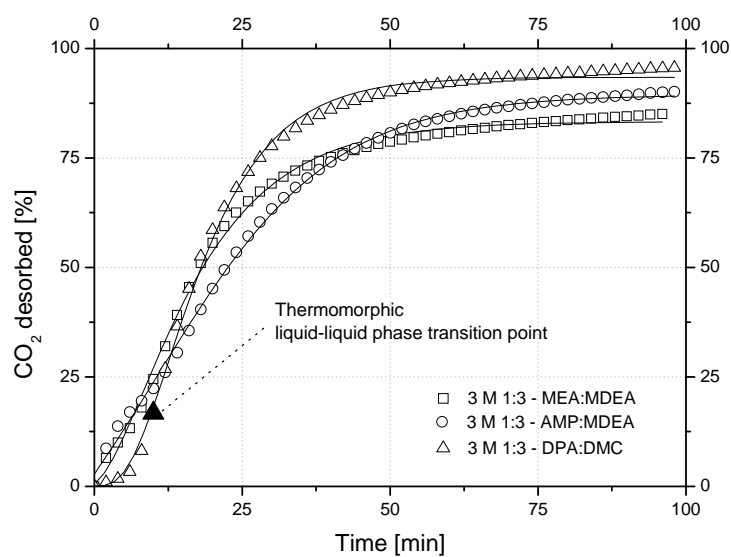


Fig. 76: Regeneration comparison: DPA-DMCA mixture with alkanolamine mixtures

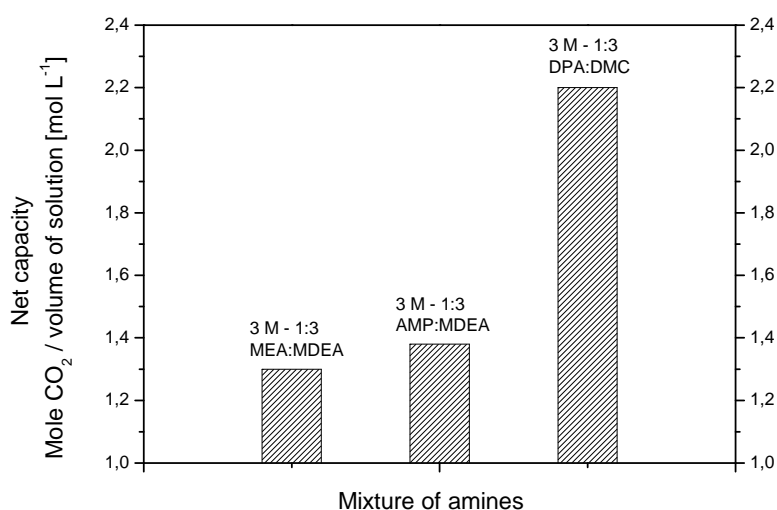


Fig. 77: Net capacity comparison: DPA-DMCA mixture with alkanolamine mixtures

A contrast high absorption reaction kinetics and capacity of lipophilic amines is observed compare to commercial alkanolamine. Desorption of lipophilic amine is enhanced by liquid phase separation. Once the liquid-liquid phase separation occurs, as shown in the figure above, desorption of CO<sub>2</sub> is enhanced rapidly. Thus the net capacity of the lipophilic amine solutions is approximately 60% higher than that of AMP-MDEA under the same experimental condition.

The thermodynamic approach to rank the solvent performance was conducted according to the method developed by Hasse – Stuttgart [55]. The method analyses the amount of minimum solvent requirement and minimum stripping steam requirement at respective pressure and temperature of the process for infinite separation capacity. For comparison purpose, CO<sub>2</sub> with inlet partial pressure 120 mbar is applied and 12 mbar CO<sub>2</sub> is expected to be present in sweet gas.

The absorption and desorption equilibrium curves are based on 1 bar pressure absorption and 2 bar regeneration providing pure 1 atm CO<sub>2</sub> is obtained at the top of the desorption column. Moreover the limiting case infinite number of separation stages was applied to link the absorption and regeneration operating line. The result of the aqueous solution 3M 1:3 DPA:DMCA with regeneration temperature 70°C is depicted in Fig. 78 and Fig. 79.

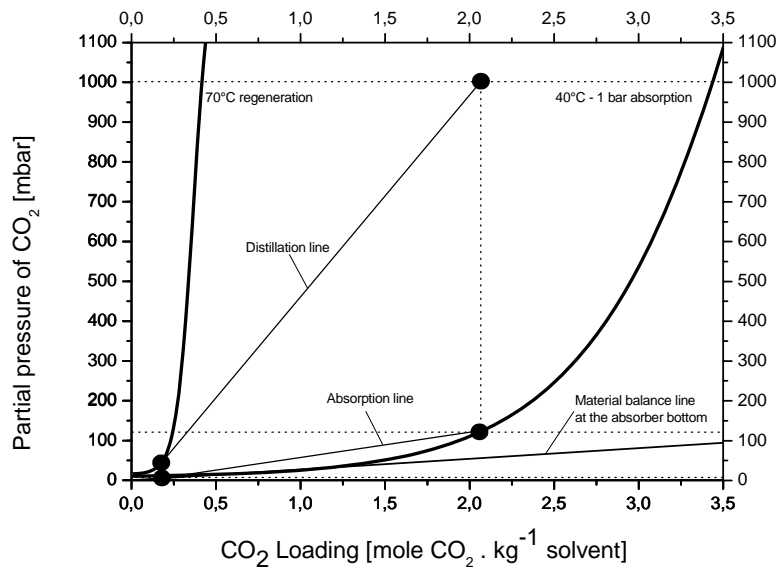


Fig. 78: Theoretical absorption-regeneration operating lines of 3 M 1:3 - DPA:DMCA

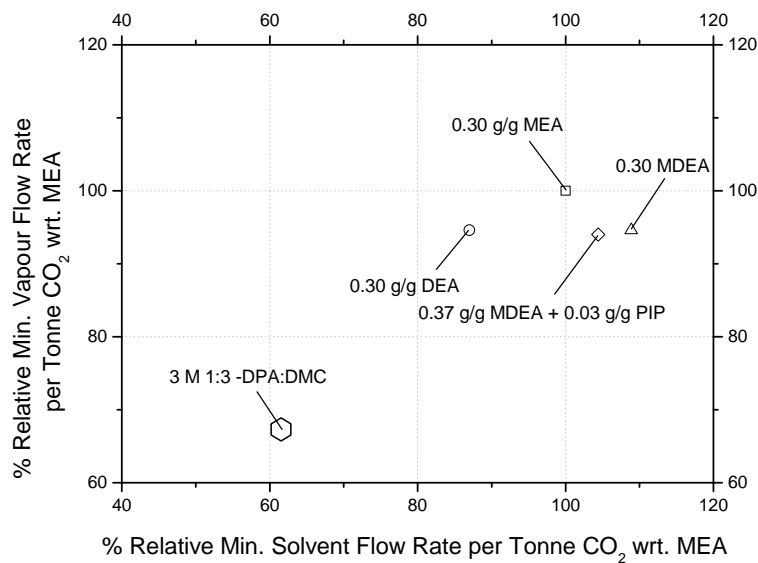


Fig. 79: Theoretical comparison of 3 M 1:3 – DPA:DMCA to standard solvents

The DPA-DMCA regeneration which was carried out at 70°C solution temperature requires approximately 30% less vapour than 0.3 g/g MEA reference solutions with regeneration using 2 bar steam (corresponds to 120°C). Moreover it is also less than other cited solutions given in the correspond literature. The minimum solvent requirement is also

approximately 35% less than that of 0.3 g/g MEA and comparable to that of other cited solutions.

Enthalpic measurement carried out with the method discussed in chapter 4.8 for CO<sub>2</sub> - 3M 1:3 DPA:DMCA yield -73.986 kJ/mol absorption enthalpy. The value agree well in between those of DPA (-84.23 kJ/mol) and DMCA (-68.997 kJ/mol) and only 7.23% higher than 3 M DMCA.

#### 4.9.5 Solvent degradation

Preliminary tests of lipophilic amines mixtures stability were also carried out. Degradation of the amines could be caused by formation of irreversible by-products from side reactions, oxidation and thermal degradation would be the main causes [43].

##### 4.9.5.1 Thermal degradation

In the experiment, the contact with free oxygen was maintained minimum, thus the degradation due to oxidation could be wiped out. Moreover, only CO<sub>2</sub> and N<sub>2</sub> were used, no COS or SO<sub>x</sub> was applied in the gas line. Thus the main deactivation amine in the experiment would be due to thermal degradation.

For the purpose of the stability test, the mixture of 3M 1:3 - DPA:DMC was applied for repetitive absorption with and regeneration at 80°C. CO<sub>2</sub> with partial pressure 400 mbar was used. The result of the run test is given in Fig. 80.

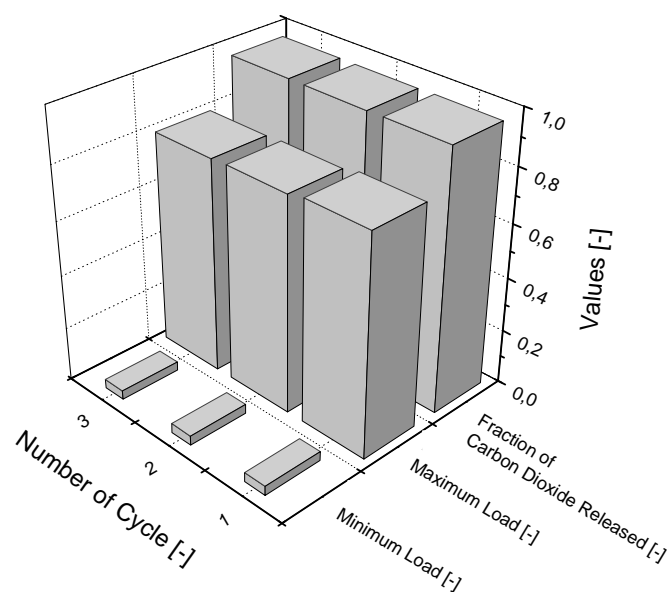


Fig. 80: 3M 1:3 – DPA:DMC repetitive absorption-regeneration performance

A good stability was observed in the experiments. This is indicated by the maximum load and net capacity of CO<sub>2</sub>, which remained stable in the range of less than 4%. A low regeneration temperature might minimise the thermal degradation of the amines. The stability is proposed also due to the low regeneration temperature below 100°C. For alkanolamine the thermal degradation is significant at temperature above 205°C, while the carbamate polymerisation is significant at temperature above 100°C [61].

#### 4.9.5.2 Oxidative degradation

The amine solvents for CO<sub>2</sub> absorption are known to be prone to oxidative degradation. The oxidative degradation product is of interest since it is formed specifically dependent on the specific amine molecule, operating temperature, gas phase composition, material of construction, etc. Numerous investigations on amine's oxidative degradation have led to numerous reactions paths with nonlinear reaction order dependent on amine concentration [13], [74]. This is caused by the complexity related to specific experimental and operational condition. Investigations carried out by Chi and Rochelle reveal the possibility of corroded column construction material, i.e. iron steel, to act as homogeneous catalyst in the amine degradation reaction [22]. Carbon dioxide was found to inhibit the oxidative degradation in amine solutions due to the competitive absorption of CO<sub>2</sub> along with O<sub>2</sub> into the amine solutions [12], [74].

In the preliminary oxidative degradation experiments, pure O<sub>2</sub> was introduced to the solutions in order to identify qualitatively the oxidative degradation product of DPA and DMCA. This way we can minimise the interference of other gases in the degradation process and obtain better insight of the oxidative degradation product. DPA-H<sub>2</sub>O and DMCA-H<sub>2</sub>O solutions at concentration 3M were contacted with pure O<sub>2</sub> for six hours at 40°C in a glass bubble column. The liquid samples were analyzed using GC/MS to identify the molecular weight fragments and thus identify the species in the solutions. The results are shown in Fig. 81 - Fig. 84.

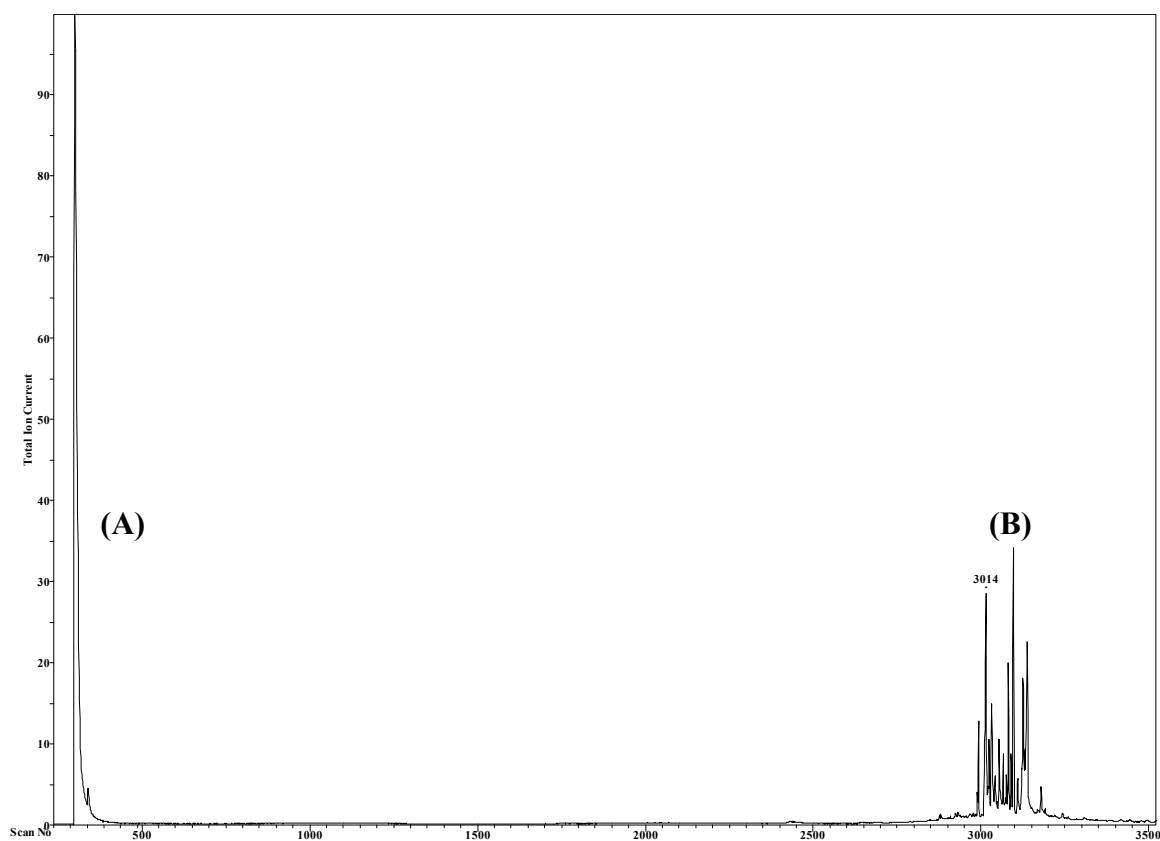


Fig. 81: Chromatogram of 3M DPA-H<sub>2</sub>O-O<sub>2</sub> system (overall)

Analysis with DPA with purum purity grade indicated that the peak A in Fig. 81 is pure DPA while the numerous peaks B are oxidative degradation products. Water is not displayed in all of the chromatograms. Due to the strong interactions among the degradation products, they could not be fully separated in this experiment. However their molecular weight fragments could be analysed to identify the molecular size of species in the sample. Multiple degradation products in peaks B have significantly higher molecular weight compare to DPA itself. This is confirmed from the molecular weight fragment diagram in Fig. 82.

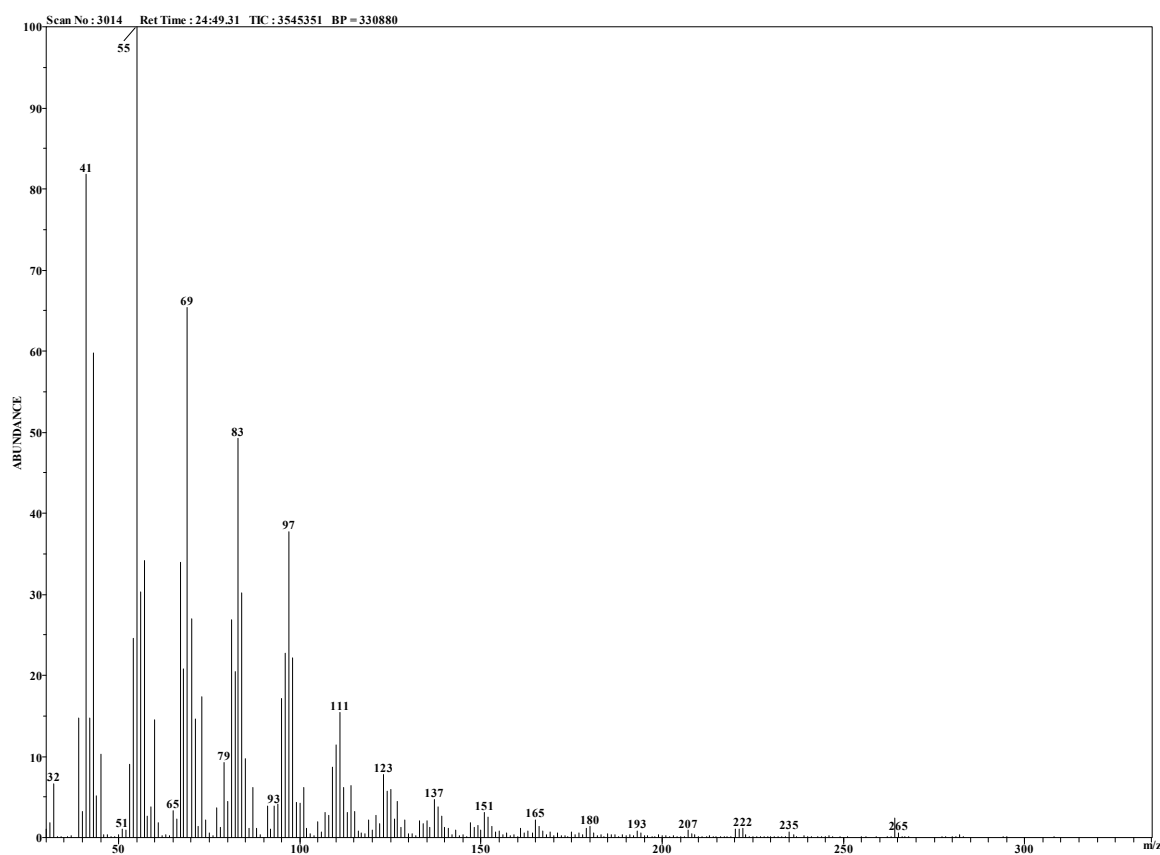
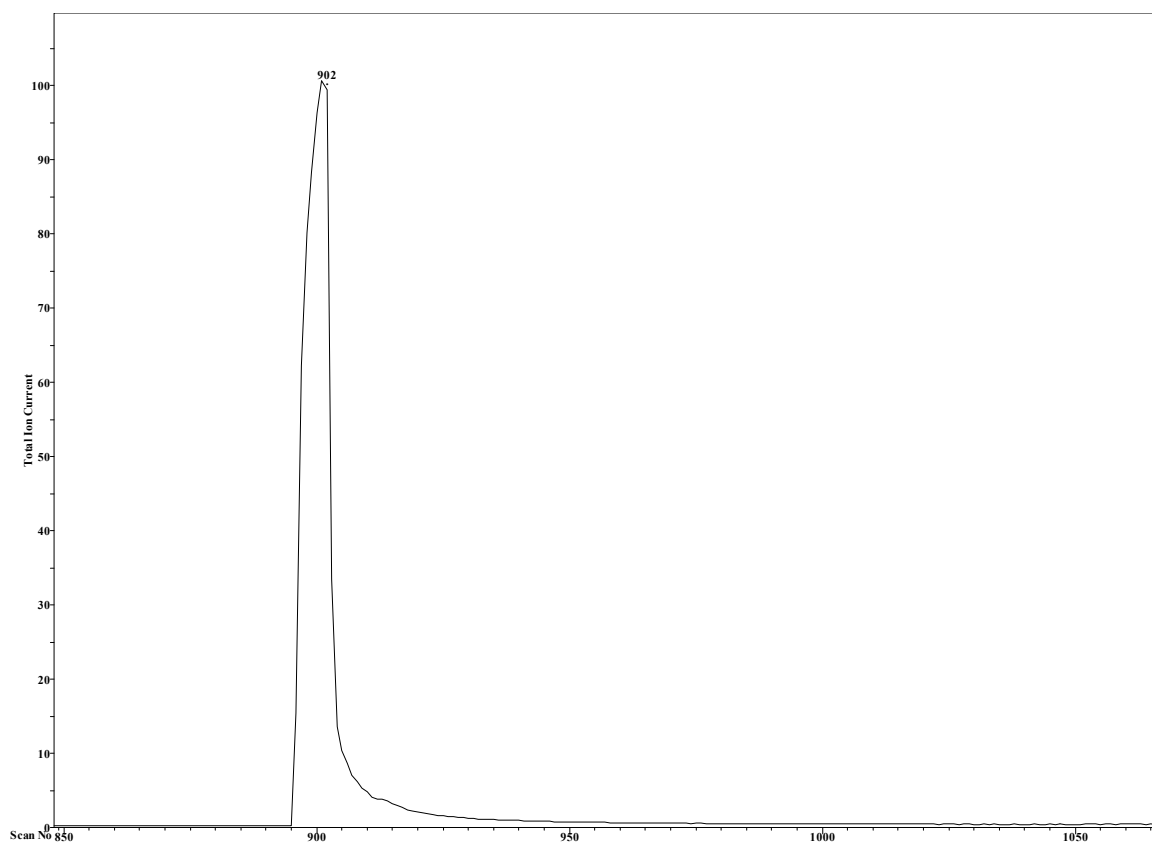
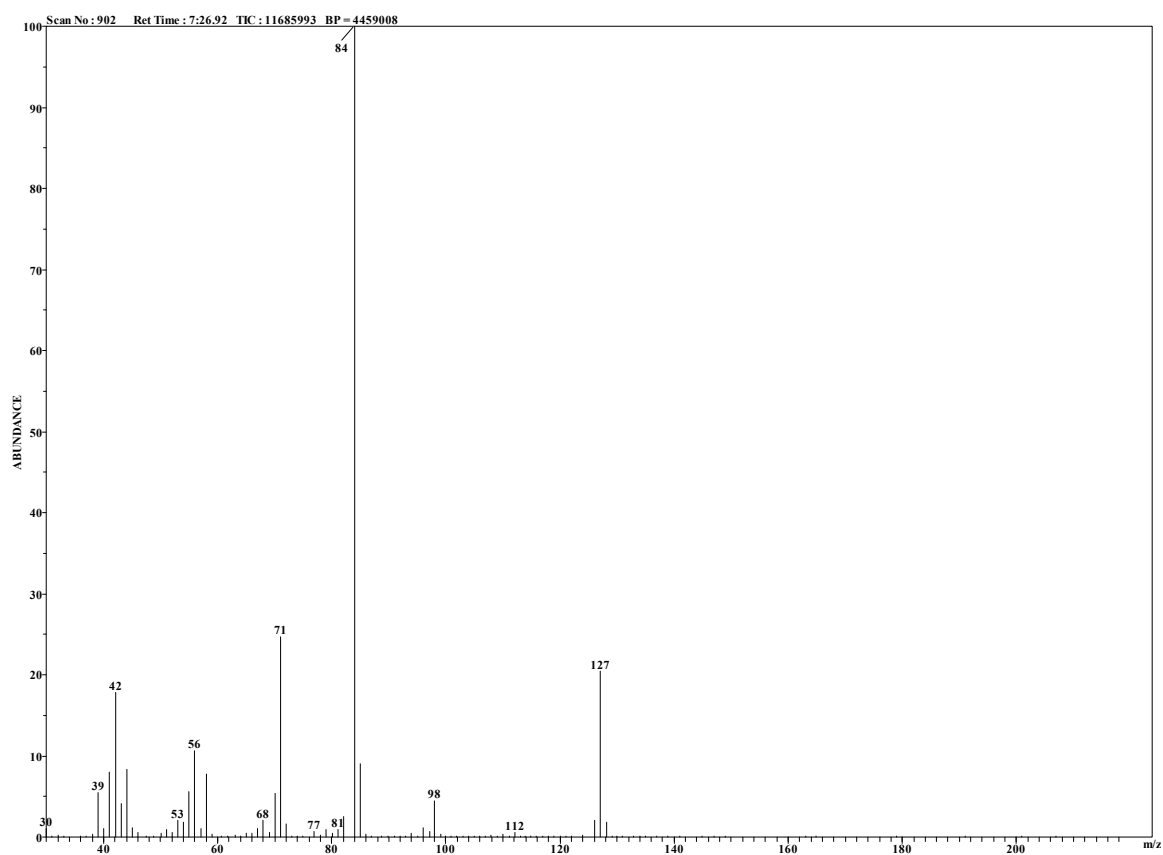


Fig. 82: Oxidative degradation product in 3M DPA-H<sub>2</sub>O-O<sub>2</sub> system (molecular weight fragments)

DPA's fragment is indicated up to fraction 97, while degradation products from DPA achieve molecular weight of dimer (fragment 193) to trimer (fragment 265) of itself. There's also a possibility of attachment of oxygen atoms to form nitrite (fragment 235-265).

DMCA as tertiary amine was found to be stable during the experiment. The analyzed liquid phase depicted in Fig. 83 shows no presence of additional degradation product other than the DMCA molecule. The molecular weight fragments diagram in Fig. 84 confirms the maximum molecular weight in the DMCA solution is 127, which is molecular weight of DMCA itself.

Fig. 83: Chromatogram of 3M DMCA-H<sub>2</sub>O-O<sub>2</sub> system (overall)Fig. 84: Oxidative degradation product in 3M DMCA-H<sub>2</sub>O-O<sub>2</sub> system (molecular weight fragments)

It should be noted that oxidative degradation products of amine do not remain only in liquid phase. Investigations have proven that gas/vapour phase oxidative degradation product, namely ammonia, is formed with the presence of iron in the amine solution [22]. This is not the case with this investigation since no steel experimental apparatus was used. Thus more extensive degradation study should be carried out also with respect to column's construction material.

## 4.10 Extractive regeneration

In industrial application, the loaded amine solution is regenerated thermally. A standard alkanolamine, namely MEA is regenerated at 120°C using low pressure steam at 2 bar. Biphasic lipophilic amine solutions can be regenerated thermally at temperature below 100°C. Biphasic lipophilic amine solutions have unique property, which undergo transformation from biphasic polar-nonpolar solutions to become homogeneous semi-polar solution after loaded by CO<sub>2</sub>. This indicates that the stability of the homogeneous loaded solution can be influenced by introducing a tertiary component whose polarity lies between that of water and lipophilic amine. Once the stability of the loaded solution is disturbed, CO<sub>2</sub> will be released from the loaded solutions and lipophilic amine is regenerated.

### 4.10.1 Concept and solvent selection

Schematic diagram in Fig. 85 describes briefly the process of CO<sub>2</sub> absorption using lipophilic amine solutions with addition of extractive regeneration unit.

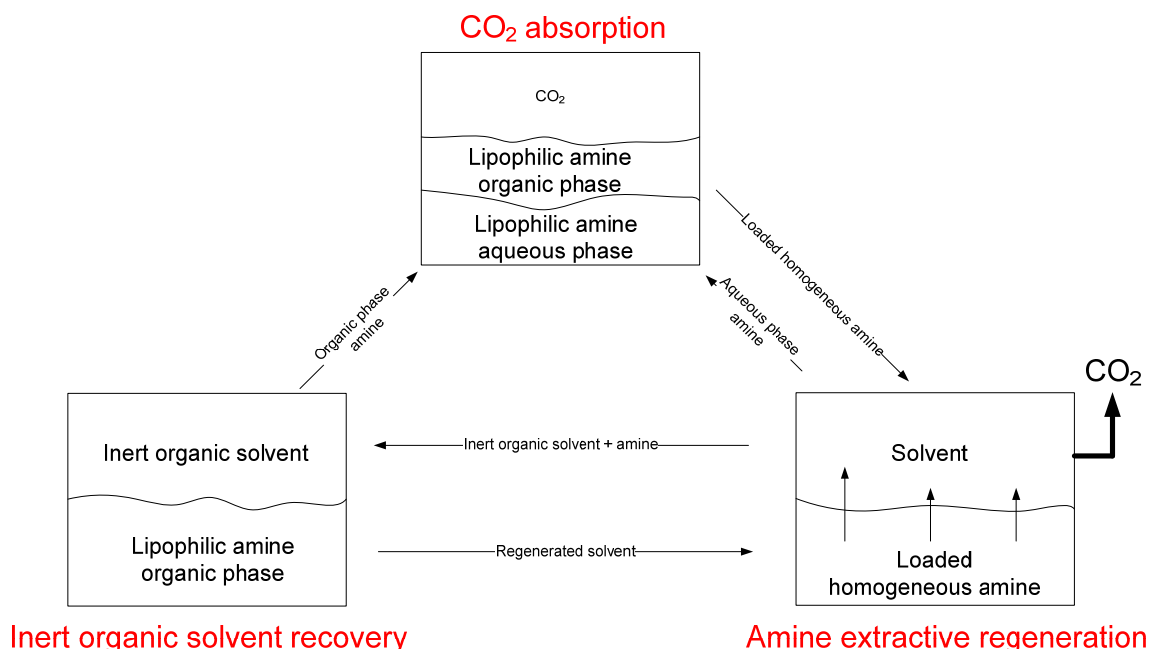


Fig. 85: Extractive regeneration concept

The process starts with CO<sub>2</sub> absorption into biphasic lipophilic amine solution to form homogeneous loaded amine solution. The regeneration of loaded amine solutions is carried out by addition of an inert solvent, which has low solubility in the loaded amine solutions.

The inert solvent acts as an extracting agent and extract the lipophilic organic from the loaded solution and thus disturbs the stability of the chemical equilibrium in it. Subsequently CO<sub>2</sub> will be released from the loaded solution.

Moreover mixture of lipophilic amine and inert solvent can be separated by any kind of separation method. In this study, thermal separation was selected. The inert solvents criteria are as follow:

- Polarity between that of organic and aqueous phase of lipophilic amine solution
- Good and easy separability. For recovery with thermal separation, the inert solvent should have low boiling point.
- Low solubility in loaded amine solution
- Minimum influence to overall absorption process if trace amount of it presents in amine solution
- Good stability

The key point in the extractive regeneration is the selection of solvents with polarity lies between polarity of aqueous phase and organic phase of lipophilic amine solutions. For the purpose of solvent identification, solubility parameter is used. Solubility parameter ( $\delta$ ) stands for the energy required to separate molecules in a fluid and create cavities to accommodate solute molecules [59]. It consists of cohesive, adhesive and hydrogen bonding interactions. As a rule of thumb, two molecules are miscible when their  $\delta$  value differ no more than 3.5 fold [5]. With refer to the selection criteria above, screening had been carried out starting from saturated as well as unsaturated hydrocarbon, with various structures as well as functional groups. As a general remark, halogen compound is not suitable because of its reactivity with amine. Ether compound is not advisable even though it is still considered in this study. The ether group is chemically unstable during thermal separation and might lead to formation of explosive vapor.

In brief, based on the criteria and literature study, nine molecules were selected for further investigation. Their solubility parameters as well as those of DPA and DMCA are given in Table 25.

Table 25: Solubility parameters of various solvents [35]

<b>Compound</b>	<b><math>\delta</math> [MPa<sup>0.5</sup>]</b>
Hexane	14.9
3-methyl pentane	14.5
Pentane	14.5
Cyclopentane	16.5
Cyclopentene	17.2
2-methyl butane	13.7
2-methyl-2-butene	14.3
MTBE	14.8
Water	47.8
DPA*	15.3
DMCA*	18.5

\* estimated based on the interactions energies, courtesy of Hansen

As observed in Table 25, all of the selected solvents are expected to have strong interaction with DPA and DMCA. Moreover their normal boiling point is below 50°C, except that of hexane (69°C).

#### 4.10.2 Inert solvent performance

Lipophilic amine solutions with preloaded optimum composition at 3 M 1:3 – DPA:DMCA are used as the standard for this experiment. The performance of various inert solvents with single-stage-equilibrium extractive regeneration at 40°C is depicted in Fig. 86.

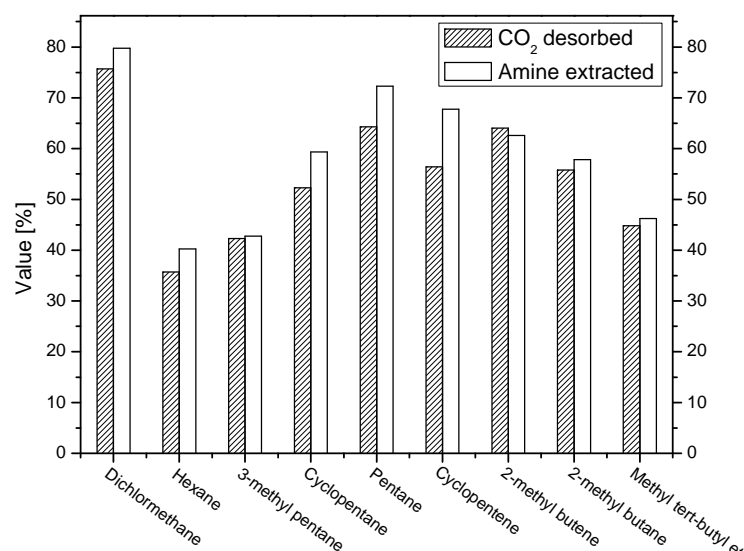


Fig. 86: Extractive regeneration performance with various solvents ( $\alpha_{\text{initial}} = 0.8$ )

For this experiment 1:1 volume ratio of inert organic phase to loaded amine solution was used. Dichloromethane, as a compound consists of halogen group, was not considered for further investigation because it reacts with the lipophilic amines through substitution mechanism to form mixtures of amines with various state of alkylation [6]. Through analysis of the liquid phase with GC, over five reaction products had been found but not identified specifically.

It was found that molecule with less number of atom carbon extracts more amine than larger molecule does. Moreover the cyclic structure does not influence much the extraction/regeneration degree. Molecules with unsaturated hydrocarbon substituents perform better (less than 10% additional CO<sub>2</sub> removal) than their saturated counterpart, however they are economically infeasible and highly reactive when they come into contact with further chemicals. Thus solubility interaction alone could be used to regenerate the loaded amine solution up to over 35% degree of CO<sub>2</sub> removal at 40°C, while it achieves over 60% for pentane. Thus pentane was selected for further study.

Based on the solubility parameters of the inert solvents, providing no interference of additional compounds, more DPA than DMCA is expected to be extracted to inert solvent phase. However the experimental results depicted in Fig. 87 indicate anomaly from the predicted solubility behaviour, in which more DMCA was extracted to the inert organic solvent phase than DPA.

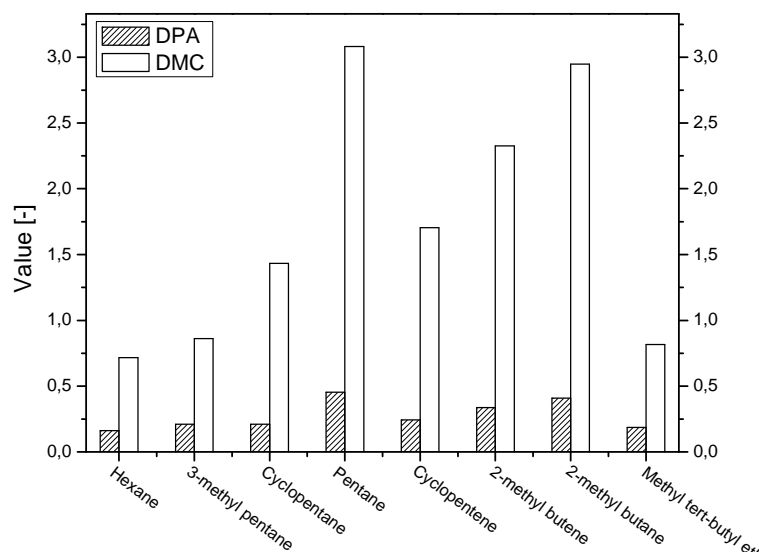


Fig. 87: DPA and DMCA partition coefficient with various solvents ( $\alpha_{\text{initial}} = 0.8$ )

This can be explained by the presence of DPA in the loaded amine solution as carbamate ions. The carbamate ions are not only relatively stable in aqueous / polar liquid phase, but also relatively polar (self-associate) compare to other chemical species in the loaded amine solution. In order to fully extract DPA from the loaded solution, the carbamate has to be hydrolysed to form free amine. However it can be carried out only at high temperature, which should be at least above 50°C as shown in Fig. 88. At elevated temperature up to 50°C, the partition coefficient of DPA in pentane remained relatively constant at average value 0.5. As long as temperature for rapid carbamate hydrolysis not yet achieved, most of the DPA will remain in the loaded amine solution.

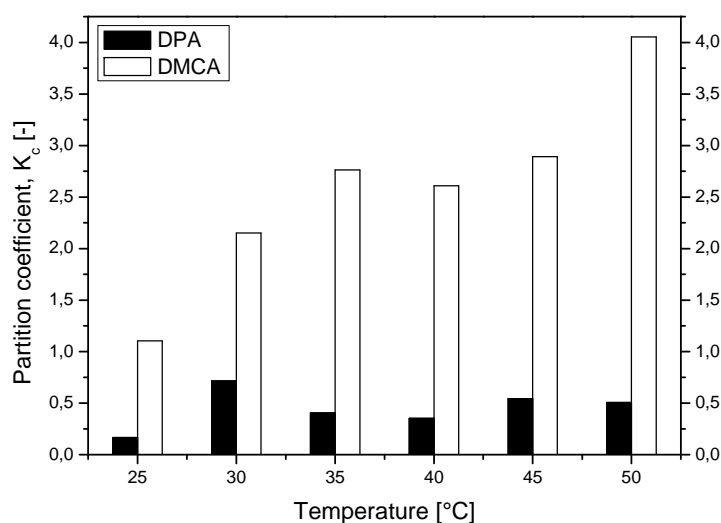


Fig. 88: DPA and DMCA partition coefficient (with pentane) at temperature increase ( $\alpha_{\text{initial}} = 0.931$ )

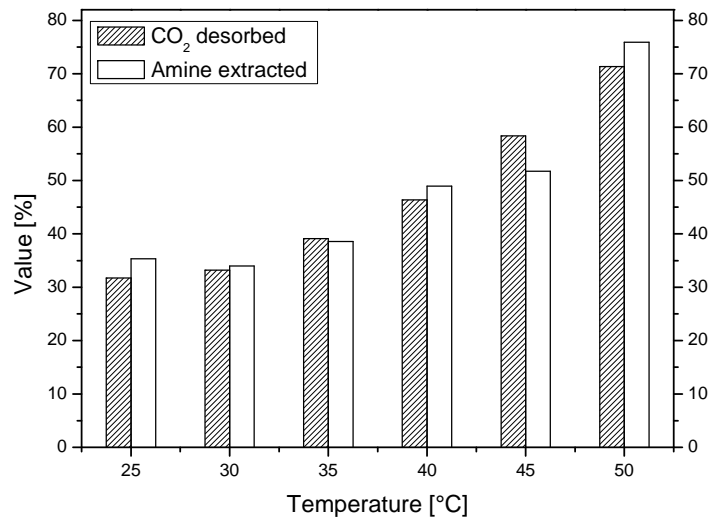


Fig. 89: Extractive regeneration using pentane at temperature increase ( $\alpha_{\text{initial}} = 0.931$ )

Increase of temperature will improve the extraction of DMCA followed by CO<sub>2</sub> release but further increase of the temperature above 50°C was not advisable due to high volatility of pentane.

Reasonable operating temperature for the extractive regeneration will be at 40°C, which is also the typical absorption temperature.

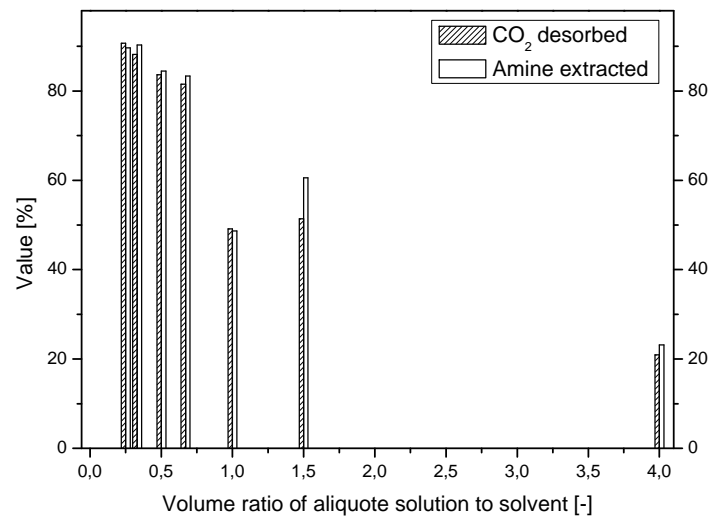


Fig. 90: Extractive regeneration using pentane at various inert solvent at 40°C ( $\alpha_{\text{initial}} = 0.952$ )

At this particular temperature, for single stage equilibrium extractive regeneration, the volume ratio of 2:1 inert solvent to loaded amine solutions will be optimum.

### 4.10.3 Inert solvent recovery

In order to determine the energy requirement for recovery of solvent, material and energy balance was carried out using ASPEN<sup>TM</sup> Plus. As a benchmark, the mixtures of 100 kmol/h of 1:1 volume ratio of pentane to amine (40°C) were used. Shortcut calculation method based on Winn-Underwood-Gilliland model was used to determine the column's operating parameter to recover 99% mole of pentane. With the given separation task, the following process parameters were obtained:

- Minimum number of stages : 3.20
- Minimum reflux ratio : 0.045
- Actual reflux ratio : 1.860

The real reflux ratio is related to the number of stages required to accomplish certain separation task. Varying the number of stages from 4 to 10, as shown in Fig. 91, shows the optimum number of stages is 7 in terms of energy requirement.

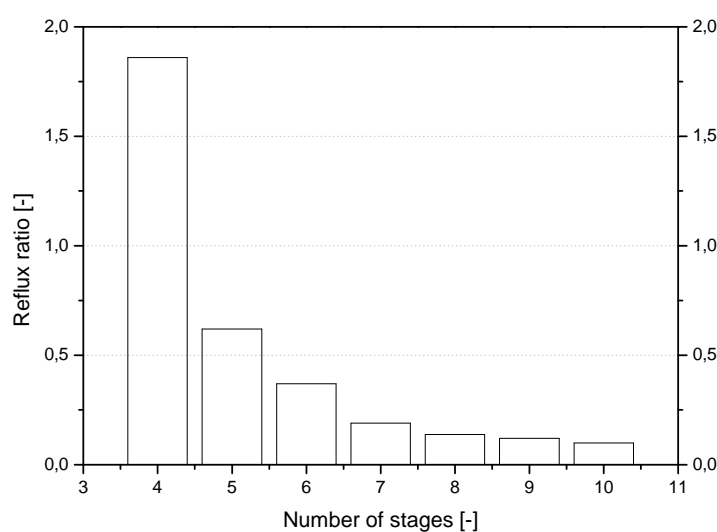


Fig. 91: Relux ratio dependent on number of stages

However economic optimisation should be done to determine whether it is feasible to increase column height or to spend more on utilities. In this work, 7 stages were applied for further mass and energy balance by using Radfrac Model and the results are given in Table 26.

Table 26: Heat duty for pentane recovery

<b>Process parameters</b>	<b>Unit</b>	<b>Value</b>
Number of stages	-	7
Actual reflux ratio	-	0.074
Pentane recovery	%	93
Specific reboiler duty	kJ/mol pentane	45.16
Specific condenser duty	kJ/mol pentane	-28.22

The calculated reboiler duty is based on single stage extractive regeneration. The performance of the process can be improved by multistage counter-current extraction. Degree of inert solvent recovery depends on the economic constraint. It should be noted that the inert solvent used in the system should not hamper the absorption process if it remains in minor amount after recovery process.

## 4.11 Exploration for new amine

Even though lipophilic amine DPA and DMCA have indicated a better performance compare to conventional alkanolamine for industrial application, they still have many disadvantages. Besides precipitation, the volatility of DPA during absorption leads to significant solvent loss. As tertiary amine DMCA has relatively high base strength which requires higher energy for regeneration than conventional tertiary alkanolamine. This can be observed from the absorption enthalpy of DMCA in chapter 4.8.

Exploration has been carried out based on information on structural influence in chapter 4.2.1 in order to identify suitable lipophilic amine for CO<sub>2</sub> absorption. Screening had been carried out with commercially-synthesized amines having linear and branched alkyl, cyclic alkyl, as well as other functional groups. This screening is an extension of the screening carried out in the previous work [86],[75]. The amine concentration used in the work is standardized to the DPA-H<sub>2</sub>O. This means, the composition of each tested amines is equal to the composition of DPA in terms of mol. All solutions with composition eq. 30%wt. DPA, have the same amount mole amount of amine and water to that of 30% wt. DPA solution. The experimental method used in this work is described in chapter 3.2.7.

### 4.11.1 Primary amines screening

Previous screening of primary amines indicated that primary lipophilic amines with carbon atom larger than six will form gel upon mixing with water. This restricts the exploration only to molecules with atom carbon less than six. There are very few primary lipophilic amine with linear and branched alkyl structures, which are economically feasible to be used for CO<sub>2</sub> absorption. Other than linear/branched alkyl amines, primary amines with cyclic alkyl substituent do not exhibit gel formation upon mixing with water. In brief, seven most promising primary lipophilic amines had been tested.

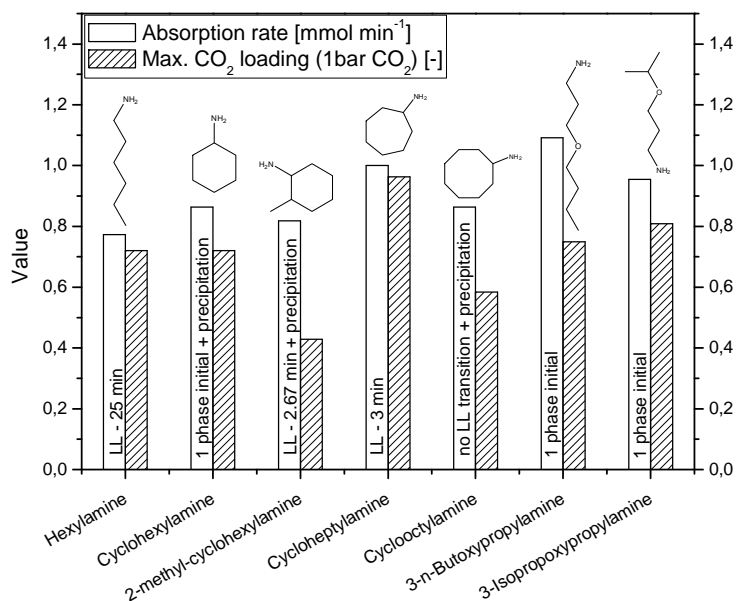


Fig. 92: Primary amines absorption (eq. 30%wt. DPA, 25°C)

Due to strong base strength of primary amines, absorption rate is not the most decisive criteria. Their application for CO<sub>2</sub> absorption is restricted by precipitation phenomena. Precipitation is however can be avoided by introducing ether functional group in the molecule with the expense of low CO<sub>2</sub> loading. Unlike cyclic alkyl amine with even number of atom carbon like cyclohexylamine and cyclooctylamine, precipitation did not occur in cycloheptylamine solution. Primary lipophilic amine solutions which form precipitate are no longer considered for further study.

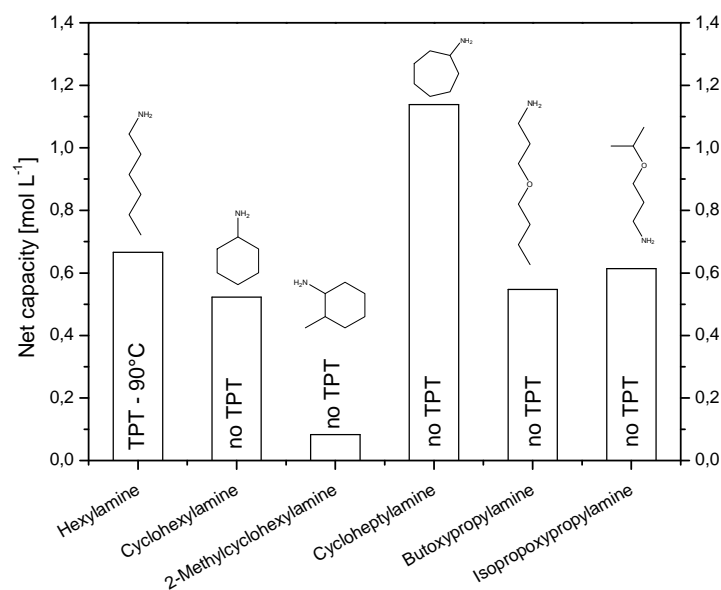


Fig. 93: Primary amines regeneration (eq. 30%wt. DPA, 80°C)

Among the tested primary lipophilic amine, the cycloheptylamine showed good absorption and regeneration characteristics. However cyclic alkyl amines with odd number of carbon are economically infeasible. Thus exploration was focused to find suitable secondary lipophilic amines for CO<sub>2</sub> absorption.

#### 4.11.2 Secondary amines screening

Secondary lipophilic amines provide more degree of freedom in the exploration. Investigation had been carried out with various structures but with number of carbon atom more than six. Even though larger molecular size will lead to decrease of absorption rate, but it will enable more effective amine regeneration at low temperature below 100°C. Due to relatively high base strength of secondary lipophilic amines, their absorption rate is not the main criterion in the selection. Instead, absorption capacity in terms of loading and precipitation phenomena are considered important.

Results of the screening are given in Fig. 94 and Fig. 95. At eq. 30%wt. composition, DPA (6 carbon atoms) exhibits minor amount of precipitation, which was soluble in amine solution at 40°C. Therefore it is still applicable for CO<sub>2</sub> absorption provided its concentration as an activator in the solution is low. After literature study, five chain structural secondary lipophilic amines were selected to be investigated.

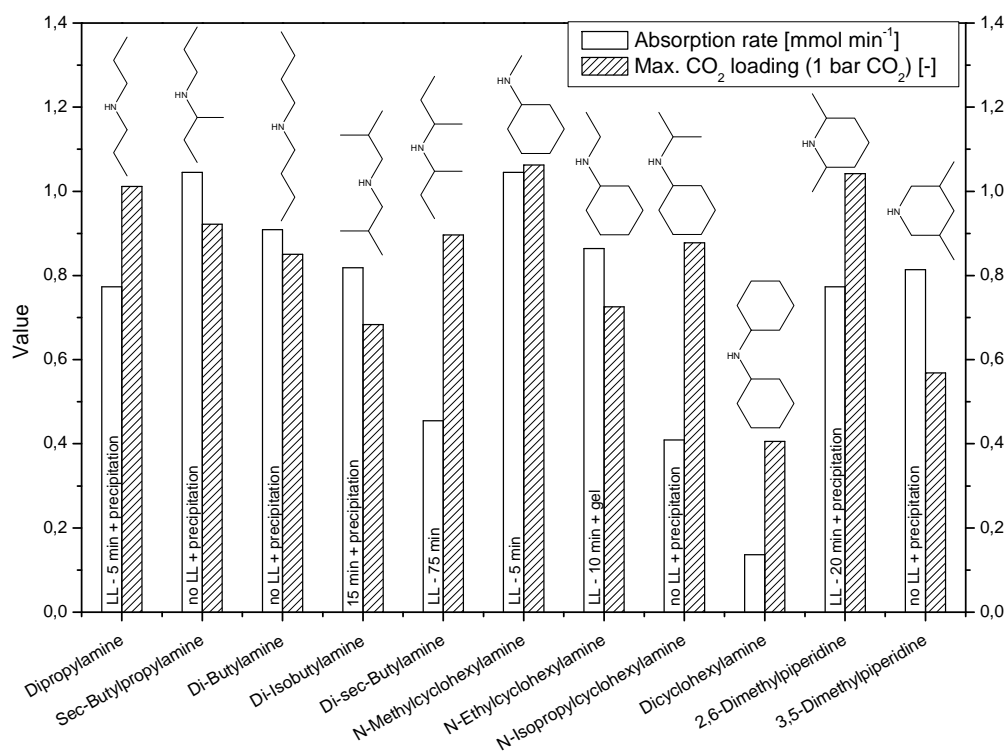


Fig. 94: Secondary amines absorption (eq. 30%wt. DPA, 25°C)

Investigation on sec-butylpropylamine is an attempt to add one carbon atom to the structure of DPA. The inductive effect discussed in chapter 4.2.1.1 suggests modifying the carbon substituents as near as possible to base central (nitrogen atom) will influence the characteristics of the molecule significantly. Thus adding one methyl group next to the amino group in the DPA molecule increases its absorption rate due to the inductive effect. The solution of sec-butylpropylamine precipitates and followed by gelation upon CO<sub>2</sub> absorption. Thus it was not considered for further study despite their high absorption capacity.

Di-butylamine was tested as an attempt to resolve the disadvantage of DPA, namely high volatility. Solutions of dibutylamine in water are biphasic over the tested amine concentration. Due to increase of molecule size, the phase transition from 2 to 1 phase during absorption takes place later than DPA. Precipitation occurred during CO<sub>2</sub> absorption into it, however it dissolved in the amine solution at 40-60°C.

Di-isobutylamine, which is an isomer of di-butylamine, exhibits a severe precipitation that it is not suitable for CO<sub>2</sub> absorption. It was found that primary and secondary lipophilic amines with iso-alkyl substituent tend to precipitate during CO<sub>2</sub> absorption.

Shifting position of each methyl substituent in di-isobutylamine toward closer to nitrogen atom, will yield di-sec-butylamine structure. It is interesting to observe the influence of modifying alkyl substituent close to the base central (nitrogen atom). Due to the sterically hindered effect, its absorption rate lies at the range of that of tertiary lipophilic amines. There's no precipitation observed during CO<sub>2</sub> absorption with di-sec-butylamine solutions at the concentration range used in this work. Its performance in regeneration, as depicted in Fig. 95, surpasses any tested secondary lipophilic amines as well as most tertiary lipophilic amines. Thus it is suitable to be applied in CO<sub>2</sub> absorption without restriction due to precipitation. Further study with secondary lipophilic amines having totally 8 carbon atoms was restricted by the economic feasibility criterion. Secondary lipophilic amines with unsymmetrical alkyl substituents are found to be economically infeasible. Thus investigation was expanded to amines with cyclo-alkyl substituents.

Along the development in the research, four amines with cyclic alkyl structure were investigated. Amines with cyclic alkyl substituent tend to form precipitation upon CO<sub>2</sub> absorption and their application is restricted by their molecular size. The larger the molecular size the larger the tendency of the amine to precipitate during absorption process.

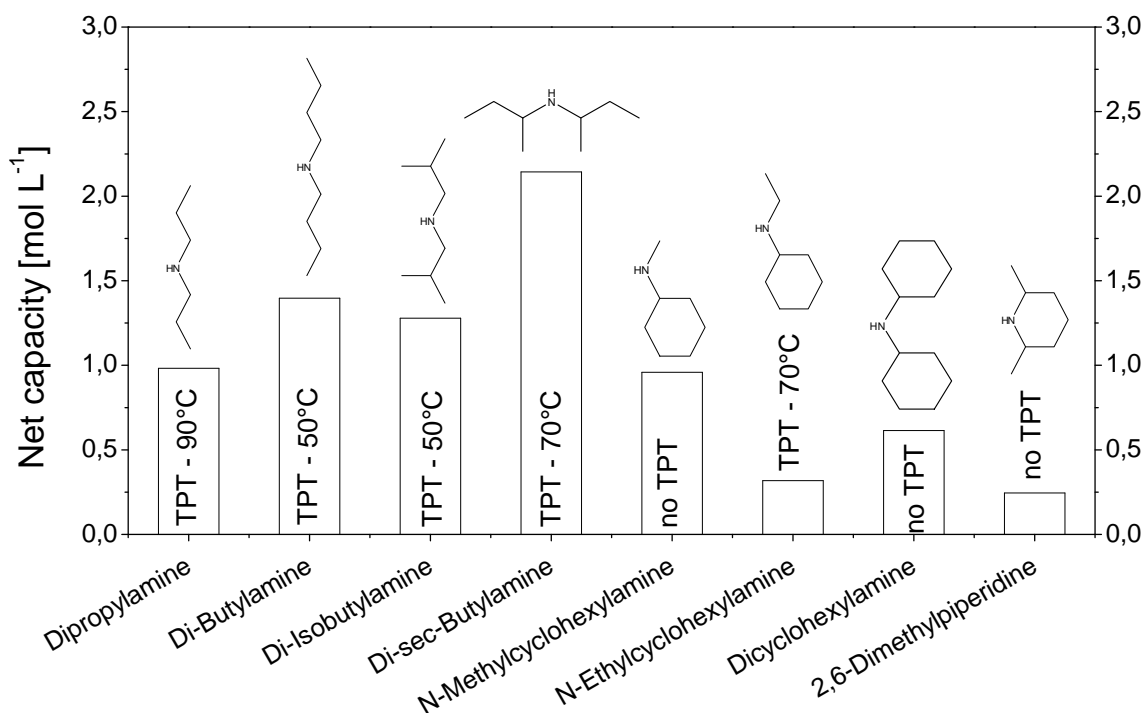


Fig. 95: Secondary amines regeneration (eq. 30%wt. DPA, 80°C)

Among the tested amines only n-methylcyclohexylamine was found to be suitable for CO<sub>2</sub> absorption. Compare to DPA, the N-methylcyclohexylamine has higher absorption rate and capacity without any precipitation disadvantage. Moreover it has a higher normal boiling point at 149°C compare to DPA at 110°C.

#### 4.11.3 Tertiary amines screening

Tertiary lipophilic amines do not form precipitation upon CO<sub>2</sub> absorption. However it was observed in the experiments that with increase of molecular size, the tertiary amine will have lower absorption capacity. This is proposed due to the solubility hindered effect discussed in the previous chapter. The larger the molecular size of tertiary amines, the larger the volume occupied by them in the aqueous phase, which acts as storage for absorption reaction products. Once the aqueous phase is saturated, the absorption will not proceed further. On the other hand, with decrease of molecular size, the regeneration of lipophilic amine will be hampered. This restricts the exploration down to only a few tertiary lipophilic amines in addition to those which were investigated in the previous work [75],[86].

Results of the investigation are given in Fig. 96 and Fig. 97.

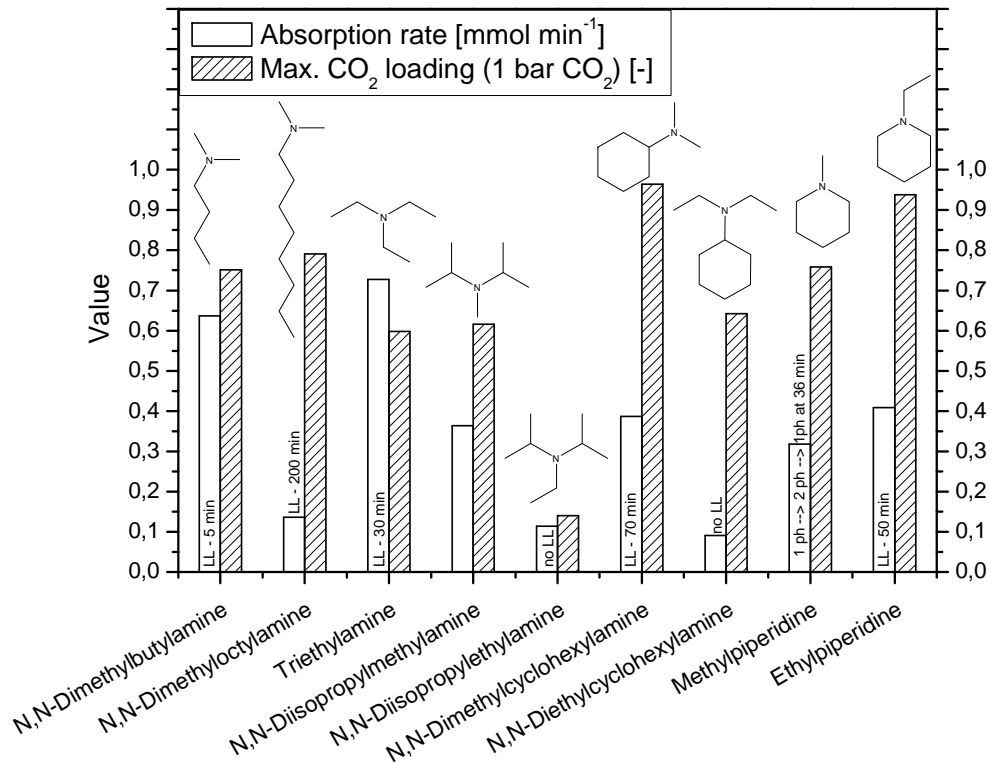


Fig. 96: Tertiary amines absorption (eq. 30%wt. DPA, 25°C)

Investigation of tertiary amine with cyclic alkyl structure was extended from the previous work [75],[86].

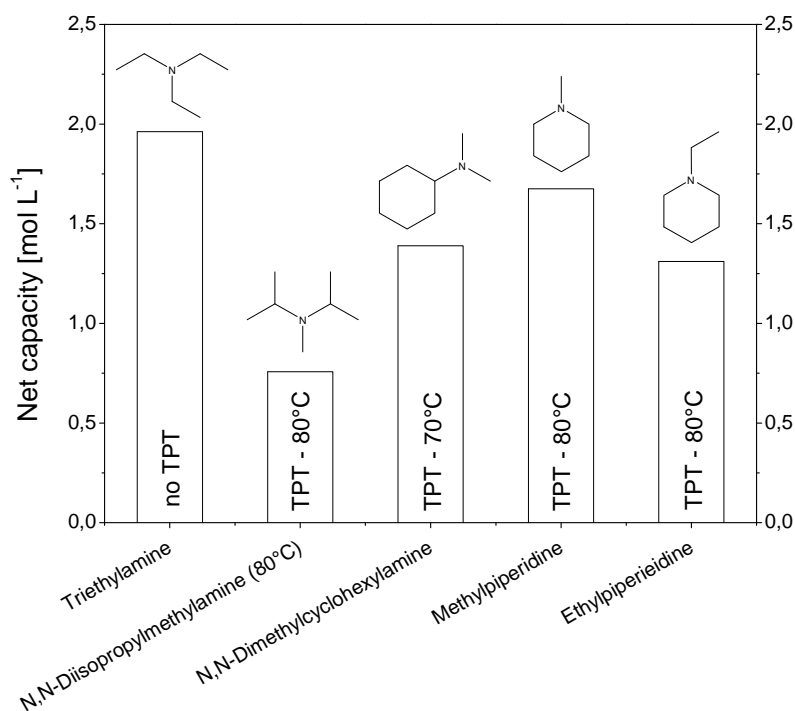


Fig. 97: Tertiary amines regeneration (eq. 30%wt. DPA, 80°C)

For tertiary lipophilic amines with chain structure alkyl substituents, increase of molecular size will decrease their absorption rate as observed from comparison of N,N-Dimethylbutylamine to N,N-Dimethyloctylamine. Moreover sterically hindered effect decreases their absorption rates significantly as observed from comparison of triethylamine, N,N-Diisopropylmethylamine and N,N-Diisopropylethylamine. Thus further increase of molecular size of chain structure tertiary amine is not advisable.

Tertiary amines with piperidine structure are found to be suitable for CO<sub>2</sub> absorption. However their performance in terms of net capacity is still below that of di-sec-butylamine, which is discussed in the previous chapter 4.11.2. Moreover their thermomorphic liquid-liquid separation takes place at 80°C, which is higher than that of DMCA. This will contribute to economic infeasibility because the regeneration will have to be carried out at higher temperature than that of mixture of DPA-DMCA discussed in chapter 4.9.

The solubility hindered effect, which occurs in tertiary lipophilic amine, is more clearly shown in Fig. 98.

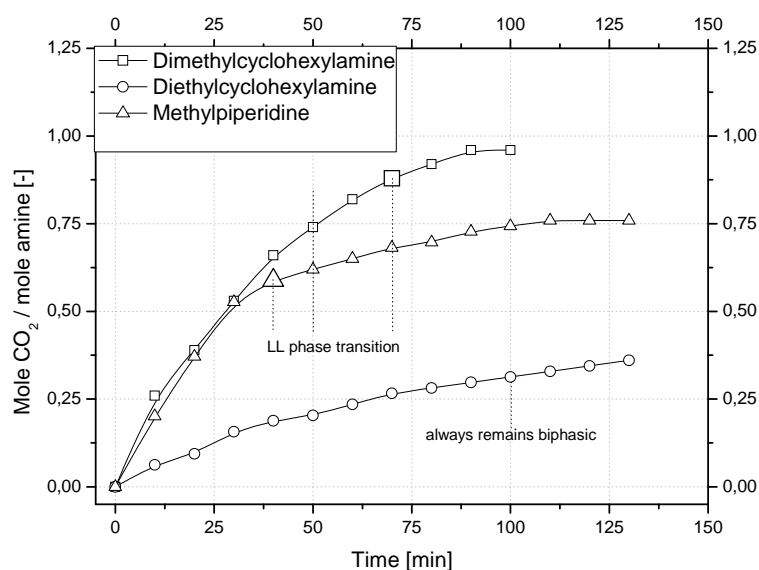


Fig. 98: CO<sub>2</sub> absorption into cyclic structure tertiary lipophilic amines

During CO<sub>2</sub> absorption process, diethylcyclohexylamine solution remained biphasic throughout the entire process. High concentration of diethylcyclohexylamine in the organic phase could not be utilised for CO<sub>2</sub> absorption, because of insufficiency of water in the aqueous phase.

#### 4.11.4 Lipophilic Amine Screening Summary

As an activator N-methylcyclohexylamine was selected for further study. Its absorption rate is relatively stable upon increase of concentration. Moreover it absorbs CO<sub>2</sub> efficiently up to the loading approaching 1:1 of CO<sub>2</sub> to amine. All biphasic aqueous n-methylcyclohexylamine solutions undergo liquid-liquid phase transition from two to one phase in relatively shorter time than other tested lipophilic amines (less than five minutes) in the experiment condition. The time required to achieve this liquid-liquid phase transition depends on the CO<sub>2</sub> loading in the liquid phase and thus absorption rate. The ability of activator to transform the solution from biphasic into homogeneous phase during absorption is important especially when applying biphasic lipophilic amine solutions. Once the loaded solution of lipophilic amines becomes homogeneous, the solubility hindered effect will not occur. This way activator does not only serve to increase absorption rate but also to ensure the utilisation of full CO<sub>2</sub> absorption capacity of the solution.

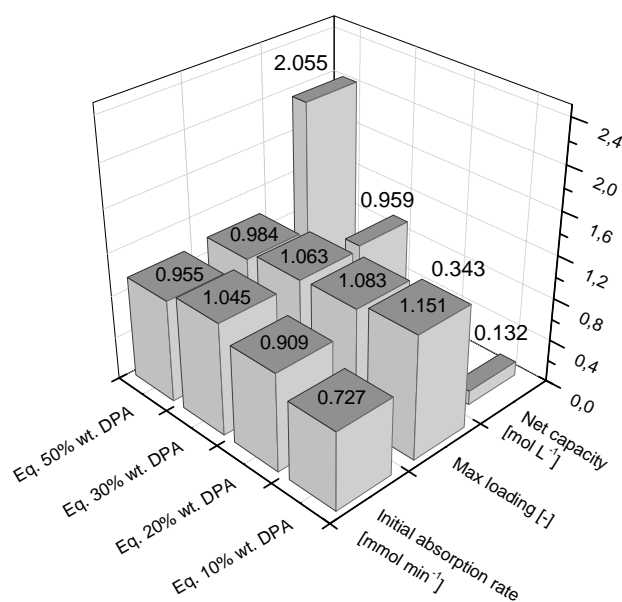


Fig. 99: N-methylcyclohexylamine absorption characteristics

Despite the high CO<sub>2</sub> loading in aqueous n-methylcyclohexylamine solution, it does not precipitate even at high concentration.

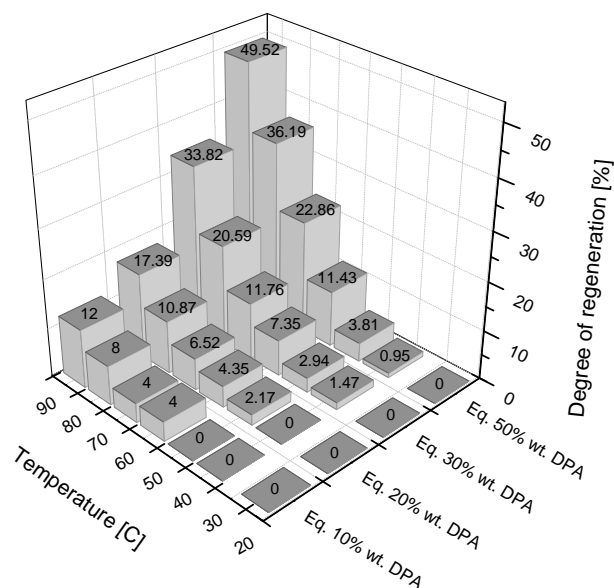


Fig. 100: N-methylcyclohexylamine regeneration characteristics

Despite there's no thermomorphic liquid-liquid separation took place during regeneration of n-methylcyclohexylamine up to 90°C, its net capacity is comparable to that of DPA. Its degree of regeneration increases exponentially with increase of temperature starting from 60°C.

Di-sec-butylamine was selected as the base amine due to its high capacity and low regeneration temperature. Due to the inductive effect and sterically hindered effect, di-sec-butylamine have characteristics of tertiary amine. Its absorption rate and net capacity lies in the range of tertiary amine.

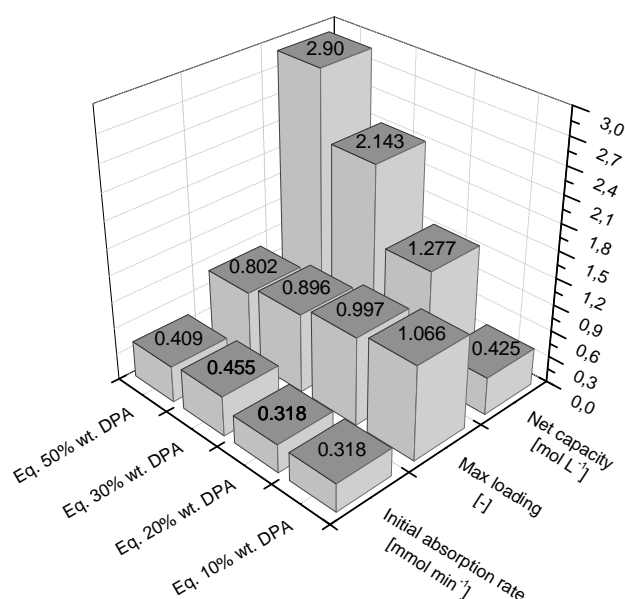


Fig. 101: Di-sec-butylamine absorption characteristics

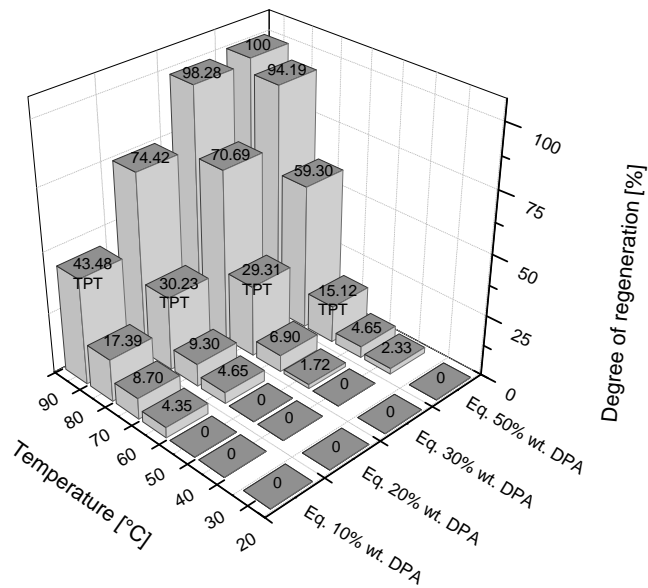


Fig. 102: Di-sec-butylamine regeneration characteristics

Upon regeneration, thermomorphic phase transition temperature (TPT) takes place starting from 60-90°C dependent on the composition of the solutions. The performance comparison of individual selected lipophilic amines is given in Fig. 103 and Fig. 104.

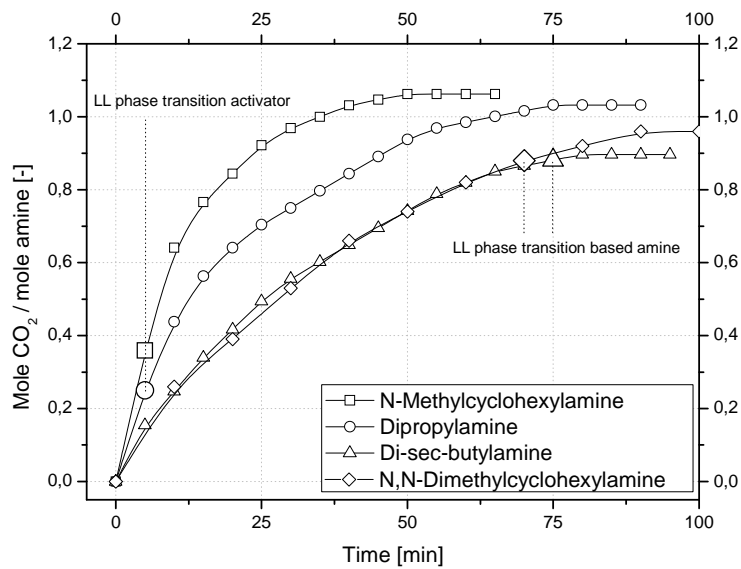


Fig. 103: Absorption comparison with 3M lipophilic amine solutions at 40°C

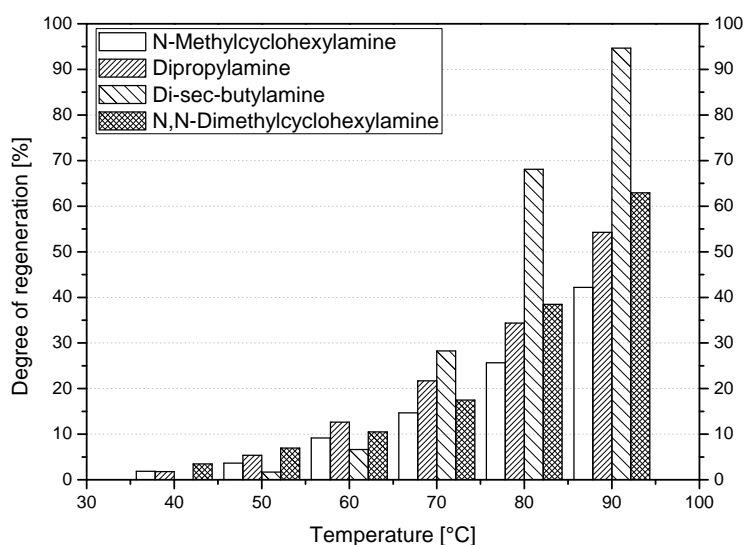


Fig. 104: Regeneration comparison with 3M lipophilic amine solutions

Among activators, n-methylcyclohexylamine surpasses DPA in terms of absorption rate. Due to the absence of thermomorphic liquid-liquid phase separation in the regeneration, n-methylcyclohexylamine's degree of regeneration is lower than DPA. However since it does not precipitate upon CO<sub>2</sub> absorption and its volatility is significantly lower than DPA, the n-methylcyclohexylamine is still considered to be more suitable for CO<sub>2</sub> absorption than DPA. Among base amine, di-sec-butylamine exhibit similar absorption rate to that of DMCA, however it outperforms the DMCA in terms of regeneration performance. Due to the relatively slow absorption rate of di-sec-butylamine, its application for CO<sub>2</sub> absorption has to be mixed with activator.

The optimum composition of the previous applied aqueous solution DPA and DMCA lies at mole ratio 1:3 - DPA:DMCA. Test carried out with methylcyclohexylamine (MCA) and di-sec-butylamine (DSBA) at the mole ratio 1:3 – MCA:DSBA at various concentration shows a comparable performance compare to that of DPA and DMCA.

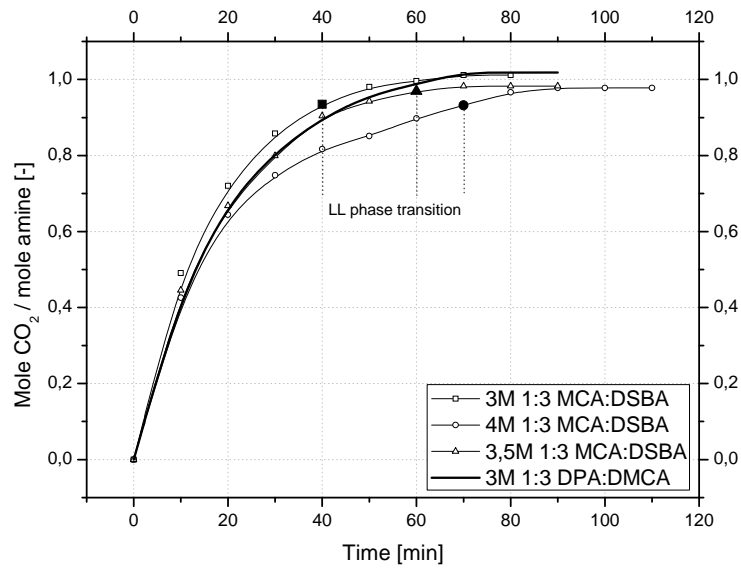


Fig. 105: CO<sub>2</sub> absorption into MCA-DSBA mixtures at various concentration (40°C, 1 bar CO<sub>2</sub>)

With increase of amine concentration, the CO<sub>2</sub> absorption capacity increases, however the CO<sub>2</sub> loading decreases. This is observed in solutions having concentration 4M of total amine. For further study, the solution having concentration 3M MCA and DSBA is used. Upon varying the ratio of MCA to DSBA at absorption condition, their absorption rate as well as CO<sub>2</sub> loading is comparable. This provides degree of freedom for tailoring of solvent composition to various CO<sub>2</sub> removal purposes.

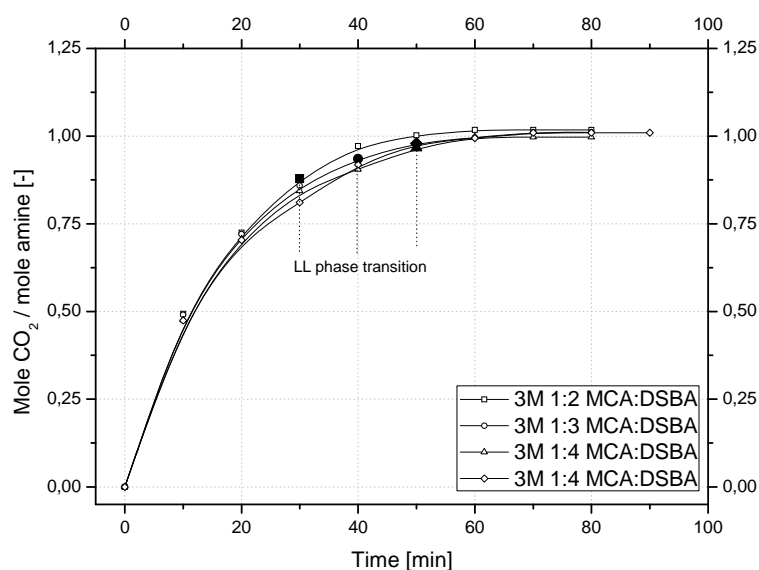


Fig. 106: CO<sub>2</sub> absorption into 3 M MCA-DSBA at various amine ratio (40°C, 1 bar CO<sub>2</sub>)

For the purpose of comparison with the previous solvent of 3M 1:3-DPA:DMCA, the new solvent with composition 3M 1:3-MCA:DSBA is furthermore tested. The result is shown in Fig. 107.

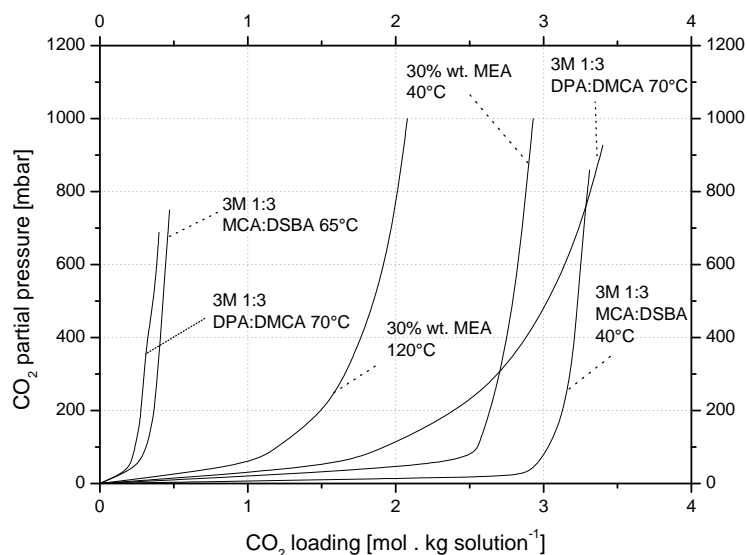


Fig. 107: Loading curve of 3M 1:3 MCA:DSBA at absorption and regeneration temperature

For industrial application, the important part of the loading curve is the loading range below 200 mbar partial pressure of CO<sub>2</sub>. Within this loading range, the MCA-DSBA mixtures absorb in average over 15% more CO<sub>2</sub> per kg solution than the previous studied DPA-DMCA system. Comparing with standard 30% wt. MEA system, it absorbs in average more 15% CO<sub>2</sub>. However the concentration of 30% wt. MEA is correspond to approximately 4.9M, while the lipophilic amine solutions are at 3M. Comparison of solvent performance was carried out baed on method developed by Hasse et.al [55]. The method enables theoretical comparison of performance of various amine solvents with various. The benchmark for comparison is CO<sub>2</sub> absorption from 120 to 20 mbar partial pressure.

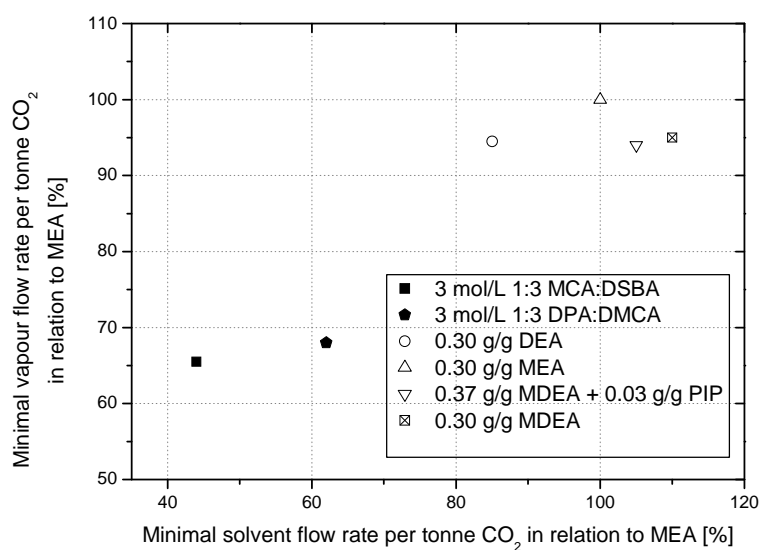


Fig. 108: Theoretical performance comparison of lipophilic amine solvent with standard alkanolamine

The result shown in Fig. 108 showed an early indication of economic feasibility of absorption process using lipophilic amine solutions due to lower solvent flow rate and utility requirement in their application for CO<sub>2</sub> absorption. The comparison shows 40% less solvent and 30% less utility are required compare to those of conventional 30% wt. MEA process. However more detail enthalpic study as well as mass and energy balance must be carried out to verify the economic feasibility besides testing in pilot plant.

## Conclusions and outlook

In the biphasic amine solutions the organic phase of lipophilic amine plays a key role to absorb CO<sub>2</sub> at a high rate. The high absorption rate is caused by the highly concentrated amine solutions in the organic phase rather than high reaction kinetics constant. However application of merely organic phase in the absorption is not recommended. Two main phenomena were found to prohibit this: Organic phase DPA precipitates upon CO<sub>2</sub> absorption, while in organic phase DMCA a “solubility hindered” effect occurs. Without the presence of sufficient amount of water, the aqueous DMCA solution (as well as its mixture with DPA) can not absorb CO<sub>2</sub> up to its full capacity.

The thermodynamic study explained clearly the phenomena occur during CO<sub>2</sub> absorption in the biphasic lipophilic amine DPA and DMCA. The organic phase serve to absorb CO<sub>2</sub> at high rate and the ionic reaction products of CO<sub>2</sub>-DPA and DMCA are extracted from organic into aqueous phase and stored in aqueous phase. Once the aqueous phase is saturated, no further absorption can be carried on. Thus water plays a decisive role in CO<sub>2</sub> absorption into biphasic lipophilic amine system.

Theoretical study on the influence of amine structure to its CO<sub>2</sub> absorption performance was done. Based on this, the exploration to find new lipophilic amines has successfully determined new lipophilic amines, which have superior absorption and regeneration characteristics compare to the former DPA and DMCA. The MCA is proposed to replace DPA. MCA solves volatility and precipitation issue arise in DPA application, moreover it has higher absorption rate than DPA while in regeneration its performance is comparable to DPA. DSBA which is a secondary amine, behaves extraordinarily similar to tertiary amine due to the influence of strong steric effect to nitrogen atom in the molecule. DSBA is proposed to replace DMCA. It has comparable absorption rate to DMCA however its performance in regeneration distinctly surpasses that of DMCA.

Additional to the project scope, the investigation of blend MCA-DSBA was carried out. 3M 1:3 MCA-DSBA was selected as suitable solution for CO<sub>2</sub> absorption. The result concludes the superiority of MCA-DSBA over DPA-DMCA mixture. The most recent update with MCA-DMCA doesn't perform as well as MCA-DSBA mixture. Added to that the oxidative degradation study as well as repetitive absorption-regeneration shows the stability of MCA-DSBA solutions even with the presence of oxygen in gas phase. The MCA-DSBA

mixture brings the biphasic system to a new step of CO<sub>2</sub> absorption with high absorption rate, high net capacity and low regeneration temperature without precipitation issue.

As a follow up to this finding, energetic measurement as well as test in bench scale absorption and regeneration unit using MCA and DSBA solution should be carried out. Moreover due to the nature of biphasic solution which is different from homogeneous solution, modification to the existing absorber to be able to accommodate biphasic solution will be important to maximise its application potency.

## References

- [1] Aboudheir A., Tontiwachwuthikul P., Chakma A. et al., Kinetics of the reactive absorption of carbon dioxide in high CO<sub>2</sub>- loaded, concentrated aqueous monoethanolamine solutions, *Chemical Engineering Science*, 58 (23-24) (2003): 5195-5210.
- [2] Al-Ghawas H.A., Hagewiesche D.P., Ruiz-Ibanez G., Sandall O.C., Physicochemical properties important for carbon dioxide absorption in aqueous Methyldiethanolamine, *Journal of Chemical and Engineering Data*, 34 (4) (1989): 385-391
- [3] Astarita G., Gas Treating with Chemical Solvents. (Wiley-Interscience Publication, New York), (1983)
- [4] Austgen D.M., Rochelle G.T., Chen C.C., Model of vapour-liquid equilibria for aqueous gas-alkanolamine systems .2. Representation of H<sub>2</sub>S and CO<sub>2</sub> solubility in aqueous MDEA and CO<sub>2</sub> solubility in aqueous mixtures of MDEA with MEA or DEA, *Industrial and Engineering Chemistry Research*, 30 (1991): 543-555
- [5] Barton, A. F. (1983). CRC Handbook of Solubility Parameters and Other Cohesion Parameters. (CRC Press, Inc., Boca Raton). p. 9 – 189.
- [6] Bruice P. Y., *Organic Chemistry*, (Prentice-Hall International, Inc., Engelwood Cliffs) (1995)
- [7] Behr A., Fängewisch C., Temperature-dependent multicomponent solvent systems – an alternative concept for recycling homogeneous catalysts, *Chemical Engineering and Technology*, 25 (2002): 143-147
- [8] Behr A., Fängewisch C., Rhodium-catalysed Synthesis of Branched Fatty Compounds in Temperature-dependent Solvent Systems, *Journal of Molecular Catalysis A: Chemical*, 197 (2003): 115-126.
- [9] Behr A., Miao Qiang, A new temperature-dependent solvent system based on Polyethyleneglycol 1000 and its use in Rhodium catalyzed cooligomerization, *Journal of Molecular Catalysis A: Chemical*, 222 (2004): 127-132
- [10] Behr A., Obst D., Turkowski B., Isomerizing hydroformylation of *trans*-4-octene to *n*-nonanal in multiphase systems: Acceleration effect of propylene carbonate, *Journal of Molecular Catalysis A: Chemical*, 226 (2005): 215-219
- [11] Behr A., Toslu N., Hydrosilylation reactions in single and two phases, *Chemical Engineering Technology*, 23 (2000): 122-125
- [12] Bello A., Idem R. O., Comprehensive study of the kinetics of the oxidative degradation of CO<sub>2</sub> loaded and concentrated aqueous monoethanolamine (MEA) with and without sodium metavanadate during CO<sub>2</sub> absorption from flue gases, *Industrial and Engineering Chemistry Research*, 45 (8) (2006): 2569-2579

- [13] Bello A., Idem R. O., Pathways for the formation of products of the oxidative degradation of CO<sub>2</sub>-loaded concentrated aqueous monoethanolamine solutions during CO<sub>2</sub> absorption from flue gases. *Industrial and Engineering Chemistry Research*, 44 (4) (2005): 945-969
- [14] Brillman E.W.F., *Mass transfer and chemical reaction in gas-liquid-liquid systems*, Thesis University of Twente, The Netherlands, 1998
- [15] Bruice P.Y., *Organic Chemistry*, Prentice-Hall International, Inc., Engewood Cliffs, (1995)
- [16] Camacho F., Sanchez S., Pacheco R., et al. Thermal Effects of CO<sub>2</sub> Absorption in Aqueous Solutions of 2-amino-2-methyl-1-propanol. *AIChE Journal*, 51 (10) (2005): 2769-2777
- [17] Caplow M., Kinetics of carbamate formation and breakdown, *Journal of American Chemical Society*, 90 (1968): 6795-6803
- [18] Carson J.K, Marsh K.N., Mather A.E., Enthalpy of solution of carbon dioxide in water + Monoethanolamine or Diethanolamine or N-methyldiethanolamine at T = 298.15K, *Journal Chemical Thermodynamic*, 32 (2000): 1285-1296
- [19] Cents A.H.G., Brillman D.W.F., Versteeg G.F., Gas absorption in an agitated gas-liquid-liquid system, *Chemical Engineering Science*, 56, 2001, pp. 1075-1083
- [20] Choi W.J., Cho K.C., Lee S.S., *Green Chemistry*, 9 (6) (2007): 594-598
- [21] Crooks J.E., Donnellan J.P., Kinetics and mechanism of the reaction between carbon dioxide and amines in aqueous solutions, *Journal of Chemical Society, Perkins Transaction*, 2 (1989): 331-333
- [22] Chi S., Rochelle G.T., Oxidative degradation of monoethanolamine, *Industrial and Engineering Chemistry Research*, 41 (17) (2002): 4178-4186
- [23] Chunxi L., Fürst W., Representation of CO<sub>2</sub> and H<sub>2</sub>S in aqueous MDEA solutions using an electrolyte equation of state, *Chemical Engineering Science*, 55 (15) (2000): 2975-2988
- [24] Clayden J., Greeves N., Warren S., Wothers, P., *Organic chemistry*, Oxford University Press, Oxford, (2005)
- [25] Danckwerts P.V., The Reaction of CO<sub>2</sub> with Ethanolamines, *Chemical Engineering Science*, 34 (1979): 443-445
- [26] Danckwerts P.V., *Gas-Liquid Reactions*, London, McGraw-Hill Book Company, (1970)

- [27] Das T.R., Bandopadhyay A., Parthasarathy R., Kumar R., Gas-liquid interfacial area in stirred vessels: the effect of an immiscible liquid phase, *Chemical Engineering Science*, 40 (2) (1985): 209-214
- [28] Desmukh R.D., Mather A., Otto F., A Mathematical Model for Equilibrium Solubility of Hydrogen Sulfide and Carbon Dioxide in Aqueous Alkanolamine Solutions, *Chemical Engineering Science*, 36 (1981): 355-362
- [29] Donaldson T.L., Nguyen Y.N., Carbon Dioxide Reaction Kinetics and Transport in Aqueous Amine Membranes, *Industrial and Engineering Chemistry Fundamentals*, 19 (1980): 260-266
- [30] Dumont E., Demas H., Mass transfer enhancement of gas absorption in oil-in-water systems: A review, *Chemical Engineering and Processing*, 42 (2003): 419-438
- [31] EIA. Annual Energy Outlook 2001 (with Projections to 2020); Energy Information Administration, U.S. Department of Energy: Washington, DC, (2000)
- [32] Franks F., Ives D.J.G., *Chemical Society*, Vol. 20 (1966):1
- [33] Gabrielsen J., Michelsen M.L., Stenby E.H., et al., Modeling of CO<sub>2</sub> absorber using an AMP Solution, *AIChE Journal*, 52 (10) (2006): 3443-3451
- [34] Gabrielsen J., Michelsen M.L., Stenby E.H., Kontogeorgis G.M., A model for estimating CO<sub>2</sub> solubility in aqueous alkanolamines, *Industrial and Engineering Chemistry Research*, 44 (2005): 3348-3354
- [35] Hansen C.M., *Hansen Solubility Parameters*, (CRC Press, Boca Raton) (2000)
- [36] Hassan I.T.M., Robinson C.W., Oxygen transfer in mechanically agitated systems containing dispersed hydrocarbon, *Biotechnology and Bioengineering*, 19 (1977): 661-682
- [37] <http://www.physicalgeography.net/fundamentals/7h.html>
- [38] Hu W., Chakma A., Modelling of equilibrium solubility of CO<sub>2</sub> in aqueous Amino Methyl Propanol (AMP) Solutions, *Chemical Engineering Communications*, 94 (1990): 53-61
- [39] IPCC Special Report, *Carbon Dioxide Capture and Storage*, Cambridge University
- [40] Jou F., Otto F.D., Mather A.E., Vapor-liquid equilibrium of carbon dioxide in aqueous mixture of Monoethanolamine and Methyldiethanolamine, *Industrial and Engineering Chemistry Research*, 33 (1994): 2002-2005
- [41] Ju L.-K., Lee J.F., Armiger W.B., Enhancing oxygen transfer in bioreactors by perfluorocarbon emulsions, *Biotechnology Progress*, 7 (1991): 323-329
- [42] Kent R.L., Eisenberg B., Better data for amine treating, *Hydrocarbon Processing*, 55 (1976): 87-89

- [43] Kohl A., Nielsen R., *Gas Purification*, (Gulf Publishing Company, Houston) (1997)
- [44] Kritpiphat W., Tontiwachwuthikul P., New modified Kent-Eisenberg model for predicting carbon dioxide solubility in aqueous 2-Amino-2-Methyl-1-Propanol (AMP) solutions, *Chemical Engineering Communications*, 144 (1996): 73-83
- [45] Laddha S.S., Diaz J.M., Danckwerts P.V., The N<sub>2</sub>O analogy: The solubilities of CO<sub>2</sub> and N<sub>2</sub>O in aqueous solutions of organic compounds, *Chemical Engineering Science*, 36 (1) (1981): 228-229
- [46] Lekhal A., Etude du transfert de matiere gaz-liquide dans les systemes gaz-liquide-liquide: application a l'hydroformilation de l'octene-1 par catalyse biphasique, Thesis, INP Toulouse, 1998
- [47] Liao C.H., Li M.H., Kinetics of absorption of carbon dioxide into aqueous solutions of Monoethanolamine + N-methyldiethanolamine, *Chemical Engineering Science*, 57 (2002): 4569-4582
- [48] Lide D.R., *Handbook of Chemistry and Physics 80<sup>th</sup> ed.*, CRC Press, Washington D.C., (1999)
- [49] Linek V., Benes P., A study of the mechanism of gas absorption into oil-water emulsions, *Chemical Engineering Science*, 31(11) (1976): 1037-1046
- [50] Littel R.J., Versteeg G.F., and Van Swaaij W.P.M., Kinetics of CO<sub>2</sub> with primary and secondary amines in aqueous solutions-II, influence of temperature on zwitterion formation and deprotonation rates, *Chemical Engineering Science*, 47 (1992): 2037-2045
- [51] Liu Y., Zhang L., Watanasiri S., Representing vapor-liquid equilibrium for an aqueous MEA-CO<sub>2</sub> system using the electrolyte Nonrandom-Two-Liquid model, *Industrial and Engineering Chemistry Research*, 38 (1999): 2080-2090
- [52] MacMillan J.D., Wang D.I.C., Mechanisms of oxygen transfer enhancement during submerged cultivation in perfluorochemical-in-water dispersions, *Annals of The New York Academy of Sciences*, 589 (1990): 283-300
- [53] Mc Ketta J.J., *Encyclopedia of chemical processing and design*, Vol. 6. (Marcel Dekker, Inc., New York) (1978): 280-309
- [54] Mehta V.D., Sharma M.M., Mass transfer in mechanically agitated gas-liquid contactors, *Chemical Engineering Science*, 26 (1971): 461-479
- [55] Notz R., Asprion N., Clausen I., Hasse H., Selection and pilot plant tests of new absorbents for post-combustion carbon dioxide capture, *Chemical Engineering Research and Design*, 85 (A4) (2007): 510-515
- [56] Othmer K., *Encyclopedia of chemical technology* 4<sup>th</sup> ed., Vol. 5. (Wiley- Interscience Publication, New York), (1993)

- [57] Perrin D.D., Dempsey B., Serjeant E. P., *pKa Prediction for Organic Acids and Bases*, Chapman and Hall, London, (1981)
- [58] Rao A.B., Rubin E.S., A technical, economic and environmental assessment of amine-based CO<sub>2</sub> capture technology for power plant greenhouse gas control, *Environmental Science and Technology*, 36 (2002): 4467-4475
- [59] Reichardt C., *Solvents and solvent effects in organic chemistry* 2<sup>nd</sup> ed. (VCH Verlagsgesellschaft mbH, Weinheim) (1988)
- [60] Rhudy D., CO<sub>2</sub> testing program an Industry/EPRI initiative to develop CO<sub>2</sub> capture and storage test capabilities, (2006)  
<http://www.co2captureandstorage.info/docs/capture/M-Rhudy.pdf>.
- [61] Rochelle G., Bishnoi S., Chi S., Dang H., Santos J., (2001). Research needs for CO<sub>2</sub> capture from flue gas by aqueous absorption/stripping. DE-AF26-99FT01029, Pittsburg, PA, USA, Federal Energy Technology Center
- [62] Rolker J., Arlt W., Abtrennung von Kohlendioxid aus Rauchgasen mittels Absorption, *Chemie Ingenieur Technik*, 78 (4) (2006): 416-424
- [63] Rolker, J., Seiler, M., Mokrushina, L., Arlt, W., Potential of branched polymers in the field of gas absorption: experimental gas solubilities and modelling, *Industrial and Engineering Chemistry Research*, 46 (2007): 6572-6583
- [64] Rols J.L., Condoret J.S., Fonade C., Goma G., Mechanism of enhanced oxygen transfer in fermentation using emulsified oxygen-vectors, *Biotechnology and Bioengineering*, 38 (1990): 427-435
- [65] Sada E., Kumazawa H., Han Z.Q., Butt M.A., Chemical Kinetics of the Reaction of Carbon Dioxide with Ethanolamines in Nonaqueous Solvents, *AIChE Journal*, 31 (1985):1297-1303
- [66] Saleh M.A., Akhtar S., Ahmed S.M., Khan M.A.R., Thermodynamic activation parameters for viscous flow of aqueous solutions of butylamines, *Physics and Chemistry of Liquids*, 44 (5) (2006): 501-512
- [67] Sartori G., Savage D.W., Sterically hindered amines for CO<sub>2</sub> removal from gases, *Industrial & Engineering Chemistry Fundamentals*, 22 (2) (1983): 239-249
- [68] Schubert S., Untersuchungen zur Anwendung immobilisierter Aktivatoren bei der Absorption von CO<sub>2</sub> mit wässrigen Methyldiethanolamine – Lösungen (Dr.-Ing. dissertation, University of Dortmund) (2004)
- [69] Schubert S., Grünewald M., Agar D.W., *Chemical Engineering Science*, 56 (2001): 6211
- [70] Sharma M.M., Ph.D. Thesis, Cambridge, (1964)

- [71] Sharma M.M., Mashelkar R.A., Absorption with reaction in bubble columns, *International Chemical Engineering Symposium Series*, 28 (1968): 10-21
- [72] Sulaiman M.Z., Aroua M.K., Benamor A., Analysis of equilibrium data of CO<sub>2</sub> in aqueous solutions of Diethanolamine (DEA), Methyldiethanolamine (MDEA) and their mixtures using the modified Kent Eisenberg model, *Transaction of The Institution of Chemical Engineers A*, 76 (1998): 961-968
- [73] Sun W.C., Yong C.B., Li M.H., Kinetics of the Absorption of Carbon Dioxide into Mixed Aqueous Solutions of 2-Amino-2-Methyl-1-Propanol and Piperazine, *Chemical engineering Science*, 60 (2005): 503-516
- [74] Supap T., Idem R., Veawab A., Aroonwilas A., Tontiwachwuthikul P., Chakma A., Kybett B.D., Kinetics of the oxidative degradation of aqueous monoethanolamine in a flue gas treating unit, *Industrial and Engineering Chemistry Research*, 40 (16) (2001): 3445-3450
- [75] Tan Y.H., *Experimental Study of CO<sub>2</sub> Absorption into Aqueous Lipophilic Amine Solution* (M. thesis), Technical Chemistry B, Universität Dortmund, (2006)
- [76] Thitakamol B., Veawab A., Foaming Behavior in CO<sub>2</sub> absorption process using aqueous solutions of single and blended alkanolamines, *Industrial and Engineering Chemistry Research*, 47 (1) (2008): 216-225
- [77] Tontiwachtuthikul P., Meisen A., Lim C.J., Solubility of CO<sub>2</sub> in 2-amino-2-methyl-1-propanol, *Journal of Chemical Engineering Data*, 26 (1991): 130-133
- [78] van der Meer A.B., Beenackers A.A.C.M., Burghard R., Mulder N.H., Fok J.J., Gas/liquid mass transfer in a four-phase stirred fermentor: effects of organic phase hold-up and surfactant concentration, *Chemical engineering science*, 47 (9/11) (1992): 2369-2374
- [79] van Ede C.J., van Houten R., Beenackers A.A.C.M., Enhancement of gas to water mass transfer rates by a dispersed organic phase, *Chemical Engineering Science*, 50 (18) (1995): 2911-2922
- [80] Versteeg G.F., Blauwhoff P.M.M., Van Swaaij W.P.M., The effect of diffusivity on gas-liquid mass transfer in stirred vessels. Experiment at atmospheric and elevated pressures, *Chemical Engineering Science*, 42 (5) (1987): 1103-1119
- [81] Versteeg G. F., Van Dijck L.A.J., Van Swaaij W.P.M., On the kinetics between CO<sub>2</sub> and alkanolamines both in aqueous and non-aqueous solutions: An overview. *Chemical Engineering Communications*, 144 (1996): 113-158
- [82] Versteeg G.F., Van Swaaij W.P.M., Solubility and diffusivity of acid gases (CO<sub>2</sub>, N<sub>2</sub>O) in Aqueous Alkanolamine Solutions, *Journal of Chemical and Engineering Data*, 33 (1988): 29-34
- [83] Xing Q. Y., *Basic organic chemistry*, Higher Education Press, Beijing, 2003

- 
- [84] Yalkowski, S. H., *Solubility and Solubilization in Aqueous Media*, Oxford University Press, New York, 1999
- [85] Yoshida F., Yamane T., Miyamoto Y., Oxygen absorption into oil-in-water emulsions. A study on hydrocarbon fermentors, *Industrial Engineering Chemistry Research and Development*, 9 (4) (1970): 570-577
- [86] Zhang, X., *Studies on Multiphase CO<sub>2</sub> Capture Systems*, Fortschritt-Berichte VDI (Dissertation), VDI Verlag GmbH, Düsseldorf, 2007

## **CURRICULUM VITAE**

Yudy Halim Tan

Born in Bandung, 28.04.1980

- |             |   |
|-------------|---|
| 1986 - 1998 | Christian Elementary – Senior High School, BPK Penabur, Indonesia   |
| 1998 - 2002 | Bachelor of Science – Chemical Engineering in Bandung Institute of Technology (ITB), Indonesia  |
| 2003 - 2005 | Master of Science – Chemical Engineering in Universität Dortmund, Germany   |
| 2006 - 2009 | Doctoral research – Department of Technical Chemistry B (Reaction Engineering Department), Faculty of Bio- and Chemical Engineering, TU Dortmund, Germany |